

TRPC5 Channel: Regulations and Functions

WONG, Ching On

**A Thesis Submitted in Partial Fulfilment
of the Requirements for the Degree of
Doctor of Philosophy**

In

Physiology

The Chinese University of Hong Kong

August 2009

UMI Number: 3514543

All rights reserved

INFORMATION TO ALL USERS

The quality of this reproduction is dependent on the quality of the copy submitted.

In the unlikely event that the author did not send a complete manuscript and there are missing pages, these will be noted. Also, if material had to be removed, a note will indicate the deletion.



UMI 3514543

Copyright 2012 by ProQuest LLC.

All rights reserved. This edition of the work is protected against unauthorized copying under Title 17, United States Code.



ProQuest LLC.
789 East Eisenhower Parkway
P.O. Box 1346
Ann Arbor, MI 48106 - 1346

Thesis/Assessment Committee

Professor YUNG Wing-ho (Chair)

Professor YAO Xiaoqiang (Thesis Supervisor)

Professor HUANG Yu (Committee Member)

Professor BEECH David (External Examiner)

Professor LI Gui-Rong (External Examiner)

Declaration of Originality

The work contained in this thesis is original research carried out by the author in the Department of Physiology, Faculty of Medicine, the Chinese University of Hong Kong, starting from August 2005 to May 2009. No part of the work described in this thesis has already been or is being submitted to any other degree, diploma or other qualification at this or any other institutions.

Abstract of the thesis entitled:

TRPC5 channel: Regulations and Functions

Submitted by WONG Ching On

for the degree of Doctor of Philosophy

at The Chinese University of Hong Kong in August 2009

Transient receptor potential (TRP) channels constitute a family of 28 mammalian cation channel members. TRPs are widely expressed in mammalian tissues, and are responsible for various physiological functions. TRP channels are regarded as signal integrators by transforming external stimuli to cation influx across the plasma membrane. Elucidating the regulatory and signaling pathway in which a TRP channel participates has shed light on many previously unknown cellular functions.

Canonical transient receptor potential isoform 5 (TRPC5) belongs to the TRPC subfamily, which is an intensively studied TRP subfamily. Expression of TRPC5 has been found in neurons, vascular endothelial and smooth muscle cells. Previous studies revealed its participation in neuronal growth cone guidance, vascular smooth muscle cell motility, synovial fluid secretion and cardiac myocyte hypertrophy. Multiple signals are capable of inducing calcium ion (Ca^{2+}) influx through TRPC5. However, the direct endogenous molecule that stimulates TRPC5 is still elusive.

The major part of my study focuses on TRPC5. Using a panel of such techniques as molecular cloning, primary culture of native cells, live cell fluorescent Ca^{2+} imaging and electrophysiology, several previously unknown properties of TRPC5 have been discovered.

Ca²⁺ signaling in vascular endothelial cells contributes to various physiological functions including nitric oxide generation, gene transcription and cell motility. Previous findings from our lab showed the expression of TRPC5 in vascular endothelial cells. Using a combination of specifically developed blocking antibody and live cell imaging technique, I found that TRPC5 is a component of the Ca²⁺ influx pathway in bovine aortic endothelial cells (BAECs). One report claimed that TRPC5 functions as a nitric oxide sensor in endothelial cell, thereby potentiating the Ca²⁺ influx after endothelial NO production. In the present study, however, NO did not stimulate TRPC5-mediated Ca²⁺ influx in human embryonic kidney (HEK) cells nor in BAECs.

Plant-derived isoflavones receive great attention for their potential health beneficial properties in protecting against many pathological conditions. Genistein is one of the most widely studied isoflavones. Apart from the inhibitory effect on tyrosine kinases and stimulation of estrogen receptors, it has been reported that genistein may exert a direct, noncatalytic modulation on several ion channels. Using live cell imaging and patch clamping technique, I found that genistein was able to stimulate the activity of heterologously expressed TRPC5 in HEK cells. The stimulatory effect was independent of tyrosine kinase activity and estrogen receptors. The genistein action on TRPC5 could be recorded in excised membrane patches, suggesting a relatively direct action. Furthermore, genistein potentiated the stimulating action of lanthanum on TRPC5 activity. Lastly, it was also found that genistein stimulates cytosolic Ca²⁺ elevation in primary endothelial cells through TRPC5. It is the first study showing an action of genistein on a TRP channel.

Mechanical force is one of the stimuli that gate TRP channel opening. The ability of

TRPC5 opening in response to mechanical force exerted on the cell membrane was tested. Hypotonic shock, induced by a reduction of osmolarity in the bath solution, caused cell swelling and TRPC5-mediated Ca^{2+} influx. Pressure suction applied to cell-attached, single-channel patches also induced TRPC5 channel opening. Expression of TRPC5 in the arterial baroreceptor neurons, from the cell body to the nerve terminals at aortic arch, was confirmed by immunodetection. Elevation of blood pressure stretches the vasculature and stimulates the action potential firing of the baroreceptor terminus. By labeling these termini, the respective baroreceptor cells were selected from the primary culture of nodose sensory neurons. It was found that hypotonic shock induced Ca^{2+} influx in the baroreceptor cells. Blocking of TRPC5 function by anti-TRPC5 blocking antibody or dominant-negative construct significantly reduced the Ca^{2+} influx. Functional contribution of TRPC5 to baroreceptor activity was examined by *in vivo* experiment. Lentiviral vector transduction of baroreceptor neurons with dominant-negative TRPC5 significantly decreased the baroreceptor activity in response to blood pressure elevation. The results indicate that TRPC5 may function as a mechanosensitive channel in baroreceptor.

In conclusion, several novel findings have been made on TRPC5. Those include: 1) TRPC5 mediates Ca^{2+} influx in vascular endothelial but is not a nitric oxide-sensitive channel; 2) activation of TRPC5 by isoflavones genistein and daidzein; 3) TRPC5 is a mechanosensitive channel that may function in the mechanotransduction of arterial baroreceptor.

論文摘要

瞬時受體電位 (Transient Receptor Potential; TRP) 通道超家族由約 28 個哺乳類非選擇性陽離子通道成員組成。TRP 通道廣泛表達於哺乳類動物組織，並負責多種生理功能。TRP 通道被視為信號集成器，傳導外部刺激，讓陽離子湧入細胞。許多前所未有的細胞功能，通過闡明 TRP 通道所參與的信號轉導通路，都得以進一步了解。

標準型瞬時受體電位亞型 5 (TRPC5) 屬於 TRPC 亞科，是一個被深入研究的 TRP 亞科。TRPC5 已發現表達於神經元、血管內皮細胞及平滑肌細胞。以往的研究發現，TRPC5 參與神經生長錐生長、血管平滑肌細胞運動、滑液分泌和心肌細胞肥大。很多信號都能夠誘導鈣離子 (Ca^{2+}) 通過 TRPC5 湧入。然而，直接刺激 TRPC5 的內源性分子，至今還沒有得到確定。

這次研究主要集中於 TRPC5。通過使用一系列技術，包括分子克隆、原代培養細胞、活細胞內 Ca^{2+} 熒光成像和電生理，發掘一些以前不為人知的 TRPC5 特性。

鈣離子信號協助血管內皮細胞的各種生理功能，包括一氧化氮 (NO) 生成、基因轉錄和細胞運動。先前我們實驗室的研究結果顯示，血管內皮細胞表達 TRPC5。是次研究運用專門開發的阻塞性抗體和活細胞 Ca^{2+} 熒光成像技術，發現 TRPC5 是一個牛主動脈內皮細胞 (BAECs) Ca^{2+} 內流途徑的組成部分。一份報告曾提出，TRPC5 能作為在內皮細胞的一氧化氮傳感器，從而增強內皮細胞 NO 生成後的 Ca^{2+} 內流。這次的研究卻有相反的結果：NO 並不能刺激人類胚胎腎 (HEK) 細胞和 BAECs 內由 TRPC5 介導的 Ca^{2+} 內流。

植物性異黃酮近年受到高度重視，因為它具潛力對抗多種病理狀況。染料木黃酮 (Genistein) 是一種最被廣泛研究的異黃酮。根據已往文獻，它除了抑制酪氨酸激酶和刺激雌激素受體外，也可透過直接和非催化性的作用調控幾種離子通道。此次研究發現，利用活細胞 Ca^{2+} 熒光成像和膜片箝技術，染料木黃酮能刺激表達在 HEK 細胞上的 TRPC5，而其刺激作用與酪氨酸激酶活性和雌激素受體並不相關。在內面向外式單通道膜片箝上，染料木黃酮對 TRPC5 的作用可以得到證實，這顯示出一個相對直接的作用機制。此外，染料木黃酮還可以增強鑷離子 (La^{3+}) 對 TRPC5 的作用。最後，研究還發現，染料木黃酮能通過刺激 TRPC5 提升血管內皮細胞內鈣離子的濃度。這是第一份研究報告顯示染料木黃酮在 TRP 通道上的作用的研究報告。

機械作用力是刺激 TRP 通道打開的因素之一。是次研究測試 TRPC5 對施加在細胞膜上的機械作用力的反應，透過減少溶液的滲透壓，引起細胞腫脹及由

TRPC5 介導的 Ca^{2+} 內流。另外，也透過施加負壓於細胞貼附式單通道膜片，引起 TRPC5 通道開放。通過免疫檢測，證實了 TRPC5 表達在動脈壓力感受器神經元，包括從細胞體到位於主動脈弓的神經末梢。血壓的升高使血管擴張並刺激動脈壓力感受器神經末梢產生動作電位。通過標記這些神經末梢，能從原代培養的結狀感覺神經元分辨出壓力感受器細胞。結果發現，低滲透壓會引起壓力感受器細胞的 Ca^{2+} 內流。阻斷 TRPC5 功能的抗 TRPC5 阻塞性抗體或 TRPC5 顯性負構 (dominant-negative construct) 大大減少了 Ca^{2+} 內流。在體動物實驗亦進一步檢測了 TRPC5 在壓力感受器生理功能中的作用。神經元被帶有顯性負 TRPC5 的慢病毒載體轉導後，因應血壓升高引起的壓力感受器活動會顯著下降。結果表明，TRPC5 是在壓力感受器上感受血壓變化的一個通道。

總括而言，是次研究對於 TRPC5 的新發現包括：1) TRPC5 介導血管內皮細胞的 Ca^{2+} 內流，但並不是一個對一氧化氮敏感的通道；2) 染料木黃酮和大豆黃酮會激活 TRPC5；3) TRPC5 是一個對機械作用力敏感的通道，並在動脈壓力感受器上有重要的生理功能。

Acknowledgements

I would like to acknowledge and extend my heartfelt gratitude to the following people for their support and encouragement which has made the completion of this thesis possible:

Professor Xiaoqiang Yao, my supervisor, who gave me the opportunity to learn and do serious research in his lab. I am in debt to him for his kindness, patience and guidance.

Professor Yu Huang, for his encouragement and insightful advices during my PhD study.

Ms Anna H.Y. Kwan, for her continuous support and encouragement. She had been a great role model to the freshmen in our lab.

Mr Bing Shen, for his technical support, especially on electrophysiology. He is also my company in the baroreceptor project.

Ms Jacqueline C.Y. Ngai and Mr Dicky Y.B. Man, for their technical support, especially on primary cell culture and antibody preparation.

Ms Natalie N.Y. Lui, for her critical revision to the Chinese version of the abstract.

Colleagues and staffs in the Department of Physiology (now Institute of Biomedical Sciences), for their experienced technical support.

Lastly, I would like to thank my family for their leniency.

Abbreviations and Units

[Ca ²⁺] _i	Cytosolic Ca ²⁺
2-APB	2-Aminoethoxydiphenyl borate
anti-TRPC5	Antibody against TRPC5 protein
BAECs	Bovine aortic endothelial cells
CCh	Carbachol
CHO	Chinese hamster ovary
DAG	Diacylglycerol
DEA	Diethylamine NONOate
DiI	1,1'-dioleyl-3,3,3',3'-tetramethylindocarbocyanine methanesulfonate
DN-T5	Dominant-negative TRPC5
HEK	Human embryonic kidney
IP3	Inositol 1,4,5-triphosphate
lenti-control	Lentiviral vector without insert
lenti-DN-T5	Lentiviral vector with DN-T5 insert
NO	Nitric Oxide
OAG	1-oleoyl-2-acetyl-sn-glycerol
Phe	Phenylephrine
PIP2	Phosphatidylinositol 4,5-bisphosphate
PKC	Protein kinase C
PLC	Phospholipase C
PVDF	Polyvinylidene difluoride
RMECs	Rat mesenteric artery endothelial cells
SNAP	S-nitroso-N-acetylpenicillamine
SOC	Store-operated Ca ²⁺ influx
T5E3	Antibody against 3 rd extracellular loop of TRPC5
TRP	Transient Receptor Potential
TRPC5	Canonical Transient Receptor Potential isoform 5
ΔC-TRPC5	TRPC5 lacking 9 amino acid residues at C-terminus
M	Molar, mole per liter
mOsm	Milli-osmolar
mV	Milli-volt
pA	Pico-ampere
pF	Pico-Farad
pS	Pico-siemens

Table of Content

Declaration of Originality.....	i
Abstract.....	ii
論文摘要.....	v
Acknowledgements.....	vii
Abbreviations and Units.....	viii
Table of Content.....	ix
Table of Figures.....	xiv

1 Chapter 1 Introduction..... 1

1.1 Introduction to Transient Receptor Potential channels.....	1
1.1.1 A superfamily of cation channels	1
1.1.2 Molecular background.....	3
1.1.3 Biological functions	6
1.2 Introduction to TRPC5.....	7
1.2.1 From gene to protein	8
1.2.2 Ion channel characteristics	11
1.2.3 Channel modulation	13
1.2.3.1 Phospholipase C-dependent activation	13
1.2.3.2 Vesicular trafficking	15
1.2.3.3 Sensitivity to store-release.....	15
1.2.3.4 Potentiation by lanthanides	17
1.2.3.5 Sensitivity to lipid molecules.....	18
1.2.3.6 Activation by S-nitrosylation	18
1.2.3.7 Activation by reduction.....	19
1.2.3.8 Sensitive to hypo-osmolarity and cell swelling	19
1.2.3.9 Endogenous inhibitory components.....	20
1.2.3.10 Artificial inhibitors/blockers.....	20
1.2.4 Protein partners.....	21
1.2.5 Expression and biological functions.....	22
1.3 Objectives of the present study	23

2 Chapter 2 Materials and Methods..... 24

2.1	Materials.....	24
2.1.1	Chemicals and reagents in functional studies	24
2.1.2	Enzymes, reagents and media in cell culture	26
2.1.3	Solutions for immuno-blotting	27
2.1.4	Solutions for agarose gel eletrophoresis.....	29
2.1.5	Solutions for molecular cloning.....	30
2.1.6	Solutions used in $[Ca^{2+}]_i$ measurement	30
2.1.7	Solutions used in isometric tension measurement	33
2.1.8	Solutions used in electrophysiology.....	33
2.1.9	Antibodies	34
2.1.10	Animals.....	35
2.1.11	$[Ca^{2+}]_i$ indicators.....	35
2.2	General Methods.....	36
2.2.1	Cell culture.....	36
2.2.1.1	Human embryonic kidney 293 cells	36
2.2.1.2	Chinese hamster ovary cells.....	36
2.2.1.3	Bovine aortic endothelial cells	36
2.2.1.4	Rat mesenteric artery endothelial cells.....	37
2.2.1.5	Nodose ganglion neurons	37
2.2.2	Transfection	38
2.2.3	Molecular biology	38
2.2.3.1	Molecular cloning	38
2.2.3.2	Western immuno-blotting	43
2.2.4	Functional studies.....	44
2.2.4.1	Cytosolic Ca^{2+} ($[Ca^{2+}]_i$) measurement	44
2.2.4.1.1	Fluoresecnt dye loading.....	44
2.2.4.1.2	$[Ca^{2+}]_i$ measurement by confocal microscopy.....	44
2.2.4.1.3	$[Ca^{2+}]_i$ measurement by Ca^{2+} -imaging.....	45
2.2.4.2	Isometric tension measurement of isolated vessels	45
2.2.4.3	Electrophysiology.....	46
2.2.5	Preparation of a TRPC5-blocking antibody T5E3	47
2.2.6	Statistical analysis.....	47
2.3	Specific Methods for each Chapter	48
2.3.1	Methods for Chapter 3	48
2.3.1.1	Cell culture and cDNA expression.....	48
2.3.1.2	Isometric tension measurement.....	48
2.3.1.3	Immunoblots	49

2.3.1.4	Ca ²⁺ -imaging experiment	49
2.3.1.5	Anti-TRPC5 blocking antibody	50
2.3.1.6	Chemicals and reagents.....	50
2.3.1.7	Data analysis and presentation.....	50
2.3.2	Methods for Chapter 4	51
2.3.2.1	Cell culture and stable transfection	51
2.3.2.2	Immunoblots	52
2.3.2.3	Immuno-detection of TRPC5 on BAECs and RMECs.....	52
2.3.2.4	Preparation of a TRPC5-blocking antibody T5E3	53
2.3.2.5	[Ca ²⁺] _i measurement.....	53
2.3.2.6	Electrophysiology.....	54
2.3.2.7	Chemicals	54
2.3.2.8	Data analysis and presentation.....	55
2.3.3	Methods for Chapter 5.....	55
2.3.3.1	Molecular cloning, cDNA transfection and expression, and stable cell lines....	55
2.3.3.2	Labeling the aortic baroreceptor neurons	56
2.3.3.3	Isolation and primary culture of nodose ganglion neurons.....	57
2.3.3.4	Construction of lentiviral vector and viral transduction.....	58
2.3.3.5	<i>In situ</i> immuno-fluorescent detection of TRPC5 and neuronal marker PGP 9.5.	58
2.3.3.6	Immunoblots detection of TRPC5 in lysates	59
2.3.3.7	[Ca ²⁺] _i measurement	60
2.3.3.8	Electrophysiology.....	61
2.3.3.9	Arterial blood pressure and baroreceptor activity recording <i>in vivo</i>	61
2.3.3.10	Data analysis and presentation	62

3 Chapter 3 TRPC5 is not stimulated by nitric oxide..... 63

3.1	Introduction.....	63
3.2	Results.....	65
3.2.1	SNAP and DEA-NONOate induce vasorelaxation.....	65
3.2.2	Lack of action of SNAP on TRPC5-mediated Ca ²⁺ influx.....	65
3.2.3	Lack of action of SNAP DEA-NONOate on TRPC5-mediated Ca ²⁺ influx.....	66
3.2.4	Mouse TRPC5 clone from other lab was not activated by SNAP.....	66
3.2.5	Inhibitory effect of T5E3 antibody on TRPC5 function.....	67
3.2.6	Inhibition of Ca ²⁺ -entry in endothelial cells (BAECs).....	67
3.3	Discussion	75

4	Chapter 4 Stimulation of TRPC5 by genistein	80
4.1	Introduction.....	80
4.2	Results.....	83
4.2.1	Effect of genistein on TRPC5-mediated $[Ca^{2+}]_i$ rise	83
4.2.2	Synergistic action of genistein and La^{3+} on TRPC5.....	83
4.2.3	Concentration-dependent stimulation of TRPC5 by genistein	84
4.2.4	Effect of tyrosine kinase inhibitors and daidzein on TRPC5-mediated $[Ca^{2+}]_i$ rise..	84
4.2.5	Independent of estrogen receptors and phospholipase C (PLC) activity.....	85
4.2.6	Action of genistein on TRPC5 current.....	85
4.2.7	Effect of genistein on TRPC5 in native endothelial cells.....	86
4.3	Discussion	104
5	Chapter 5	109
	TRPC5 mechanosensitivity and functional role in arterial	
	baroreceptor	109
5.1	Introduction.....	109
5.2	Results.....	114
5.2.1	Cell swelling at hypotonicity induces Ca^{2+} influx via TRPC5.....	114
5.2.2	Intact cytoskeletal function is critical to cell swelling-activation of TRPC5	115
5.2.3	Membrane stretch stimulate single TRPC5 channels on membrane	116
5.2.4	Expression of TRPC5 at rat arterial baroreceptor neurons	128
5.2.5	Labeling and Isolation of baroreceptor neurons for <i>in vitro</i> experiments.....	129
5.2.6	TRPC5 participates in mechanosensitive Ca^{2+} influx pathway in baroreceptor	
	neurons	130
5.2.7	TRPC5 contributes to baroreceptor activity <i>in vivo</i>	130
5.3	Discussion	140
6	Chapter 6 General Conclusion and Future Work.....	146

6.1	Concluding remarks	146
6.2	Future work.....	148
	References.....	150

Table of Figures

Table 1.1	Mammalian TRP isoforms	2
Figure 1.1	Typical topology of a TRP protein	4
Figure 1.2	TRPC5 from gene to channel subunit	10
Figure 1.3	Modulations of TRPC5	14
Table 2.1	Chemical and reagents in functional studies	24
Table 2.2	Enzymes, reagents and media in cell culture	26
Table 3.4	Fluorescent dyes for tracing $[Ca^{2+}]_i$	35
Table 3.5	Information of recombinant DNA vectors	42
Figure 3.1	Relaxation to SNAP or DEA-NONOate in mice aortic segments.	68
Figure 3.2	SNAP on TRPC5-dependent Ca^{2+} -entry in HEK293 cells.	69
Figure 3.3	Comparable effects SNAP on HEK cells transfected with TRPC5 or vector control.	70
Figure 3.4	DEA-NONOate on TRPC5-dependent Ca^{2+} -entry.	71
Figure 3.5	Ca^{2+} -imaging experiments with TRPC5 and SNAP from Dr Y. Mori	72
Figure 3.6	T5E3 antibody blocked Ca^{2+} influx through TRPC5.	73
Figure 3.7	Inhibition of Ca^{2+} -entry by SNAP in endothelial cells	74
Figure 4.1	Expression of TRPC5 in HEK cells and elevation of $[Ca^{2+}]_i$ by genistein ...	88
Figure 4.2	TRPC5-mediated Ca^{2+} influx after genistein pretreatment	89
Figure 4.3	Potential effect of La^{3+} on genistein-induced TRPC5 activation.	90
Figure 4.4	Potential effect of genistein on La^{3+} -induced TRPC5 activation.	91
Figure 4.5	Concentration-dependent stimulation of TRPC5 by genistein.	92
Figure 4.6	Effect of a panel of tyrosine kinase inhibitors and inactive genistein analog daidzein on TRPC5-mediated $[Ca^{2+}]_i$ rise.	93
Figure 4.7	Summary of the effect of tyrosine kinase inhibitors and inactive genistein analog daidzein on TRPC5-mediated $[Ca^{2+}]_i$ rise.	94
Figure 4.8	Effects of estrogen receptor antagonist ICI-182780 on TRPC5-mediated $[Ca^{2+}]_i$ rise.	95
Figure 4.9	Effects of phospholipase C inhibitor U73122 on TRPC5-mediated $[Ca^{2+}]_i$ rise.	96
Figure 4.10	Stimulating action of genistein on the whole-cell currents in TRPC5-expressing HEK cells.	97
Figure 4.11	Stimulating action of genistein on the whole-cell currents due to TRPC5.	98
Figure 4.12	Single channel recording of genistein-modulated channels in excised inside-out patches from TRPC5-transfected HEK cells.	99
Figure 4.13	Single channel conductance of the genistein-sensitive channel	100
Figure 4.14	Expression of TRPC5 protein in primary cultured bovine aortic endothelial	

	cells (BAECs).....	101
Figure 4.15	Effect of genistein on TRPC5-mediated $[Ca^{2+}]_i$ rise in bovine aortic endothelial cells (BAECs).....	102
Figure 4.16	Effect of genistein on TRPC5-mediated $[Ca^{2+}]_i$ rise in rat mesenteric artery endothelial cells (RMECs).....	103
Figure 5.1	Gating modes of mechanosensitive channel.....	112
Figure 5.2	Schematic depiction of arterial baroreceptors anatomy and activation mechanism.....	113
Figure 5.3	Hypotonicity-induced cell swelling and $[Ca^{2+}]_i$ rise in TRPC5-expressing HEK cells.....	118
Figure 5.4	Hypotonicity-induced $[Ca^{2+}]_i$ rise is resulted from Ca^{2+} influx and independent of phospholipase C activity	119
Figure 5.5	TRPC5 mediates hypotonicity-induced Ca^{2+} influx.....	120
Figure 5.6	TRPC5-blockade abolished hypotonic $[Ca^{2+}]_i$ rise.....	121
Figure 5.7	The osmolarity threshold to trigger Ca^{2+} influx through TRPC5.....	122
Figure 5.8	Cytoskeletal function is critical to hypotonic activation of TRPC5.....	123
Figure 5.9	The hypotonic activation of TRPC5 is independent of C-terminal PDZ-binding domain.....	124
Figure 5.10	Expression of TRPC5 in CHO cells.....	125
Figure 5.11	Suction induced TRPC5 single channel opening at membrane patch.....	126
Figure 5.12	Single channel conductance of the stretch-activated channel matches TRPC5 identity	127
Figure 5.13	Expression of TRPC5 at rat aortic baroreceptor, depressor nerve and nodose ganglia.....	132
Figure 5.14	DiI-labeling of baroreceptor neurons.....	133
Figure 5.15	Hypotonic $[Ca^{2+}]_i$ rise in baroreceptor neurons is inhibited by T5E3.....	134
Figure 5.16	Dominant-negative TRPC5 inhibits hypotonic $[Ca^{2+}]_i$ rise in baroreceptor neurons	135
Figure 5.17	DN-TRPC5 carried by lentiviral vector inhibits TRPC5 function.....	136
Figure 5.18	<i>in vivo</i> measurement of baroreceptor activity	137
Figure 5.19	Baroreceptor activity as a function of arterial pressure elevation.....	138
Figure 5.20	Baroreceptor activity is diminished by TRPC5 functional knock-down...	139

1 Chapter 1 Introduction

1.1 Introduction to Transient Receptor Potential channels

1.1.1 A superfamily of cation channels

Transient receptor potential was named after the identification of a mutated gene in *Drosophila* displaying phenotype of a transient, rather than sustained, response to light (Montell *et al.*, 1989). Further studies revealed that the gene codes for a cation influx channel, which elevates intracellular calcium level ($[Ca^{2+}]_i$) after phospholipase C (PLC) activation (Hardie *et al.*, 1993). PLC is a membrane-anchored enzyme which catalyzes the conversion of phosphatidylinositol 4,5-bisphosphate (PIP₂) to diacylglycerol (DAG) and inositol 1,4,5-triphosphate (IP₃) (Hughes *et al.*, 1988). PLC activity is crucial to many cellular activities governed by phosphoinositide-mediated Ca^{2+} homeostasis (Hardie, 2003). The discovery of TRP channel in *Drosophila* served as a search light to identify the previously unknown cation channels on mammalian species. Up-to-date, 28 mammalian TRP proteins have been identified and cloned from mouse, 27 of which are found in human.

TRP channels form a superfamily of non-selective cation channels comprising seven subfamilies. In mouse and human, the 28 (mouse) or 27 (human) TRP isoforms are classified by the sequence similarity into six subfamilies (Table 1.1): the canonical TRPs (TRPC); melastatin TRPs (TRPM); vanilloid receptor TRPs (TRPV), ankyrin TRP (TRPA), polycystins (TRPP) and mucolipins (TRPML). Most of the characterized TRP channels are non-selective Ca^{2+} -permeable channels, except TRPM5

and TRPM6, which conduct monovalent cations only. TRPM6 and TRPM7 are highly permeable to Mg^{2+} . Other cations that are in trace amount in normal physiology can also permeate TRP channels, for example Cs^+ , Ba^{2+} , Sr^{2+} and Mn^{2+} .

Table 1.1 Mammalian TRP isoforms

	Mouse		Human	
TRPC	7	C1, C2, C3, C4, C5, C6, C7	6	C1, C3, C4, C5, C6, C7
TRPM	8	M1, M2, M3, M4, M5, M6, M7, M8	8	M1, M2, M3, M4, M5, M6, M7, M8
TRPV	6	V1, V2, V3, V4, V5, V6	6	V1, V2, V3, V4, V5, V6
TRPP	3	P1 (PKD2), P2 (PKD2L1), P3 (PKD2L2)	3	P1 (PKD2), P2 (PKD2L1), P3 (PKD2L2)
TRPA	1	A1	1	A1
TRPML	3	ML1, ML2, ML3	3	ML1, ML2, ML3
Total	28		27	

Although most of the isoforms are capable of forming functional homo-oligomeric channels, accumulating evidences suggest that different isoforms from different subfamilies come together to constitute the heteromeric native channels. One example is the hetero-oligomeric TRPC1-TRPC5 native channel in neurons (Strubing *et al.*, 2003). The electrophysiological properties of this heteromeric channel differ from that of homomeric TRPC5 channel. A recent study on mesangial cells revealed PKD2, a TRPP isoform, as a subunit in partner with TRPC1 and TRPC4 (Du *et al.*, 2008). The complex composition gives rise to a large number of

native hetero-oligomeric TRP channels with distinct and unique properties arisen from their subunit compositions. Such characteristic correlates well with the widespread tissue distribution of TRP channels, allowing native TRP channels to participate in versatile roles in various biological functions (Kunert-Keil *et al.*, 2006).

1.1.2 Molecular background

Although high resolution of TRP protein structure is unavailable, the protein sequence analysis of TRP shows topological similarity to voltage-gated potassium channels (Clapham *et al.*, 2005). A TRP protein contains six transmembrane domains S1-S6 (Figure 1.1). In contrast to the voltage-gated cation channels, TRPs lack positively charged residues on S4, implicating a non-voltage-dependent gating of TRP channels (Clapham *et al.*, 2005). A putative pore-forming loop links the S5 and S6 domains. It is assumed that the subunits form tetrameric TRP channels, and the four linkers construct the ion conducting pore. Mutations on the amino acid residues on the putative pore-loop render the channel non-functional to conduct ions. Through electrostatic interaction with ions, residues on this linker may contribute to the conduction properties of the pore. Targeted mutation of the charged residues, for example aspartate and glutamate, altered the ion permeability on TRPC1/5, TRPM4, and TRPV1/4/5/6 (Garcia-Martinez *et al.*, 2000; Hoenderop *et al.*, 2003; Jung *et al.*, 2003; Liu *et al.*, 2003b; Nilius *et al.*, 2005; Voets *et al.*, 2003; Voets *et al.*, 2002).

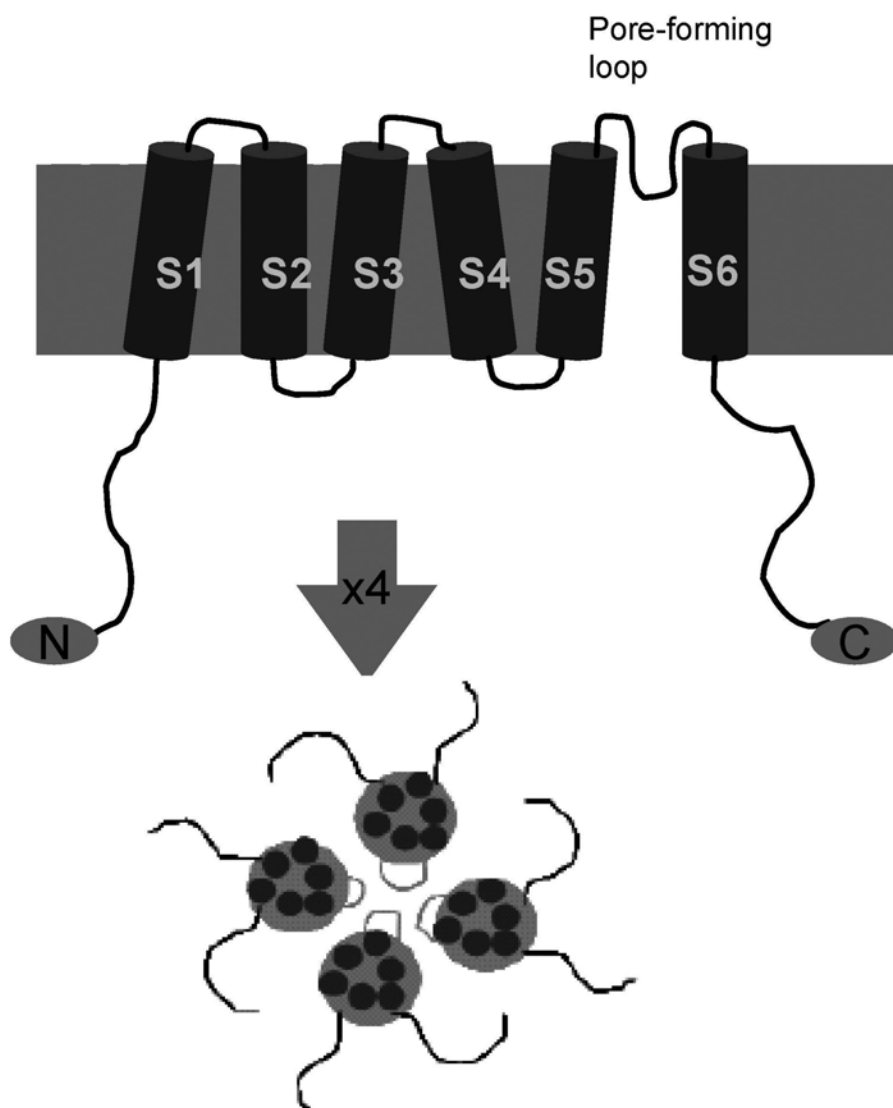


Figure 1.1 Typical topology of a TRP protein

Shown on top is a topographic depiction of a TRP protein embedded in membrane. S1-S6, transmembrane segment 1-6; N, cytosolic N-terminus; C, cytosolic C-terminus. Four TRP proteins couple together, with the pore-forming loop facing each other to form the ion-conducting pore.

There is no detailed information on the exact spatial orientation of the pore-forming linker of each TRP isoform. However, peptide sequence in this region may serve as specific target for channel blockade. A method known as E3-targeting, which utilizes antibody raised to react to a particular part of the third extracellular loop, i.e. the putative pore-loop, has

been applied to specifically block certain TRP isoforms, for example TRPC1, TRPC5, TRPM3 and TRPV1 (Klionsky *et al.*, 2006; Naylor *et al.*, 2008; Xu *et al.*, 2005b).

Images from the electron microscopy revealed the structural outline of TRP channels (Kedei *et al.*, 2001; Mio *et al.*, 2005; Moiseenkova-Bell *et al.*, 2008). The transmembrane domains together with the extracellular loops form only the tip of an iceberg, while a significantly large volume of the structure is immersed in the cytosol. From sequence analysis, clearly the majority of amino acids lay on the cytosolic amino- (N-) and carboxyl- (C-) terminal tails of a TRP protein. Numerous docking sites for signaling molecules situate on the two tails.

Indeed, many of the TRP channel functions are mediated by the protein-protein or protein-lipid interactions occur at the cytosolic domains. A stretch of five amino acids, VTTRL, forms the PDZ-binding domain at the C-terminus of TRPC4 and TRPC5, and is crucial to membrane distribution of the channels and interactions with other PDZ domain-containing proteins (Tang *et al.*, 2000). Another example is the calmodulin-binding domains found in TRPC isoforms. Calmodulin and inositol 1,4,5-triphosphate (IP₃) compete for a binding site on the C-terminus of TRPC3, and exert opposite effects on the channel function (Zhang *et al.*, 2001). Certain amino acid residues on the cytosolic tails are targets of phosphorylation (Yao *et al.*, 2005b). Specific threonine and serines on TRPC3 can be phosphorylated by protein kinase C and G to inhibit the channel activity (Kwan *et al.*, 2004; Trebak *et al.*, 2005). There

is a growing number of TRP isoforms being modulated by phosphatidylinositol 4,5-bisphosphate (PIP₂) (Voets *et al.*, 2007). Putative PIP₂-binding domains, on which targeted mutations or deletions altered the channel sensitivity to PIP₂, have been found on the C-termini of TRPC4, TRPV1, TRPV5, TRPM4 and TRPM5 (Lee *et al.*, 2005; Liu *et al.*, 2003a; Nilius *et al.*, 2006; Otsuguro *et al.*, 2008; Prescott *et al.*, 2003).

Altogether, the distinctive signature of a TRP isoform is not only determined by the ion-conducting pore-loop, but also by a combination of functional domains located on the cytosolic tails. By interacting with other signaling molecules, TRP channels are capable to form signaling microdomains to translate signal into cellular response (Ambudkar *et al.*, 2007a; Minke *et al.*, 2002).

1.1.3 Biological functions

The widespread tissue distribution of TRP isoforms implicates that the TRP channels participate in a diversity of functions in both excitable and non-excitable cells. TRP channels can be activated by a variety of chemical and physical stimuli, and can thus act as cellular sensors. Previous studies have demonstrated the critical roles of TRP channels in sensory processes ranging from taste and olfactory sensation to phototransduction, thermosensation, nociception, osmosensation and mechanosensation (Voets *et al.*, 2005). External stimuli either act on the channel directly or trigger signaling pathways which lead channel modulation. TRP channels sense and amplify the upstream signal to coordinate the downstream signal transduction pathways. Ion influx through TRP channel triggers

downstream signaling cascade which eventually leads to cellular response. For example, Ca^{2+} and Na^+ influx through TRPC4 and TRPC6 channels regulate the vascular tone (Dietrich *et al.*, 2007). TRP channels also regulate intracellular ion, e.g. Ca^{2+} and Mg^{2+} , homeostasis. One example is the impaired intestinal absorption of Mg^{2+} in patient with hypomagnesaemia due to non-functional TRPM6 (Bodding, 2007).

Given the versatile yet important physiological roles played by TRP channels, pathological conditions are inevitably resulted from malfunction of native TRP channels. A rapidly growing number of TRP channel studies demonstrate that knock-downs of specific TRP isoforms correspond to impairment or loss of functions in normal physiology, for instance, control of vascular tone, vascular cells proliferation and motility, neuronal growth, salivary secretion. Pathological conditions with defined genetic defects in TRP genes are regarded as channelopathy. There are six channelopathies directly linked to TRP channels. Those include:

1. TRPC6 – focal segmental glomerulosclerosis;
2. TRPML1 – type IV mucopolipidosis;
3. TRPM6 – hypomagnesemia with secondary hypocalcemia;
4. TRPP1/2 – polycystic kidney disease;
5. TRPM7 – Guamanian amyotrophic lateral sclerosis;
6. TRPM7 – Guamanian Parkinsonism dementia.

1.2 Introduction to TRPC5

The cloning and characterization of the first mammalian TRPC5 dated back to 1998, as reported by two independent groups. It is active in homomultimer or by

forming heteromultimeric channels with other TRPC isoforms. Reports suggested that TRPC5 displays multiple modes of activation. The electrophysiological profile of TRPC5 shows its voltage dependence. Its biological relevance has been demonstrated by a handful of studies conducted on neuron, vascular smooth muscle and fibroblast. In line with most of the TRP isoforms, TRPC5 is widely distributed across different tissues and interacts with many signaling molecules. Report on TRPC5 knock-out model is still not available and in depth functional study on TRPC5 expressed in other tissues/cells is lacking. In the course of my PhD study, TRPC5 has been the main focus. The theme of this thesis is constructed on my findings related to TRPC5.

1.2.1 From gene to protein

TRPC5 belongs to the canonical TRP family, which consists of 7 mammalian isoforms (Figure 1.2) (Beech, 2007b). The first member of the TRPC family is TRPC1, which is also the first identified mammalian TRP isoform (Zhu *et al.*, 1995). Existence of TRPC5 transcript was reported by Zhu *et al.* in 1996 (Zhu *et al.*, 1996). Full length TRPC5 cDNA was later cloned from mouse brain in 1998 (Okada *et al.*, 1998). Cloning and characterization of rabbit and mouse TRPC5 were also reported by another group at about similar time (Philipp *et al.*, 1998). The cloning of human TRPC5 followed in 1999 (Sossey-Alaoui *et al.*, 1999). Interestingly, the exons for TRPC5 lay on a region related to several X-linked mental disorders, the locus Xq23 (Sossey-Alaoui *et al.*, 1999). Phylogenetic analysis of TRPCs revealed close relationship between TRPC5 and TRPC4, and the two isoforms are classified into one subfamily, alongside with the

TRPC3/6/7 subfamily.

Human TRPC5 is 973 amino acids in length, while the mouse TRPC5 975 amino acids. Their amino acid sequences share over 96% homology. By analogy with voltage-gated potassium channel and by sequence analysis, the TRPC5 protein processes six transmembrane domains (S1-6) with a putative pore-forming loop between S5 and S6 (Figure 1.2). S1-6 spans around 300 amino acids. The N- and C-termini extend intracellularly. It is conceivable that TRPC5 forms tetrameric channel, as supported by several TRP channel studies using electron-microscopy or chemical cross-linking (Kedei *et al.*, 2001; Mio *et al.*, 2005; Moiseenkova-Bell *et al.*, 2008). Over-expression of TRPC5 in cell lines that endogenously express low level of TRP isoforms results in functional channel, suggesting a homomeric composition of TRPC5. Although there is no information on the exact subunit stoichiometry of a TRPC5 containing channel, several lines of evidence have suggested that other TRPC isoforms heteromerize with TRPC5 to form functional channels: 1) the current-voltage (I-V) relationship and single-channel conductance in cells over-expressing TRPC5 are different from that in TRPC5 co-expressing with TRPC1 (Strubing *et al.*, 2001; Xu *et al.*, 2008), or TRPC1+TRPC3 (Strubing *et al.*, 2003); 2) TRPC5 co-immunoprecipitates with TRPC4 (Goel *et al.*, 2002), TRPC1 (Goel *et al.*, 2002; Strubing *et al.*, 2001), TRPC1+TRPC3 (Strubing *et al.*, 2003) or TRPC1+TRPC6 (Strubing *et al.*, 2003); 3) blockade of TRPC5 at pore-region by specific antibody or introduction of non-functional TRPC5 inhibits the function of native channels that contain TRPC1 and TRPC5 (Strubing *et al.*, 2003; Xu *et al.*, 2008).

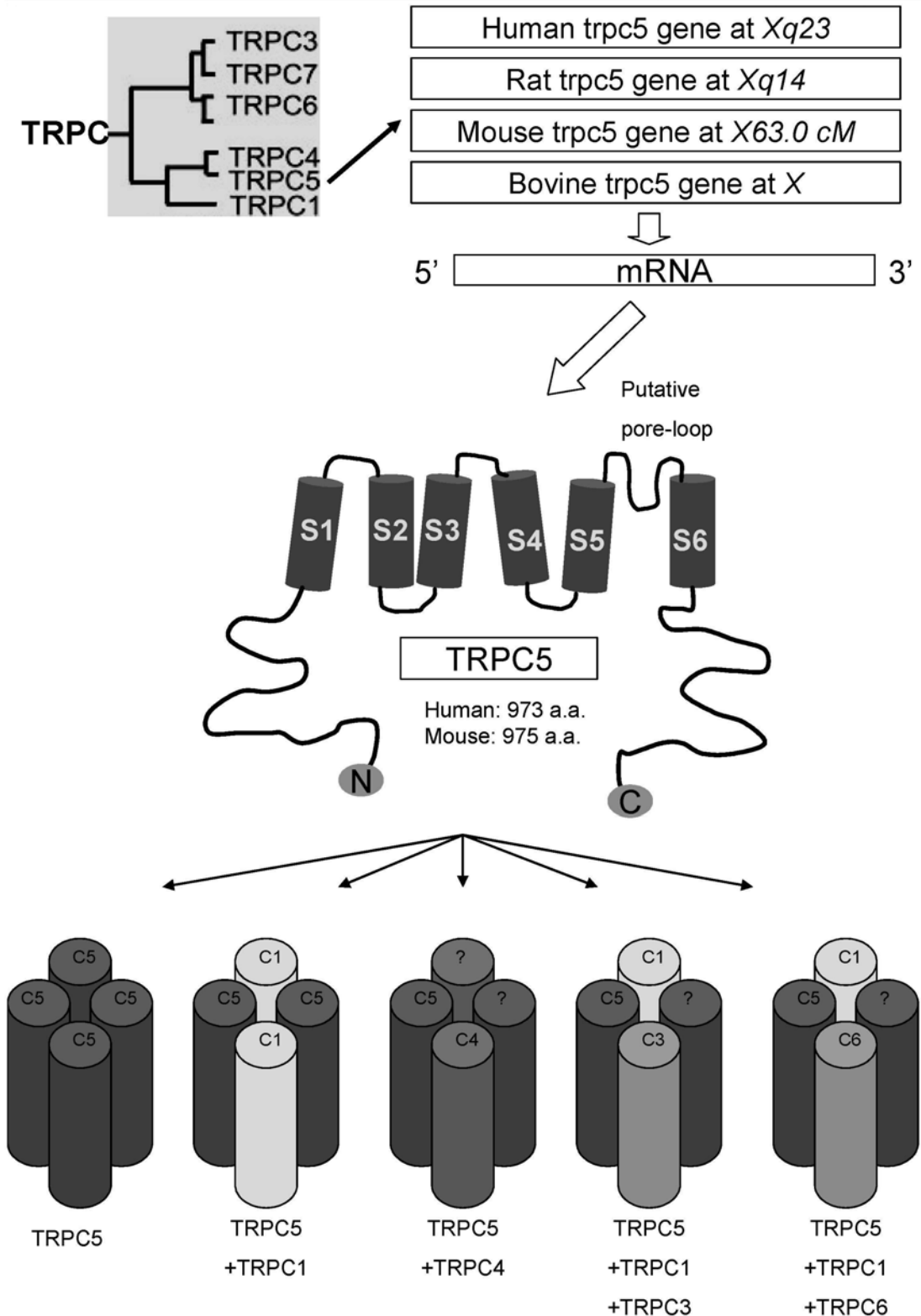


Figure 1.2 TRPC5 from gene to channel subunit

Among the TRPC isoforms, TRPC5 has closest phylogenetic relationship with TRPC4. The gene coding for human TRPC5 resides on locus *Xq23*. TRPC5 is capable of forming homomeric channel on its own. Heteromeric partners with TRPC1, TRPC4, TRPC3 and TRPC6 have been evident.

1.2.2 Ion channel characteristics

One common way to identify TRPC5 channel is by referring to its reported electrophysiological properties. TRPC5 is expressed and translocated onto the plasma membrane in both native cells and in over-expression system (Strubing *et al.*, 2003; Yamada *et al.*, 2000). The channel is functional and constitutively active on the plasma membrane (Yamada *et al.*, 2000). Reported single channel conductance varies from 38 to 47.6 pS (Alfonso *et al.*, 2008; Jung *et al.*, 2003; Strubing *et al.*, 2001; Yamada *et al.*, 2000). The channel opens and is not switched off at voltage between -100 and +100mV (Obukhov *et al.*, 2008). TRPC5 is thus not a voltage-gated channel, but the activity of the channel is voltage-regulated. At negative membrane potential, i.e. 0 to -60 mV, the channel opening increases (Obukhov *et al.*, 2008; Yamada *et al.*, 2000). Further hyperpolarization, however, results in decrease in open-probability (Obukhov *et al.*, 2008; Yamada *et al.*, 2000). At positive voltage, the current-voltage (I-V) relationship is non-linear, with an increase both in conductance and open-probability as voltage increases (Obukhov *et al.*, 2008). The channel activity is low at weakly positive voltage, i.e. 0 to +60 mV, a characteristic related to intracellular Mg^{2+} blockade of TRPC5 (Obukhov *et al.*, 2005). The complex mode of voltage-dependence of TRPC5 gives rise to its signature double-rectifying I-V relationship, with outward-rectification at positive potentials and inward-rectification at negative potentials.

The channel properties of hetero-multimeric TRPC5-TRPC1 are different from homo-multimeric TRPC5, as evident in both native cells and over-expressing cells (Strubing *et al.*, 2001; Xu *et al.*, 2008). Single

channel conductance of TRPC5-TRPC1 is much smaller than that of TRPC5 alone, and was reported to be 5 pS and 7pS (Alfonso *et al.*, 2008; Strubing *et al.*, 2001). Activity of TRPC5-TRPC1 does not increase progressively as voltage decrease from 0 to -100mV (Obukhov *et al.*, 2005; Strubing *et al.*, 2001). Slight outward-rectification at positive potentials is observed (Obukhov *et al.*, 2005; Strubing *et al.*, 2001). Although TRPC5 is capable of partnering with other TRPC isoforms in functional channels, there is yet insufficient data describing their channel properties.

One integral function of TRPC5 is to conduct cations. TRPC5 is permeable to sodium, calcium and potassium, but not chloride or large cations like N-methyl-D-glucamine (Lee *et al.*, 2003; Okada *et al.*, 1998; Strubing *et al.*, 2001). Caesium, barium, manganese and strontium also permeate the channel, thus allowing experimental studies using electrophysiological methods or ion-sensitive fluorescent dye (Lee *et al.*, 2003; Okada *et al.*, 1998; Schaefer *et al.*, 2000; Xu *et al.*, 2005a). It is conceivable that three amino acids laying on the putative pore-loop are critical in mediating the ion conduction. Mutating the highly conserved LFW motif (leucine-phenylalanine-tryptophan, at position 575-577 in mouse TRPC5) to three alanines results in a non-functional TRPC5 protein, termed as dominant negative TRPC5 (Strubing *et al.*, 2003). Since expressing and localization of the dominant negative TRPC5 showed no difference from those of wild-type TRPC5, the LFW motif is involved in the architecture of the ion-conducting pore. A parallel dominant negative construct was also demonstrated on TRPC6 (Hofmann *et al.*, 2002).

1.2.3 Channel modulation

Figure 1.3 shows a schematic diagram summarizing TRPC5 modulations

1.2.3.1 Phospholipase C-dependent activation

Several G-protein coupled receptor agonists are known to activate TRPC5. Those include: histamine, adenosine 5'-triphosphate (ATP), carbachol, bradykinin, uridine 5'-triphosphate, thrombin, prostaglandin E2 and sphingosine-1-phosphate (Schaefer *et al.*, 2000; Tabata *et al.*, 2002; Venkatachalam *et al.*, 2003; Xu *et al.*, 2006b; Zeng *et al.*, 2004). The downstream of receptor-agonist coupling involves GTP-bound G proteins, because intracellular application of GTP- γ -S was sufficient to activate TRPC5. G proteins comprise of a large family with a plethora of subunit combinations (Kaziro *et al.*, 1991). One particular type of G-protein, $G_{q/11}$, has been shown to mediate receptor activation of TRPC5 (Kanki *et al.*, 2001; Lee *et al.*, 2003). Based on the results from several groups which showed that PLC inhibitor U73122 suppresses the receptor-activation of TRPC5 and depletion of PIP_2 enhances TRPC5 activity, it is believed that the PIP_2 -hydrolysis activity of phospholipase C (PLC) confers TRPC5 activation downstream of G-proteins, (Lee *et al.*, 2003; Schaefer *et al.*, 2000; Trebak *et al.*, 2008). PLC hydrolyses PIP_2 into diacylglycerol (DAG) and inositol triphosphate (IP_3). DAG does not activate TRPC5 (Schaefer *et al.*, 2000; Venkatachalam *et al.*, 2003). IP_3 activates IP_3 -receptors on endoplasmic reticulum membrane and triggers Ca^{2+} -store release. Report by Kanki *et al.* shows IP_3 -receptor-dependent TRPC5 activation (Kanki *et al.*, 2001), but other reports argue against such scenario (Schaefer *et al.*, 2000;

Venkatachalam *et al.*, 2003; Xu *et al.*, 2005a). A recent report by Trebak *et al.* suggests that TRPC5 may be activated upon relief from a PIP₂-dependent inhibition, and that may explain the PLC-dependent TRPC5 activation (Trebak *et al.*, 2008).

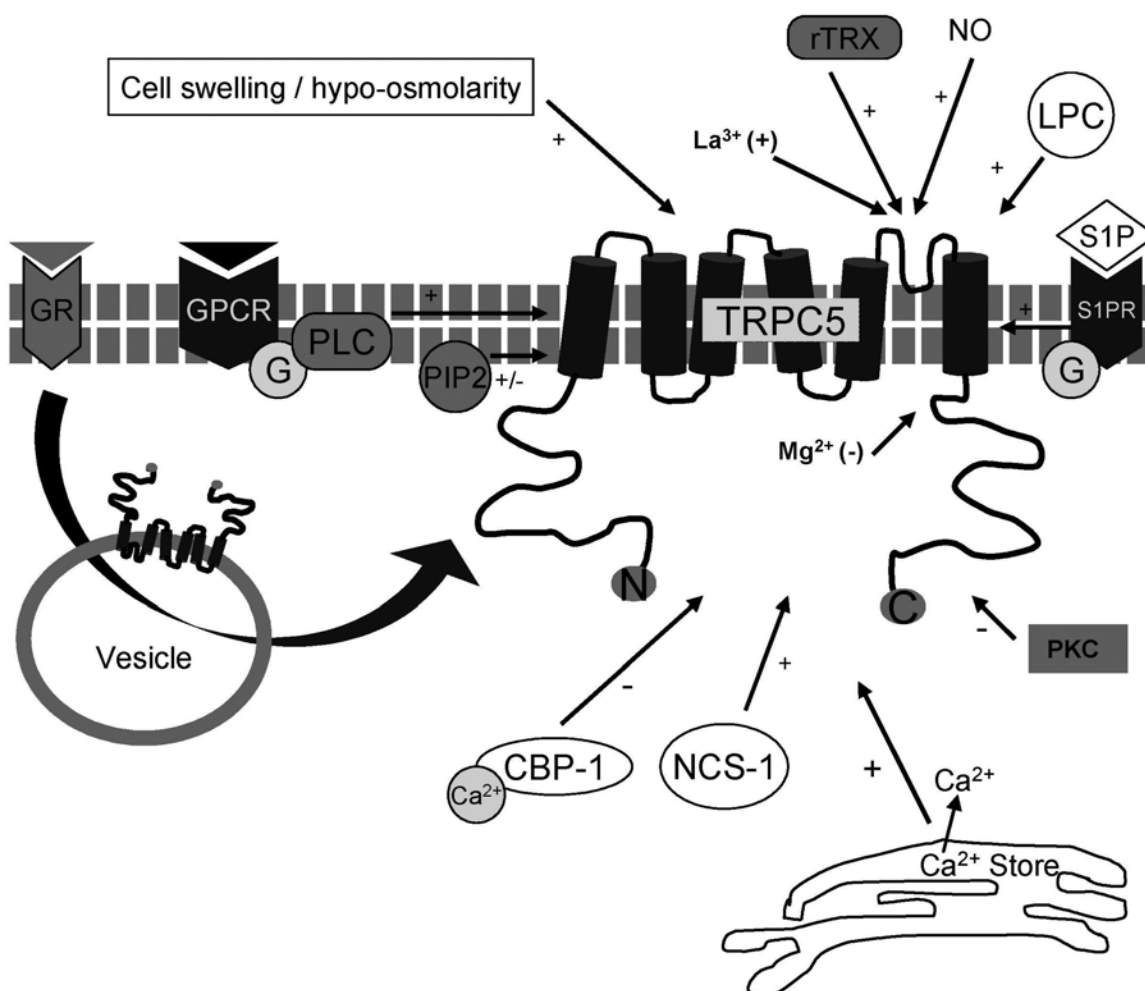


Figure 1.3 Modulations of TRPC5

Schematic diagram illustrating known modulations (indicated by arrows) of TRPC5 function; +, stimulatory action; -, inhibitory action. GR, growth-factor receptor; GPCR, G-protein-coupled receptor; G, G-protein; PLC, phospholipase C; PIP₂, phosphatidylinositol 4,5-bisphosphate; CBP-1, calcium-binding protein-1; rTRX, reduced thioredoxin; NO, nitric oxide; LPC, lysophosphatidylcholine; S1P, sphingosine-1-phosphate; S1PR, S1P receptor; PKC, protein kinase C; NCS-1, neuronal calcium sensor-1.

1.2.3.2 Vesicular trafficking

Apart from PLC-coupled receptor-activation pathways, receptor-activation can trigger Ca^{2+} influx through TRPC5 via vesicular trafficking. TRPC5 resides in punctate vesicles that were found to be just underneath the plasma membrane (Bezzarides *et al.*, 2004; Mery *et al.*, 2002; Schaefer *et al.*, 2000). Stimulation of the cells by epidermal growth factor (EGF) triggers the migration of the TRPC5-containing vesicles towards the membrane and subsequent lateral diffusion of the TRPC5 protein (Bezzarides *et al.*, 2004). Subsequent increase in surface expression of TRPC5 results in an elevated Ca^{2+} influx (Bezzarides *et al.*, 2004). Further data suggest that the vesicle fusion is mediated by the signaling pathway formed by EGF receptors, phosphatidylinositol 3-kinase, Rho GTPase Rac1 and phosphatidylinositol 4-phosphate 5-kinase (Bezzarides *et al.*, 2004). Furthermore, stimulation of the primary hippocampal neurons with other growth factors, including brain-derived neurotrophic factor, nerve-growth factor and insulin-like growth factor 1, enhances the surface expression of TRPC5 (Bezzarides *et al.*, 2004). TRPC5-TRPC1 heteromultimer seems not involved since co-expression with TRPC1 prevents the vesicle fusion (Bezzarides *et al.*, 2004). Given that TRPC5 regulates the neurite outgrowth (Greka *et al.*, 2003), the growth factor-evoked vesicular trafficking of TRPC5 may participate in neuronal development.

1.2.3.3 Sensitivity to store-release

Store depletion activates the store-operated calcium entry channels

(SOC), which mediates various cellular functions (Potier *et al.*, 2008). TRPC isoforms have been suggested as SOC candidates, although there is still controversy. Studies on TRPC5 show inconsistent results of its role in SOC, with some showing independent of store-depletion and others showing TRPC5 involved (Venkatachalam *et al.*, 2003; Zeng *et al.*, 2004). In addition, it has been suggested that TRPC1 may link TRPC5, and other TRPCs, to SOC (Ambudkar *et al.*, 2007b). On experimental settings, store-depletion can be triggered by three common ways: blockade of the sarco-endoplasmic-reticulum ATPase calcium pump (SERCA); passive store-depletion by Ca^{2+} chelators; and agonist-evoked store-release through IP_3 receptor. However, almost certainly, these methods may trigger secondary pathways, by for example a transient intracellular Ca^{2+} rise, which would modulate the TRP channel under study (Beech, 2009). Hence, it is technically challenging in dissecting the SOC component, if any, out of TRP channels. It is also notable whether TRPC5 opens in response to a depletion of Ca^{2+} in store or to the cytosolic Ca^{2+} released from store, since it is sensitive to intracellular Ca^{2+} level (Schaefer *et al.*, 2000; Zeng *et al.*, 2004). Absence of necessary endogenous SOC components in some cell types may hinder the study of SOC property in TRPC channels; particularly because store-depletion is not the sole activation mechanism in any of the TRPC channel (Ambudkar *et al.*, 2007a). The discovery of stromal interaction molecules (STIM) and Orai protein as essential SOC components steers the field into a new direction (Potier *et al.*, 2008). STIM has been found to interact with TRPC isoforms and regulate their activity (Liao *et al.*, 2008; Worley *et al.*, 2007).

Functional coupling between STIM1-TRPC1-TRPC5 may thus confer TRPC5 capable as an SOC component (Ambudkar *et al.*, 2007b; Worley *et al.*, 2007; Yuan *et al.*, 2007).

1.2.3.4 Potentiation by lanthanides

The potentiation of TRPC5 by lanthanum or gadolinium is perhaps the most distinctive feature solely possessed by TRPC4 and TRPC5. At micromolar range, lanthanum is commonly used as a blocker for non-selective cation channels. However, Jung *et al.* discovered that opening of TRPC5 is augmented when exposed to 1-100 μM lanthanum or gadolinium (Jung *et al.*, 2003). It is of note that the enhancement in open probability is accompanied by a decrease in single channel current amplitude by lanthanum in a concentration-dependent manner (Jung *et al.*, 2003). Neutralizing the negatively-charged residues E543, E595 or E598, which lay on the putative pore-loop, abrogates the lanthanum potentiation, suggesting that charge-charge interactions close to the pore region modulate the ion conduction (Jung *et al.*, 2003). Human body contains only trace amount of lanthanum. Such potentiation has little physiological relevance but serves as a useful tool to identify native TRPC5 channel. Other cations that potentiate TRPC5 include Ca^{2+} and proton (H^+). The latter has been found to act via E543 and E595, the two residues responsible for lanthanum effect (Semtner *et al.*, 2007). Decrease in single channel current amplitude was also observed when extracellular pH was decreased to pH 6.5. Ca^{2+} at supra-physiological concentrations (over 5 mM) also activates TRPC5 (Okada *et al.*, 1998; Zeng *et al.*, 2004); however, whether similar charge-charge interactions

with acidic amino acid residues occur is undetermined.

1.2.3.5 Sensitivity to lipid molecules

TRP channels are emerging as lipid sensors with the accumulating evidences showing cross-talk between phosphatidylinositol phosphates and TRPs (Nilius *et al.*, 2008). While it is evident that PIP₂ is critical to the receptor activation of TRPC5 (Kim *et al.*, 2008; Trebak *et al.*, 2008), TRPC5 was found to be a receptor to certain lipids. Lysophosphatidylcholine and sphingosine-1-phosphate (S1P) are two signaling phospholipids found in atherosclerotic lesion, and are related to vascular remodeling (Gouni-Berthold *et al.*, 2004). TRPC5 is strongly activated by these two lipids (Flemming *et al.*, 2006; Xu *et al.*, 2006b). TRPC5 as a lipid receptor in biological system is further substantiated by the correlation between channel activity and smooth muscle cell motility upon S1P stimulation (Xu *et al.*, 2006b).

1.2.3.6 Activation by S-nitrosylation

A report by Yoshida *et al.* shows that TRPC5 was activated by S-nitrosylation (Yoshida *et al.*, 2006). The authors found that high concentration of nitric oxide (NO) donors elevated intracellular Ca²⁺ level via TRPC5. It is suggested that C553 and C558 mediate the action of NO. TRPV1, TRPV3 and TRPV4, which contain the conserved cysteines, were also activated by NO donors. In addition, the authors found that TRPC5 is responsible for the NO-stimulated calcium influx in bovine aortic endothelial cells. The concept that TRPC5, also other NO-sensitive TRPs, acts as NO sensor is suggested based on these

findings (Yoshida *et al.*, 2006). However, the findings by Yoshida *et al.* are in contrast to another report that shows no activation of TRPC5 by the NO donor SNAP (Xu *et al.*, 2008).

1.2.3.7 Activation by reduction

While Yoshida *et al.* found that nitrosylation, which is one kind of oxidation, activates TRPC5, Xu *et al.* found that reducing agents activate TRPC5 (Xu *et al.*, 2008). By using Ca^{2+} imaging and electrophysiological techniques, the report shows that TRPC5 is activated by dithiothreitol and thioredoxin, a biologically reducing agent. The data suggest that the residues C553 and C558, which are suggested by Yoshida *et al.* as the nitrosylation targets, mediate the activation, possibly by reduction of the cysteine-cysteine disulphide bridge. Patients with rheumatoid arthritis have high level of thioredoxin at their joints, the activity of which is related to the severity of the disease. The authors provide striking evidence that TRPC5-TRPC1 heteromultimer expressed in fibroblast-like synoviocytes responds to thioredoxin, and the channel activity correlates with the secretion of matrix metalloproteinases (Xu *et al.*, 2008).

1.2.3.8 Sensitive to hypo-osmolarity and cell swelling

Channel opening in response to membrane stretch has been indicated for TRPC1, TRPC6, TRPM4, TRPM7, TRPV1, TRPV2 and TRPV4 (Lin *et al.*, 2005; Maroto *et al.*, 2005; Pedersen *et al.*, 2007; Spassova *et al.*, 2006). A recent report suggests that TRPC5 may join the list. Gomis *et al.* found an elevated cation influx through TRPC5 when the cell was

exposed to hypotonic solution (Gomis *et al.*, 2008). Secondary messengers derived from PLC and phospholipase A2 are not the mediators, as specific inhibitors did not abolish the channel activation in hypotonic condition. The authors also applied pressure intracellularly through the patch pipette to induce TRPC5 activation. However, direct evidence showing TRPC5 channel activation by direct mechanical stretch is lacking. Biological relevance is lacking since the study was conducted on heterologous expression system. It is thus yet pre-mature to define TRPC5 as mechanosensitive.

1.2.3.9 Endogenous inhibitory components

Although multiple signals have been known to activate TRPC5, little is known about the deactivation of the channel. Desensitisation of TRPC5 after receptor-activation was found to be mediated by protein kinase C and diacylglycerol (Venkatachalam *et al.*, 2003; Zhu *et al.*, 2005). Another study found that calcium-binding protein-1 prevents the receptor-activation of TRPC5, and the inhibition depends on Ca²⁺-binding of the inhibitory protein (Kinoshita-Kawada *et al.*, 2005).

1.2.3.10 Artificial inhibitors/blockers

There are many pharmacological tools to inhibit TRPC5 activity, for instance SKF96365 (Okada *et al.*, 1998), millimolar lanthanum (Jung *et al.*, 2003), flufenamic acid (Lee *et al.*, 2003), halothane and chloroform (Bahnasi *et al.*, 2008). One of the blockers, 2-aminoethoxydiphenyl borate (2-APB), was found to inhibit TRPC5 in a relatively direct mechanism (Xu *et al.*, 2005a). It is useful in blocking over-expressed

TRPC5 in cell lines but may not be applicable to endogenous TRPC5 in native cells, because 2-APB also modulates other TRP channel activity (Pena *et al.*, 2008; Xu *et al.*, 2005a). While there is a lack of chemical that can specifically block TRPC5, antibodies raised against TRPC5 may be used as channel blockers. Using a stretch of peptide that uniquely corresponds to the putative pore region of TRPC5, Xu *et al.* immunized rabbits with the peptide and raised the polyclonal immunoglobulin G (IgG) that remarkably blocks TRPC5 (Xu *et al.*, 2005b). With the advantage of specificity, the technique has been applied to study native TRPC5 containing channels (Xu *et al.*, 2006a).

1.2.4 Protein partners

Many proteins have been found to interact with TRPC5. Via the calmodulin-IP₃ receptor binding site (Tang *et al.*, 2001), which is also possessed by other TRPCs, and another C-terminal binding site (Ordaz *et al.*, 2005), calmodulin interacts and modulates the channel activity (Kim *et al.*, 2006; Ordaz *et al.*, 2005). The PDZ-binding domain at the end of C-terminus of TRPC5, which is conserved in TRPC4 but not other TRPCs, mediates the binding of PLC beta via Na⁺-H⁺ exchanger regulatory factor (NHERF), a PDZ-protein (Tang *et al.*, 2000). NHERF-1 seems to delay the peak activation of TRPC5 in response to receptor agonist (Obukhov *et al.*, 2004). Stathmin 3, a regulatory protein of microtubule dynamics, binds to TRPC5 and mediates the trafficking of TRPC5 from the neuronal cell body to growth cone (Greka *et al.*, 2003). Growth cone guidance is regulated by subtle change in Ca²⁺ homeostasis (Gomez *et al.*, 2006). The neuronal calcium sensor-1 (NCS-1) protein was found to bind TRPC5 at C-terminus

(Hui *et al.*, 2006). Inhibitory mutant of NCS-1 suppresses channel activity, suggesting a positive modulatory role of NCS-1 on TRPC5 (Hui *et al.*, 2006).

1.2.5 Expression and biological functions

Transcript for TRPC5 protein exists at high abundance in the brain (Riccio 2002). The best-characterized biological function of TRPC5 has been demonstrated on neuronal growth cone. Greka et al found that suppressing native TRPC5 activity by dominant-negative construct reduces neuronal growth cone extension (Greka *et al.*, 2003). The proposal was further substantiated by another report, which identified NCS-1 as a calcium sensor and interacting with TRPC5 to retard neurite outgrowth (Hui *et al.*, 2006). Apart from functioning at growth cone, TRPC5 mediates the initiation of neurite outgrowth from soma induced by cross-linking of ganglioside GM1 with integrin (Wu *et al.*, 2007).

In addition to steering neurite outgrowth, TRPC5 is related to the cell motility in the cardiovascular system. TRPC5 is expressed in vascular smooth muscle cells (Flemming *et al.*, 2006; Xu *et al.*, 2006b; Yip *et al.*, 2004). Smooth muscle cell motility evoked by SIP was found to be mediated through TRPC5 (Xu *et al.*, 2006b). In endothelial cells, lysophosphatidylcholine triggers the elevation of intracellular Ca^{2+} level through a TRPC6-TRPC5 cascade, and eventually leads to restriction of cell migration (Chaudhuri *et al.*, 2008). In addition, upregulated TRPC5 expression has been found in the failing heart of patients with idiopathic dilated cardiomyopathy (Bush *et al.*, 2006). These reports collectively

suggest that TRPC5 has functional role in cardiovascular remodeling.

Additional functional roles of TRPC5 in other physiological contexts have been hinted, albeit not fully elucidated, by other reports. Dexamethasone-induced upregulation of TRPC5 in adrenal medulla may be associated with metabolic syndrome (Hu *et al.*, 2009). Activation of TRPC5 by thioredoxin inhibits the synovial secretion in patients with rheumatoid arthritis (Xu *et al.*, 2008). Studies of TRPC5 expression in other cells/tissues, for instance sperm head (Sutton *et al.*, 2004) and neuroendocrine cells (Dalmazzo *et al.*, 2008), monocytes from hypertensive patients (Liu *et al.*, 2007) and baroreceptor (Glazebrook *et al.*, 2005), suggest that more un-characterized functional roles of TRPC5 exist.

1.3 Objectives of the present study

The aims of the present study are to use comprehensive techniques that cover molecular biology, cell biology, virus-based gene transfer, fluorescent imaging, electrophysiology, and in vivo experiments to elucidate the previously unknown properties and physiological functions of TRPC5. The study also emphasizes the biological relevance of endogenous TRPC5 in the cardiovascular physiology.

The study is planned as follows:

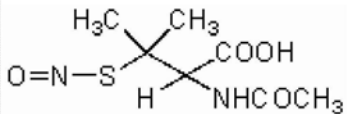
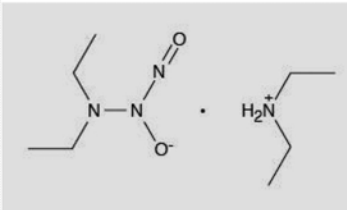
1. To test whether TRPC5 activity is modulated by nitric oxide-mediated pathways or tyrosine kinases.
2. To study the participation of TRPC5 in endothelial cells.
3. To study the potential role of TRPC5 as a mechanosensitive channel; and the relevant physiological function in arterial baroreceptor.

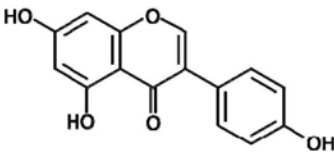
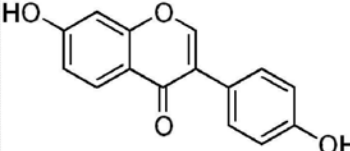
2 Chapter 2 Materials and Methods

2.1 Materials

2.1.1 Chemicals and reagents in functional studies

Table 2.1 Chemical and reagents in functional studies

<i>Chemicals (synonym, abbreviation)</i>	<i>Description</i>	<i>Solvent (storage °C; [stock])</i>	<i>Company (Catalog No.)</i>
Carbachol (carbamylcholine, Cch)	A cholinergic agent that binds and activates acetylcholine receptor	H ₂ O (4°C; 100 mM)	Calbiochem (212385)
Lanthanum chloride (LaCl ₃ , La ³⁺)	A blocker of divalent cation channels; potentiator of TRPC5	H ₂ O (23°C; 100 mM)	Sigma (L4131)
2-Aminoethoxydiphenyl borate (2-APB)	A chemical that inhibits IP3 receptors and modulates TRP channels	DMSO (4°C; 100 mM)	Calbiochem (100065)
S-nitroso-N-acetylpenicillamine (SNAP) 	An S-nitrosothiol that spontaneously releases nitric oxide radical (NO) in aqueous solution	DMSO (-20°C; 300 mM)	Sigma /Calbiochem (N3398/487910)
Diethylamine NONOate (DEA-NONOate, DEA) 	An NO donor that spontaneously dissociates in a pH-dependent, first-order process with a half-life of 2 minutes and 16 minutes at 37°C and 22-25°C, pH 7.4, respectively, to liberate 1.5 moles of NO per mole of parent compound	Ethanol purged with helium (-80°C; 100 mM)	Cayman (82100)
Phenylephrine hydrochloride (Phenylephrine, Phe)	α1-adrenoceptor agonist; induces vasoconstriction	H ₂ O (-20°C; 100mM)	Tocris (2838)
Genistein	An isoflavone naturally found in soybean; estrogenic at low concentration; non-specific tyrosine kinase inhibitor at high concentration	DMSO (-20°C; 100 mM)	Calbiochem (345834)

			
<p>Daidzein</p> 	<p>An isoflavone naturally found in soybean; estrogenic at low concentration; inactive to tyrosine kinases</p>	<p>DMSO (-20°C; 50 mM)</p>	<p>Sigma (D7802)</p>
<p>PP2</p>	<p>Src-family tyrosine kinase inhibitor</p>	<p>DMSO (-20°C; 50 mM)</p>	<p>Calbiochem (529576)</p>
<p>Lavendustin A</p>		<p>DMSO (-20°C; 100 mM)</p>	<p>Calbiochem (428150)</p>
<p>Herbimycin</p>		<p>DMSO (-20°C; 20 mM)</p>	<p>Sigma (H6649)</p>
<p>ICI-182780 (Fulvestrant)</p>	<p>An estrogen receptor antagonist</p>	<p>DMSO (-20°C; 50 mM)</p>	<p>Tocris (1047)</p>
<p>U73122</p>	<p>A phospholipase C inhibitor</p>	<p>DMSO (-20°C; 100 mM)</p>	<p>RBI (U107)</p>
<p>U73343</p>	<p>Inactive analog to U73122</p>	<p>DMSO (-20°C; 100 mM)</p>	<p>RBI (U112)</p>
<p>D-Mannitol (mannitol)</p>	<p>A sugar alcohol for calibration of solution osmolarity</p>	<p>H₂O</p>	<p>Calbiochem (443907)</p>
<p>1-oleoyl-2-acetyl-sn-glycerol (OAG)</p>	<p>A membrane-permeable analog to diacylglycerol; activator of TRPC3/6/7</p>	<p>DMSO (-20°C; 100 mM)</p>	<p>Calbiochem (495414)</p>
<p>Cytochalasin D</p>	<p>A cell-permeable and potent inhibitor of actin polymerization by association with barbed ends</p>	<p>DMSO (-20°C; 10 mM)</p>	<p>Sigma (C8273)</p>
<p>Pentobarbitol sodium</p>	<p>A short-acting barbiturate used as anesthetic to animal</p>	<p>H₂O</p>	<p>Sigma (P5178)</p>
<p>1,1'-dioleoyl-3,3',3'-tetramethylindocarbocyanine methanesulfonate (Δ9-DiI, DiI)</p>	<p>A lipophilic membrane stain that diffuses laterally to stain the entire cell; weakly fluorescent until incorporated into membranes.</p>	<p>DMSO</p>	<p>Invitrogen (D3886)</p>

Complete protease inhibitor cocktail tablets	A mixture of protease inhibitors with broad specificity for the inhibition of serine, cysteine, aspartic proteases and aminopeptidases	H ₂ O	Roche (046931-24001)
Triton X-100	A non-ionic surfactant used to isolate and purify functional membrane protein complexes		Sigma (NP40)
EDTA	Divalent-ion chelator	H ₂ O	Sigma (431788)
Pluronic acid (F-127)	To facilitates permeability of fluorescent dye	DMSO	Sigma (P2443)

2.1.2 Enzymes, reagents and media in cell culture

Table 2.2 Enzymes, reagents and media in cell culture

<i>Reagent and enzymes</i>	<i>Description</i>	<i>Company</i>	<i>Catalog No.</i>
Collagenase (Type I)	To dissociate endothelial cells for primary culture	Sigma	C0130
EBM basal medium	For rat mesenteric artery endothelial cell isolation	Lonza	CC-3129
DNase I	To dissociate nodose ganglion neurons for primary culture	Sigma	DN25
Trypsin	To dissociate nodose ganglion neurons for primary culture	Calbiochem	6502
Collagenase IA	To dissociate nodose ganglion neurons for primary culture	Sigma	C9891
Trypsin inhibitor	To stop enzyme digestion during isolation of nodose ganglion neurons	Calbiochem	65035
7S NGF	A neural growth factor for primary culture of nodose ganglion neurons	Invitrogen	13290-010
Cytosine arabinofuranoside (Ara-C)	An antimetabolic agent to arrest dividing cells; used in primary culture of nodose ganglion neurons	Sigma	C1768
Penicillin-streptomycin	As antibiotics in cell culture	Invitrogen	15140-122
Antibiotic-antimycotic	As antibiotics in cell culture	Invitrogen	15240-112

Dulbecco's Modified Eagle Medium (DMEM)	Culture medium of HEK cells	Invitrogen	11965-092
RPMI Medium 1640 (RPMI)	Culture medium of BAECs	Invitrogen	22400-089
EGM complete medium	Culture medium of rat mesenteric artery endothelial cells	Lonza	CC-3024A
F-12/Ham medium	Culture medium of CHO cells	Invitrogen	11765-054
L-15 medium	Culture medium of primary nodose ganglion neurons	Invitrogen	11415-064
Fetal bovine serum (FBS)	Supplement to culture medium	Invitrogen	10270-106

2.1.3 Solutions for immuno-blotting

Lysis buffer (pH 7.3)

<u>Reagents</u>	<u>Concentration</u>
Tris-HCl (pH 7.3)	20 mM
NaCl	150 mM
Triton X-100	0.5% (v/v)
EGTA	1 mM
Complete protease inhibitor cocktail tablets	1 tablet/50 ml

3X SDS-PAGE loading dye

<u>Reagents</u>	<u>Concentration</u>
Tris-HCl (pH 6.8)	150 mM
Bromophenol Blue	0.3% (w/v) □
SDS	6% (w/v) □
Glycerol	30% (v/v)

DTT 300 mM

SDS-PAGE Resolving gel (7.5%)

<u>Reagents</u>	<u>Concentration</u>
H ₂ O	4.8 ml
40 % acrylamide	1.68 ml
1.5 M Tris-HCl (pH 8.8)	2.3 ml
10 % SDS	90 µl
10 % Ammonium persulfate (APS)	90 µl
TEMED	9 µl

SDS-PAGE Stacking gel (4%)

<u>Reagents</u>	<u>Concentration</u>
H ₂ O	2.5 ml
40 % acrylamide	0.4 ml
0.5 M Tris-HCl (pH 6.8)	1 ml
10 % SDS	40 µl
10 % Ammonium persulfate (APS)	40 µl
TEMED	4 µl

SDS-PAGE Running buffer (pH 8.6)

<u>Reagents</u>	<u>Concentration</u>
Tris-base	25 mM
Glycine	192 mM
SDS	0.1% (w/v)

Semi-dry Transfer buffer (pH 9.2)

<u>Reagents</u>	<u>Concentration</u>
Tris-base	48 mM
Glycine	39 mM
SDS	0.05 %
Methanol	20% (v/v)

Membrane washing buffer: Phosphate-buffer saline + Tween-20

(PBS-T, pH 7.4)

<u>Reagents</u>	<u>Concentration</u>
NaCl	140 mM
Na ₂ HPO ₄	10 mM
KCl	3 mM
KH ₂ PO ₄	2 mM
Tween-20	0.1% (v/v)

Blocking buffer (pH 7.4)

5% % non-fat milk in PBS-T

2.1.4 Solutions for agarose gel eletrophoresis

1 X TAE buffer (pH 7.4)

<u>Reagents</u>	<u>Concentration</u>
Tris-HCl	40 mM
Sodium acetate	20 mM

EDTA	1 mM
------	------

6 X DNA sample loading buffer

<u>Reagents</u>	<u>Concentration</u>
Bromophenol blue	0.25% (w/v)
Xylene cyanol FF	0.25% (w/v)
Sucrose	40% (w/v)

2.1.5 Solutions for molecular cloning

Luria-Bertani Media (LB Media)

<u>Reagents</u>	<u>Concentration</u>
Tryptone	10 g/L
Yeast extract	5 g/L
NaCl	5 g/L

LB agar (1.5%)

15 g agar in 1 L LB media.

2.1.6 Solutions used in $[Ca^{2+}]_i$ measurement

Normal physiological saline solution (NPSS, pH 7.4 with NaOH)

<u>Reagents</u>	<u>Concentration</u>
NaCl	140 mM

KCl	5 mM
MgCl ₂	2 mM
CaCl ₂	1 mM
HEPES	10 mM
Glucose	10 mM

Ca²⁺-free physiological saline solution (OPSS, pH 7.4 with NaOH)

<u>Reagents</u>	<u>Concentration</u>
NaCl	140 mM
KCl	5 mM
MgCl ₂	2 mM
HEPES	5 mM
Glucose	10 mM

HEPES-buffered saline solution (HBS, pH 7.4 with NaOH)

<u>Reagents</u>	<u>Concentration</u>
NaCl	107 mM
KCl	6 mM
MgSO ₄	1.2 mM
CaCl ₂	2 mM
HEPES	20 mM
Glucose	11.5 mM

Calcium-free HEPES-buffered saline solution (HBS-EGTA, pH 7.4 with NaOH)

<u>Reagents</u>	<u>Concentration</u>
-----------------	----------------------

NaCl	107 mM
KCl	6 mM
MgSO ₄	1.2 mM
EGTA	0.5 mM
HEPES	20 mM
Glucose	11.5 mM

Isotonic bath solution (300 mOsm, pH7.4 with NaOH)

<u>Reagents</u>	<u>Concentration</u>
NaCl	65 mM
KCl	5 mM
MgCl ₂	1 mM
CaCl ₂	1 mM
HEPES	10 mM
Mannitol	~140 mM

Hypotonic bath solution (210 mOsm, pH7.4 with NaOH)

<u>Reagents</u>	<u>Concentration</u>
NaCl	65 mM
KCl	5 mM
MgCl ₂	1 mM
CaCl ₂	1 mM
HEPES	10 mM

Bath solutions at 240 mOsm, 255 mOsm, 270 mOsm and 360 mOsm were formulated based on hypotonic bath solution (210 mOsm) and the respective osmolarity calibrated by addition of mannitol.

2.1.7 Solutions used in isometric tension measurement

Krebs-Henseleit solution (pH 7.4, bubbled with 95 % O₂ + 5 % CO₂)

<u>Reagents</u>	<u>Concentration</u>
NaCl	118 mM
KCl	4.7 mM
CaCl ₂	2.5 mM
KH ₂ PO ₄	1.2 mM
MgSO ₄ (7H ₂ O)	1.2 mM
NaHCO ₃	25.2 mM
Glucose	11.1 mM

2.1.8 Solutions used in electrophysiology

Patch clamp bath solution for recording genistein-stimulated whole-cell current: NPSS as described above

Patch clamp bath solution for recording genistein-stimulated inside-out single-channel current: (pH 7.2 with NaOH)

<u>Reagents</u>	<u>Concentration</u>
CsCl	135 mM
MgCl ₂	2 mM
EGTA	1 mM
HEPES	20 mM

Patch clamp bath solution for recording stretch-sensitive single channel current at cell-attached configuration:

NPSS as described above

Patch clamp pipette solution for recording genistein-stimulated whole-cell current (pH 7.2 with CsOH)

<u>Reagents</u>	<u>Concentration</u>
CsCl	145 mM
MgCl ₂	2 mM
ATP	0.2 mM
HEPES	10 mM
Glucose	10 mM

Patch clamp pipette solution for recording genistein-stimulated inside-out single-channel current:

NPSS as described above

Patch clamp pipette solution for recording stretch-sensitive single channel current at cell-attached configuration: (pH7.4 with CsOH)

<u>Reagents</u>	<u>Concentration</u>
Cs-aspartate	140 mM
CsCl	5 mM
MgCl ₂	1 mM
CaCl ₂	1 mM
HEPES	10 mM

2.1.9 Antibodies

Table 3.3 List of primary antibodies.

<i>Antibodies</i>	<i>Host</i>	<i>Company</i>	<i>Catalog No.</i>
Anti-TRPC5	Rabbit	Alomone Labs	ACC-020
T5E3	Rabbit	Home-made	—
Anti-PGP 9.5	Rabbit	Abcam	ab11145-50
Anti- β -tubulin	Rabbit	Santa Cruz Biotechnology Inc.	sc-9104

2.1.10 Animals

Male Sprague-Dawley rats and C57BL mice were supplied from Laboratory Animal Services Center of the Chinese University of Hong Kong.

2.1.11 $[Ca^{2+}]_i$ indicators

Table 3.4 Fluorescent dyes for tracing $[Ca^{2+}]_i$

<i>Dye</i>	<i>Excitation/Emission (nm)</i>	<i>Loading Concentration</i>	<i>Company</i>	<i>Catalog No.</i>
Fluo-3/AM	488/515	5 μ M	Invitrogen	F-23915
Fura-2/AM	340/380/510	5 μ M	Invitrogen	F-14185

2.2 General Methods

2.2.1 Cell culture

2.2.1.1 Human embryonic kidney 293 cells

Human embryonic kidney (HEK) 293 cells were obtained from the American Type Culture Collection (ATCC). Cells were cultured in DMEM supplemented with 10% FBS and 100 IU/ml penicillin G and 0.1 mg/ml streptomycin. Cells were grown at 37°C, in 95 % air and 5 % CO₂ in a humidified incubator.

2.2.1.2 Chinese hamster ovary cells

Chinese hamster ovary (CHO) cells were a gift from Dr. H. Wise, CUHK. Cells were cultured in F-12/Ham medium supplemented with 10% FBS and 100 IU/ml penicillin G and 0.1 mg/ml streptomycin. Cells were grown at 37°C, in 95 % air and 5 % CO₂ in a humidified incubator.

2.2.1.3 Bovine aortic endothelial cells

The primary cultured bovine aortic endothelial cells (BAECs) were isolated from bovine aorta obtained from the local abattoir. Aortic segments were cut open longitudinally. The intima layer was peeled off and then digested with 0.1% collagenase in phosphate-buffered saline (PBS) (in mM: 140 NaCl, 3 KCl, 25 Tris, pH 7.4) for 15 min at 37°C under vigorous shaking. Dissociated cells were centrifuged, re-suspended and then grown in a culture medium RPMI-1640 supplemented with 10% FBS. Cells were cultured at 37°C, in a humidified incubator with 95 % air and 5 % CO₂.

2.2.1.4 Rat mesenteric artery endothelial cells

Rat mesenteric artery endothelial cells (RMECs) were isolated from the mesentery of male Sprague-Dawley rats. The rat was anesthetized with pentobarbital. The abdomen was opened and the heart was perfused with ~150 ml of PBS to remove blood cells from the mesenteric vessels. The intestine was removed from the abdominal cavity and the mesentery was isolated. The mesentery was digested with 0.02% collagenase in phenol red-free EBM basal medium (Lonza) for 45 minutes at 37°C. The resulting suspension was placed in a centrifuge tube containing EGM complete medium and centrifuged. The cell pellet was resuspended and cultured in EGM complete medium (Lonza) containing 1% penicillin-streptomycin.

2.2.1.5 Nodose ganglion neurons

Primary nodose ganglion neurons were obtained from male Sprague-Dawley rat. Rat was anesthetized and the left nodose ganglion was dissected out quickly. The peripheral tissues were severed and the ganglion was minced in L-15 medium at 4 °C. They were then transferred to an enzyme solution containing 0.1 mg/ml DNase I, 1 mg/ml trypsin, and 1 mg/ml collagenase IA. After 1 hour, the enzyme digestion was terminated by adding 2 mg/ml trypsin inhibitor, 3 mM CaCl₂ and 1.5 mg/ml bovine serum albumin. The single neurons were dispersed by gentle trituration, centrifugation and resuspension. The neurons were then washed twice and resuspended in a modified L-15 media supplemented with 10% fetal bovine serum, 5 % antibiotic-antimycotic, and 8 ng/ml 7S NGF and then plated onto poly-L-lysine-coated glass coverslips. 10 μM cytosine arabinofuranoside (Ara-C) was included in the culture medium for the first 4 days to inhibit

growth of dividing cells.

2.2.2 Transfection

4 μg of DNA plasmid were transfected into cultured cells using 6 μl of Lipofectamine 2000 in 1000 μl Opti-MEM reduced serum medium (Invitrogen) in 6-well plates, which contained $\sim 6 \times 10^4$ cells per well. After 6-hour incubation, the transfection medium was replaced by fresh complete culture medium. Cells were trypsinized 24 hours post-transfection and seeded for functional studies or further culture. Stable cell line was obtained by addition of appropriate antibiotics into the culture medium for selection.

2.2.3 Molecular biology

2.2.3.1 Molecular cloning

Preparation of DH5 α competent cells

Modified RbCl method was used to prepare DH5 α competent cells. Briefly, a single colony on a LB agar plate was picked and placed into a 10 ml tube which contained 5 ml LB broth and then the tube was vigorously shaken (~ 250 rpm) at 37 $^{\circ}\text{C}$ until optical density at 260nm (OD_{260}) reached 0.3-0.4 (~ 3 hours). 2.5 ml of the 5 ml culture was inoculated into 50 ml LB medium with shaking (~ 250 rpm) at 37 $^{\circ}\text{C}$ to grow the cells until the OD_{260} reached 0.4-0.5 (~ 2 hours). After then, the cells were chilled on ice for 5 minutes and collected by centrifuging at 5000 rpm for 10 minutes at 4 $^{\circ}\text{C}$. The cell pellet was gently resuspended in 40 ml ice-cold Buffer 1 and was incubated on ice for 5 minutes. The cells were collected by centrifuging again and gently resuspended in 2 ml Buffer 2. The suspension was placed on ice for 5 minutes. Then the cell

suspension was aliquot (100 μ l/1.5 ml tube) and quick-frozen by liquid nitrogen. The tubes containing DH5 α competent cells were stored at -70 $^{\circ}$ C.

Buffer 1 contained (mM):

30 mM KAc, 100 mM RbCl₂, 10 mM CaCl₂, 50 mM MnCl₂, 15% glycerol, Adjust pH to 5.8 with HAc.

Buffer 2 contained (mM):

10 mM MOPS, 75 mM CaCl₂, 10 mM RbCl₂, 15% glycerol, Adjust pH to 6.5 by KOH.

Subcloning of cDNA

Polymerase Chain Reaction (PCR)

cDNA cloning was carried out by PCR reaction using a pair of designed primers. The primers flanked out a desired region on the cDNA-containing plasmid DNA template to allowed PCR for amplification.

Components of PCR reaction (1 x)

dH ₂ O	41 μ l
10x buffer	5 μ l
dNTP (10mM)	1 μ l
forward primer (0.1 nM)	1 μ l
reverse primer (0.1 nM)	1 μ l
<i>Taq</i> polymerase (1 U/ μ l)	0.5 μ l
Template	0.5 μ l

Total volume 50 μ l

Agarose Gel Electrophoresis of DNA

The agarose gels were prepared with 1.0-2.0% (w/v) agarose dissolved in 50 ml 1x TAE buffer with 0.5 μ g/ml ethidium bromide. 6x DNA sample loading buffer was added to the DNA sample in 1 to 5 ratio to make up the final volume. Electrophoresis was performed at constant voltage of 120 V in the gel tank containing 1X TAE buffer. When electrophoresis was finished, DNA was visualized and the image captured using a transilluminator (302nm) by FluorChem 8000 system.

Restriction Enzyme Digestion

Compatible ends of the DNA fragments were generated by enzyme digestion with appropriate restriction enzymes (New England Biolab) in the experiment. The volume of the restriction enzyme digestion was about 20-60 μ l in the appropriate buffers provided by the suppliers. The reaction mixture was incubated at 37°C for three hours for digestion. The products of digestion were separated by agarose gel electrophoresis.

Components of Restriction Enzyme Digestion

	<u>PCR product</u>	<u>Plasmid vector</u>
10 x digestion buffer	3 μ l	2 μ l
DNA (1 μ g/ μ l)	5 μ l	1 μ l
Enzyme 1	1.5 μ l	1 μ l
Enzyme 2	1.5 μ l	1 μ l

H ₂ O	Added to total 30 μ l	Added to total 20 μ l
------------------	---------------------------	---------------------------

Ligation of DNA fragment

Ligation was carried out to ligate two DNA fragments (insert & vector) together by T4 DNA ligase (New England Biolab) at 14°C overnight in the ligation buffer provided by the suppliers.

Components of DNA Ligation (1 x)

10 x ligation buffer	2 μ l
Digested DNA insert (100 ng/ μ l)	1.5 μ l
Digested vector DNA (100 ng/ μ l)	0.5 μ l
T4 DNA ligase	1 μ l
Total volume	20 μ l

Transformation of ligation product to *E. coli* competent cell

An aliquot (100 μ l) of *E. coli* DH5 α was thawed on ice. 5 μ l of the whole ligation product was added into the cells. The cells were allowed to stand on ice for 30 minutes. Then the cells were heat-shocked at 42°C for 1.5 minutes without disturbance. The cells were again cold-shocked on ice for 10 minutes. 400 μ l of LB was added to the cells, and the cells were shaken at 37°C at 280rpm for 45 minutes. The transformants were centrifuged at 6400 rpm for 2 minutes and then 400 μ l of the supernatant was discarded. The cell pellet was resuspended gently in the remaining 100 μ l medium and spread on an LB-Agar plate supplemented with appropriate antibiotics. Then the plate was incubated at 37°C for 16

hours.

Amplification and confirmation of the clones

Single colonies from the DH5 α transformed with ligation product were picked and inoculated into medium for growth. Cell pellet was harvested after overnight culture. Plasmid DNA was extracted by Mini Prep Kit (QIAprep Spin Miniprep Kit, QIAGEN GmbH, Germany).

The purified recombinant plasmid DNA was first verified by restriction enzyme digestion and gel electrophoresis. Plasmid clones that release appropriate masses of DNA fragment were further verified by automated sequencing. DNA sequencing was performed by Tech Dragon Limited, Hong Kong.

Table 3.5 Information of recombinant DNA vectors

<i>Recombinant construct</i>	<i>Insert</i>	<i>Origin of insert</i>	<i>Vector</i>	<i>Restriction sites</i>
pcDNA6-IRES-GFP	IRES-GFP	PCR amplified from pCAGGS/IRES-GFP vector, given by B. Nilius	pcDNA6A	<i>XhoI / XbaI</i>
TRPC5-IRES-GFP	TRPC5	PCR amplified from mouse TRPC5 in pcDNA3, given by L. Birnbaumer	pcDNA6-IRES-GFP	<i>EcoRI/XhoI</i>
Δ C-TRPC5	Δ C-TRPC5	PCR amplified from mouse TRPC5 in pcDNA3, flanking 1 st to 2901 st nucleotides of TRPC5 cDNA	pcDNA6	<i>KpnI / ApaI</i>
pSL6-DN-T5 (lentiviral vector)	DN-TRPC5	PCR amplified from dominant-negative TRPC5 construct in vector, given by D. Clapham	pSL6	<i>EcoRI/XhoI</i>

2.2.3.2 Western immuno-blotting

The cultured cells were trypsinized and washed three times with ice-cold PBS. The cell pellet was collected by 1,600 rpm centrifugation, followed by gentle shaking in 500 μ l ice-cold freshly prepared lysis buffer for 15 min. The lysate was centrifuged at 12,000 rpm for 30 min at 4 °C. The supernatant were collected and the protein concentration was determined by Bradford assay.

Bradford assay: BSA (0.325 mg/ml) with final concentration ranging from 0-39 μ g/ml was used as protein standards. The cell lysate was diluted in H₂O at 1:3 ratios. 40 μ l Bradford assay buffer, 2 μ l diluted lysate and 158 μ l H₂O were mixed in a well of 98-well plate. Protein samples were assayed in triplicate. Absorbance at 595 nm was read by a Microplate UV/VIS Spectrophotometer. The concentration of protein was calculated with reference to the standard protein curve.

Protein samples were calibrated to equal amounts, boiled with SDS-PAGE loading dye and loaded at ~80 μ g into each lane of polyacrylamide gel and separated by a 7.5% SDS-PAGE gel. Proteins were transferred to a PVDF membrane, and the membrane was then immersed in a blocking solution containing 5% non-fat milk and 0.1% Tween-20 in PBS for 1 hour at room temperature with constant shaking. Proteins were blotted with the primary antibodies. Immunodetection was accomplished with secondary antibody conjugated with horseradish

peroxidase, followed by reaction with ECL western blotting detection system (Amersham) and fluorescent exposure to X-ray film. Beta-tubulin was used as reference to confirm that an equal amount of proteins was loaded onto each lane. The intensity of the protein blotting bands was captured and analyzed by FluorChem 8000 system.

2.2.4 Functional studies

2.2.4.1 Cytosolic Ca^{2+} ($[\text{Ca}^{2+}]_i$) measurement

2.2.4.1.1 Fluorescent dye loading

The cells were seeded on coverslips and cultured according to above protocol. 5 μM Fluo-3/AM or Fura-2/AM dye and 0.02% pluronic F-127 were added to the culture medium for 1 hour inside the culture incubator. Coverslip of cells was then taken out and washed in NPSS, followed by mounting onto a recording chamber which contain 400 μl bath solution.

2.2.4.1.2 $[\text{Ca}^{2+}]_i$ measurement by confocal microscopy

The coverslip of cells was mounted onto the recording chamber and placed on the stage of an inverted microscope (Olympus IX81). The $[\text{Ca}^{2+}]_i$ fluorescence was recorded using the FV1000 laser scanning confocal imaging system (Olympus) at room temperature ($\sim 23^\circ\text{C}$). The excitation wavelength was at 488 nm and the fluorescence signals were collected using a 515 nm long pass emission filter. The data was analyzed by FV-10 ASW 1.5 software (Olympus). The changes in $[\text{Ca}^{2+}]_i$ were indicated by the changes of the ratio of real time fluorescence (F_t) relative to the fluorescence at the beginning of the recording (F_0) (F_t/F_0). Chemicals were added to the chamber by diluting in 1/10 of the bath

solution prior to addition. In case of changing bath solution was needed, 3/5 volume of the original bath solution was discarded and replaced by 3/5 volume of the new bath solution for at least four times.

2.2.4.1.3 $[Ca^{2+}]_i$ measurement by Ca^{2+} -imaging

Coverslip of cells was mounted onto a recording chamber and placed on the stage of an inverted microscope (Motic AE31), For ratiometric $[Ca^{2+}]_i$ measurement with Fura-2, fluorescence was recorded at 340 and 380 nm excitation and 510 nm emission wavelengths. For single-wavelength $[Ca^{2+}]_i$ measurement with Fluo-3, fluorescence was recorded at 490 nm excitation and 510 nm emission wavelengths. The real-time fluorescent images were captured and analyzed by InCytIm Basic live cell imaging system (Intracellular Imaging Inc. USA) at room temperature ($\sim 23^\circ C$). For fura-2 fluorescent dye, $[Ca^{2+}]_i$ was indicated by the real-time fluorescence ratio at 340 and 380 nm excitation (F_{340}/F_{380}). Change in $[Ca^{2+}]_i$ ($\Delta F_{340}/F_{380}$) was given by the difference between initial F_{340}/F_{380} ratio and the F_{340}/F_{380} ratio at a specific time. For fluo-3 fluorescent dye, changes in $[Ca^{2+}]_i$ were indicated by the changes of the ratio of real time fluorescence (F_t) relative to the fluorescence at the beginning of the recording (F_0) (F_t/F_0).

2.2.4.2 Isometric tension measurement of isolated vessels

The male C57BL mice (~ 5 week-old) were killed by cervical dislocation. Thoracic aorta was rapidly cut out and placed into an ice-cold Krebs Henseleit solution bubbled with a gas mixture of 95% O_2 and 5% CO_2 . Under dissection microscope, the fat and peripheral tissues were severed. The aorta

was cut into 2-mm segments and then the vessel rings were mounted onto two thin stainless steel holders (model 610M, DMT, Denmark) in 5 ml organ baths containing Krebs Henseleit solution bubbled with a gas mixture of 95% O₂ and 5% CO₂ at 37°C. One holder was connected to a force displacement transducer and the other one to a movable device that allowed the application of a 3 mN passive tension, which was determined to be the optimal resting tension for obtaining the maximal active tension induced by 60 mM K⁺ solution (in mM: 58 NaCl, 64.7 KCl, 2.5 CaCl₂, 1.2 KH₂PO₄, 1.2 MgSO₄·7H₂O, 25.2 NaHCO₃, and 11.1 glucose, bubbled with 95% O₂ + 5% CO₂). The endothelium was removed by rubbing against a thin stainless steel wire. The absence of endothelial function was verified by a loss in relaxation to 1 μM acetylcholine in vessels precontracted by 10 μM phenylephrine. After an equilibration period in the passive tension for about 30 minutes, the contractile function of the aortic rings were first tested twice by 60 mM K⁺ solution. Following a washout period, the aortic rings were precontracted with 10 μM phenylephrine to achieve sustained contraction and relaxed with cumulative addition of chemicals into the bath solution. Data were acquired and analyzed using PowerLab and LabChart (AD Instruments).

2.2.4.3 Electrophysiology

In patch clamp experiments, cell-attached, whole-cell or inside-out patch clamp recording was achieved by an EPC 9 patch clamp amplifier (HEKA Elektronik, Lambrecht-Pfalz, Germany) in voltage-clamp mode, controlled by Pulse+PulseFit 8.7 software (HEKA). Patch pipettes (resistance: 3-5MΩ for whole-cell, 6-10MΩ for single-channel) were filled with pipette solution. Pipette and membrane capacitance were automatically compensated. The

formulations of bath and pipette solutions are listed before. Whole-cell currents were recorded in response to successive voltage pulses of 500 ms duration, increasing in 20 mV increments from -80 to $+80$ mV. All currents were sampled at 50 kHz and filtered at 3 kHz (single-channel) or 5 kHz (whole-cell). Data were analyzed with PulseFit software (HEKA). For whole-cell recording, the currents were normalized by cell capacitance to current densities (pA/pF). All experiments were performed at room temperature (~ 23 °C).

2.2.5 Preparation of a TRPC5-blocking antibody T5E3

T5E3 was raised in rabbits using the strategy developed by Xu *et al.* (Xu *et al.*, 2005b). Briefly, a peptide corresponding to TRPC5 putative pore region (CYETRAIDEPNNCKG) conjugated to keyhole limpet hemocyanin (KLH) (Alpha Diagnostics) was subcutaneously injected to the back of a rabbit followed by two boost doses. T5E3 antiserum was collected 4 weeks after the second boost. T5E3 IgG was purified from T5E3 antiserum using a protein G column. Pre-immune serum IgG purified from the rabbit before immunization was used as control, and was termed as “pre-immune”.

2.2.6 Statistical analysis

Data were expressed as mean \pm SEM. The “n” numbers in Ca^{2+} measurement represent number of independent recordings. The “n” numbers in isometric tension measurement represent individual artery segments. In electrophysiology, “n” represents number of individual recordings. Statistical comparisons of two groups of data were made using Student’s t-test. Differences were considered significant when $p < 0.05$.

2.3 Specific Methods for each Chapter

2.3.1 Methods for Chapter 3

2.3.1.1 Cell culture and cDNA expression

Mouse TRPC5 clone, a generous gift from L Birnbaumer (NIH) was subcloned into pcDNA3 and stably transfected into HEK293 cells. Transfection and cell culture were done as described in Chapter 2 Section 2.2.1-2.2.2). A stable cell line was established using 1 mg/ml G-418 (Invitrogen) added to the culture medium DMEM (Invitrogen). Expression of TRPC5 was validated by western blotting. The primary cultured bovine aortic endothelial cells (BAECs) were isolated from bovine aorta obtained from the local abattoir and using methodology described previously (Cheng *et al.*, 2008). Briefly, aortic segments were cut open longitudinally. The intima layer was peeled off and then digested with 0.1% collagenase in phosphate-buffered saline (PBS) (in mM: 140 NaCl, 3 KCl, 25 Tris, pH 7.4) for 15 min at 37°C under vigorous shaking. Dissociated cells were centrifuged, re-suspended and then grown in a culture medium RPMI-1640 supplemented with 10% FBS. All cells were cultured in 95 % air and 5 % CO₂.

2.3.1.2 Isometric tension measurement

Segments of mouse aorta ~2 mm in length were dissected from ~5 week-old male C57BL/6 mice and the endothelial layer was rubbed off. The segments were mounted in a wire myograph (610M, Danish Myograph Technology) under a normalized tension as previously described (1). The aortic segments were precontracted with 10 µM phenylephrine to achieve sustained contractions. NO donors were then added in a cumulative fashion

to the bath solution, which was Krebs solution containing, in mM: 118 NaCl, 4.7 KCl, 2.5 CaCl₂, 1.2 MgSO₄, 1.2 KH₂PO₄, 25.2 NaHCO₃, 11.1 glucose, gassed with 95% O₂–5% CO₂. Experiments were performed at 37°C. Data were acquired and analyzed using PowerLab and LabChart (AD Instruments).

2.3.1.3 Immunoblots

The procedures were as described in Chapter 2 Section 2.2.3.2. The membrane-blot was incubated at 4°C overnight with anti-TRPC5 antibody (dilution 1:200; Alomone Lab) in PBS buffer containing 0.1% Tween 20 and 5% nonfat dry milk. Immunodetection was accomplished with horseradish-conjugated secondary antibodies, followed by ECL detection system. Immunoblots with anti-β-tubulin antibody (Santa Cruz Biotechnology) were used to confirm that an equal amount of proteins was loaded onto each lane. The intensity of the bands was analyzed by Fluorchem 8000 imaging system.

2.3.1.4 Ca²⁺-imaging experiment

[Ca²⁺]_i was measured as described in Chapter 2 Section 2.2.4.1 with slight modification. Cells seeded on coverslips were loaded with 5 μM fura-2/AM in culture medium for 30 min and then mounting in a recording chamber containing bath solution. Chemicals were added to the chamber by diluting in 1/10 of the bath solution prior to addition. Normal physiological saline solution (NPSS) contained, in mM: 140 NaCl, 5 KCl, 2 MgCl₂, 1 CaCl₂, 10 glucose, 10 HEPES (pH titrated to 7.4 with NaOH). HEPES-buffered saline (HBS) was formulated as described elsewhere

(Yoshida *et al.*, 2006), and contained in mM: 107 NaCl, 6 KCl, 1.2 MgSO₄, 2 CaCl₂, 11.5 glucose, 20 HEPES (pH titrated to 7.4 with NaOH). HBS-EGTA contained in mM: 107 NaCl, 6 KCl, 1.2 MgSO₄, 0.5 EGTA, 11.5 glucose, 20 HEPES (pH titrated to 7.4 with NaOH). Fura-2 was excited by light at 340 and 380 nm and emission was filtered at 510 nm. Fluorescent signals were captured and analyzed by InCyt Basic Im2 live cell system (Intracellular Imaging). The change in intracellular calcium is indicated as the ratio of fura-2 fluorescence emission intensities for 340 nm and 380 nm excitation.

2.3.1.5 Anti-TRPC5 blocking antibody

The methods were described in Chapter 2 Section 2.2.5.

2.3.1.6 Chemicals and reagents

Carbachol (Calbiochem) and LaCl₃ (Sigma) were prepared as 100 mM stock solutions in H₂O. 2-Aminoethoxydiphenyl borate (2-APB) (Calbiochem) was prepared as 100 mM stock solutions in dimethyl sulfoxide (DMSO). S-nitroso-N-acetylpenicillamine (SNAP) (Sigma) was prepared as a 300 mM stock dissolved in DMSO. Diethylamine NONOate (DEA-NONOate) (Cayman) was prepared as a 100 mM stock dissolved in ethanol purged with helium.

2.3.1.7 Data analysis and presentation

Data from Ca²⁺-imaging were plotted as traces and expressed as mean ± SEM of cells in one experiment. Bar charts show data in mean ± SEM of individual experiments. Number of individual recordings “n” is given in

parenthesis. Student's t-test was used for statistical comparison, with probability $p < 0.05$ (*) as a significant difference.

2.3.2 Methods for Chapter 4

2.3.2.1 Cell culture and stable transfection

Mouse TRPC5 clone was a generous gift from Dr. L Birnbaumer, NIH. The full length cDNA was subcloned into pcDNA3 and transfected into HEK293 cells (ATCC). Transfection was done as described in Chapter 2 Section 2.2.2. 1 mg/ml G-418 (Invitrogen) was added during culture to establish a stable TRPC5-expressing cell line. The primary cultured bovine aortic endothelial cells (BAECs) were isolated from bovine aorta as described previously in Chapter 3 Section 2.2.1.3. Cells were grown in culture medium RPMI-1640 (Invitrogen) supplemented with 10% FBS. Ca^{2+} -imaging experiments with BAECs were carried out two days after seeding the cells on glass coverslips. Rat mesenteric artery endothelial cells (RMECs) were isolated from the mesentery of male Sprague-Dawley rats (weight between 260-280 grams). The rat was anesthetized with pentobarbital sodium (100mg/kg). The abdomen was opened and the heart was perfused with ~150 ml of PBS to remove blood cells from the mesenteric vessels. The intestine was removed from the abdominal cavity and the mesentery was isolated. The mesentery was digested with 0.02% collagenase in phenol red-free EBM basal medium (Lonza) for 45 minutes at 37°C. The resulting suspension was placed in a centrifuge tube containing EGM complete medium and centrifuged. The cell pellet was resuspended with EGM complete medium (Lonza) containing 1% penicillin-streptomycin and seeded onto 0.5% gelatin-coated glass

coverslips. The cells were allowed to adhere to the coverslips for one hour while the nonadherent cells were removed. Ca^{2+} -imaging experiments with RMECs were carried out two days later.

2.3.2.2 Immunoblots

The procedures were as described in Chapter 2 Section 2.2.3.2. The membrane-blot was incubated at 4°C overnight with anti-TRPC5 antibody (dilution 1:200; Alomone Lab) in PBS buffer containing 0.1% Tween 20 and 5% nonfat dry milk. Immunodetection was accomplished with horseradish-conjugated secondary antibodies, followed by ECL detection system. Immunoblots with anti- β -tubulin antibody (Santa Cruz Biotechnology) were used to confirm that an equal amount of proteins was loaded onto each lane.

2.3.2.3 Immuno-detection of TRPC5 on BAECs and RMECs

BAECs and RMECs were fixed with 3.7% formaldehyde in phosphate-buffered saline (PBS; Invitrogen) and permeabilized with 0.1% Triton X-100. For immuno-detection with T5E3 antibody, cells were not permeabilized. Nonspecific immunostaining was blocked by preincubating the cells with 5% BSA. The fixed cells were incubated with or without primary antibody anti-TRPC5 (dilution 1:100, Alomone Lab) or T5E3 (dilution 1:50) at 4°C overnight, followed by incubation with secondary anti-rabbit IgG conjugated to Alexa Fluor 546 or Alexa Fluor 488 (1:200, Molecular Probe). Immunofluorescence was detected by FV1000 confocal system (Olympus). Fluorescence signals were acquired at the settings under which the signals from the control cells (without primary antibody)

were absent.

2.3.2.4 Preparation of a TRPC5-blocking antibody T5E3

The methods were described in Chapter 2 Section 2.2.5.

2.3.2.5 $[Ca^{2+}]_i$ measurement

$[Ca^{2+}]_i$ was measured as described in Chapter 2 Section 2.2.4.1 with slight modification. Briefly, cells were seeded onto poly-L-lysine-coated glass discs one day before intracellular Ca^{2+} measurement. The cells were loaded for 1 h in dark with 5 μ M Fluo-3/AM and 0.02% pluronic F-127 in culture media, before mounting onto a microscope chamber containing bath solution. Normal physiological saline solution (NPSS) contained in mM: 140 NaCl, 5 KCl, 2 MgCl₂, 1 CaCl₂, 10 Glucose, 10 HEPES, pH 7.4. Calcium-free saline solution (0Ca²⁺-PSS) contained in mM: 140 NaCl, 5 KCl, 2 MgCl₂, 10 glucose, 0.2 EGTA, 10 HEPES, pH 7.4. When needed, cells were pretreated with genistein or LaCl₃ for 10 min. In experiments with BAECs, cells were loaded with Fura-2/AM for ratiometric Ca^{2+} -fluorescent measurement. HEPES-buffered saline solution (HBS) was used in experiments with BAECs and RMECs. HBS contained in mM: 107 NaCl, 6 KCl, 1.2 MgSO₄, 2 CaCl₂, 11.5 Glucose, 20 HEPES, pH 7.4. Ca^{2+} -free (0[Ca²⁺]_o) HBS was equivalent to HBS except that there was no CaCl₂. Fluorescence $[Ca^{2+}]_i$ signals was recorded by InCyt Basic Fluorescence Imaging System (Intracellular Imaging, Cincinnati, OH). Changes in $[Ca^{2+}]_i$ were displayed as a ratio of real-time fluorescence relative to the intensity at the beginning of the experiment (F_t/F_0) or ratio of the fluorescence signal from excitation at 340nm to that at 380nm

(F_{340}/F_{380}). Two-tailed Student's t-test was used for statistical evaluation, with 0.05 as the level of significance. All experiments were performed at room temperature (~ 23 °C).

2.3.2.6 Electrophysiology

TRPC5 channel activity was measured in whole-cell or excised inside-out patch mode as described elsewhere (Shen *et al.*, 2008). Briefly, whole-cell or single channel activity was recorded using an EPC9 patch clamp amplifier (HEKA) controlled by Pulse software (HEKA). Whole-cell currents were recorded in response to successive voltage pulses of 500 ms duration, increasing in 20 mV increments from -80 to +80 mV. The recordings were made immediately before and 5 min after bath application of genistein or vehicle (0.1% DMSO). For whole-cell recording, the patch pipette contained in mM: 145 CsCl, 2 MgCl₂, 10 Glucose, 0.2 ATP, 10 HEPES, pH 7.2 titrated with CsOH, and the bath was NPSS. For the excised inside-out patches, the pipette solution was NPSS, and the bath solution contained in mM: 135 CsCl, 2 MgCl₂, 1 EGTA, 20 HEPES, pH 7.2 titrated with CsOH. The recordings were made both before and after bath application of genistein. All currents were sampled at 50 kHz and filtered at 3 kHz, and the data were analyzed with PulseFit and TAC. Student's t-test was used for statistical evaluation, with 0.05 as the level of significance. Electrophysiological experiments were performed at room temperature (~ 23 °C).

2.3.2.7 Chemicals

Genistein, PP2, lavendustin A, carbachol and 2-Aminoethoxydiphenyl

borate (2-APB) were from Calbiochem. Daidzein, herbimycin, LaCl_3 , U73122, U73343 and dimethyl sulfoxide (DMSO) were from Sigma. ICI-182780 was from Tocris.

2.3.2.8 Data analysis and presentation

Data from Ca^{2+} -imaging were plotted as traces and expressed as mean \pm SEM of cells in one experiment. Bar charts show data in mean \pm SEM of individual experiments. Current-voltage curves in electrophysiology were mean \pm SEM of individual experiments. Number of individual recordings “n” is given in parenthesis. Student’s t-test was used for statistical comparison, with probability $p < 0.05$ (*) as a significant difference.

2.3.3 Methods for Chapter 5

2.3.3.1 Molecular cloning, cDNA transfection and expression, and stable cell lines

Mouse TRPC5 clone and mouse TRPC6 clone were a generous gift from Dr. L Birnbaumer, NIH. The full length cDNAs of TRPC5 and TRPC6 were in pcDNA3 vector and transfected into HEK293 (HEK) cells (ATCC). Transfection was done as described in Chapter 2 Section 2.2.2. 1 mg/ml G-418 (Invitrogen) was added during culture to establish stable TRPC5- or TRPC6- expressing cell line. To construct ΔC -TRPC5, which lacks the last 27-nucleotide sequence at 3'-end of the open reading frame, a pair of primers was used to PCR-amplify the fragment flanking 1st to 2901st nucleotide of TRPC5 cDNA. The fragment was subcloned into pcDNA6 vector. ΔC -TRPC5 in vector was transfected into HEK cells. Transfected cells were cultured under selection with 3 $\mu\text{g}/\text{ml}$ blasticidin (Invitrogen).

To construct a bicistronic expression vector that allows separate expression of TRPC5 and green fluorescent protein (GFP) on a single mRNA, TRPC5 was subcloned by PCR into pCDNA6-IRES-GFP vector as described in Chapter 2 Section 2.2.3.1, resulting the TRPC5-IRES-GFP construct. This construct was transfected into CHO cells (a gift from Dr. H. Wise, CUHK) as described in Chapter 2 Section 2.2.2. 6 µg/ml blasticidin was added to the culture medium F-12/Ham (Invitrogen). GFP-positive cells were selected under fluorescence microscope for stable culture. Dominant-negative TRPC5 (DN-T5) was constructed by alanine replacement of a conserved LFW motif (amino acids 575–577) within the TRPC5 pore region as described by Struebing *et al.*, and is a generous gift from Dr D. Clapham, Harvard Medical School (Strubing *et al.*, 2003). This DN-T5 construct was transfected into isolated nodose ganglion cells by electroporation. 5 µg of DN-T5 plasmid DNA or pCDNA6 plasmid DNA was electroporated into the dissociated cells from two rat nodose ganglia by Amaxa Transfection Device (Amata Inc.). The defaulted protocol G-013 for neuron chicken DRG was used.

2.3.3.2 Labeling the aortic baroreceptor neurons

The animal study was conducted in conformity with the Animal Experimental Ethics Committee of the Chinese University of Hong Kong. All animals used for data collections were male Sprague-Dawley rats obtained from the Laboratory Animal Research Centre of the University, and were kept in cages supplied with adequate water and food in a temperature- and humidity-controlled holding room. The nodose baroreceptor neurons were labeled as described previously (Li *et al.*, 1998).

Briefly, male Sprague-Dawley rat between 260-280 grams was anaesthetized with 100 mg/kg pentobarbital sodium and mechanically ventilated. With right thoractomy, approximately 1~2 μ l DiI (1,1'-dioleoyl-3,3,3',3'-tetramethylindocarbocyanine methanesulfonate, Δ^9 -DiI, Molecular Probes) was injected onto the adventitia of aortic arch. Under sterile condition, the chest was closed following with reestablishing negative intrapleural pressure by suction via a syringe. The rats were allowed to recover and raised for at least 1 week to allow DiI dye to diffuse retroactively along the cell membrane to the soma at nodose ganglion.

2.3.3.3 Isolation and primary culture of nodose ganglion neurons

Nodose ganglion neurons were dissociated and primary cultured as described elsewhere (Li *et al.*, 1998). Briefly, rat was anesthetized and the left nodose ganglion was dissected out quickly. The peripheral tissues were severed and the ganglion was minced in L-15 medium (Invitrogen) at 4 °C. They were then transferred to an enzyme solution containing 0.1 mg/ml DNase I (Sigma), 1 mg/ml trypsin (Calbiochem), and 1 mg/ml collagenase IA (Sigma). After 1 hour, the enzyme digestion was terminated by adding 2 mg/ml trypsin inhibitor (Calbiochem), 3 mM CaCl₂ and 1.5 mg/ml bovine serum albumin (Sigma). The single neurons were dispersed by gentle trituration, centrifugation and resuspension. The neurons were then washed twice and resuspended in a modified L-15 media supplemented with 10% fetal bovine serum, 5 % antibiotic-antimycotic, 8 ng/ml 7S NGF (Invitrogen), and then plated onto poly-L-lysine-coated glass coverslips (De Koninck *et al.*, 1993). 10 μ M cytosine arabinofuranoside (Ara-C) (Sigma) was included in the culture medium for 4 days to inhibit growth of

dividing cells. The cells were cultured for 3-7 days before functional studies. In some experiments, neurons were transiently transfected with DN-T5 or empty vector by electroporation after single cells were separated. The transfected cells were cultured for 72 hours before experiments.

2.3.3.4 Construction of lentiviral vector and viral transduction

A lentiviral vector that carries DN-T5 was generated based on the published pRRL-cPPT-CMV-X-PRE-sin vector (pSL6) (kindly provided by Dr. Y Chen, CUHK) (Barry *et al.*, 2001; Chen *et al.*, 2007). Full length DN-T5 was amplified from the original vector by PCR with a pair of primers containing *EcoRI* and *XhoI* restriction sites. The *EcoRI/XhoI* insert was subcloned into pSL6, following the CMV promoter. DN-T5 containing pseudotyped lentivirus (lenti-DN-T5) or control lentivirus (lenti-control) was produced by cotransfecting HEK293T cells with pSL6±DN-T5 and 3 packaging vectors: pMDLg/pRRE, pRSV-REV, and pCMV-VSVG. To transduce HEK cells, 9×10^6 copies of lentivirus and 8 $\mu\text{g/ml}$ polybrene (Sigma) were incubated with each well of the cells seeded on 48-well plate for ~16 hours. To transduce rat nodose ganglion cells *in vivo*, 1.5×10^7 copies of virus were topically applied to the left nodose ganglion.

2.3.3.5 *In situ* immuno-fluorescent detection of TRPC5 and neuronal marker PGP 9.5

Cultured rat nodose ganglion cells were fixed with 3.7% formaldehyde in phosphate-buffered saline (PBS) (Invitrogen). Nonspecific immunostaining was blocked by preincubating the cells with 5% donkey serum. The fixed cells were incubated with or without primary antibody T5E3 (dilution 1:50)

at 4°C overnight, followed by incubation with secondary anti-rabbit IgG conjugated to Alexa Fluor 488 (1:200, Molecular Probe). For *in situ* detection of TRPC5 in rat baroreceptor neurons, the left nodose ganglion, the left aortic depressor nerve and the aortic arch adventitia were dissected out, trimmed of peripheral tissues, and fixed with 3.7% formaldehyde in PBS. The fixed adventitia was permeabilized by 1% Triton X-100 in PBS for 3 hours. The nodose ganglion and depressor nerve were embedded in media and frozen, followed by cryosectioning. The cryosections were mounted on glass slides and washed with PBS. The cryosections and the isolated aortic arch adventitia were blocked by 5% donkey serum and incubated with or without 1:100 anti-TRPC5 rabbit-antibody (Alomone Lab) and 1:100 anti-PGP 9.5 goat-antibody (Abcam) at 4°C overnight, followed by incubation with secondary anti-rabbit IgG conjugated to Alexa Fluor 488 and anti-goat IgG conjugated to Alexa Fluor 546 (1:200, Molecular Probe). The stained adventitia was gently stretched flat and mounted on glass slide. Immunofluorescence was detected by FV1000 confocal system (Olympus). Fluorescence signals were acquired at the settings under which the signals from the control cells (without primary antibody) were undetectable.

2.3.3.6 Immunoblots detection of TRPC5 in lysates

The procedures were as described in Chapter 2 Section 2.2.3.2. Protein lysate from rat nodose ganglion was prepared by mechanically homogenizing the isolated ganglion in lysis buffer at 4°C. The membrane-blot was incubated at 4°C overnight with anti-TRPC5 antibody (dilution 1:200; Alomone Lab) in PBS buffer containing 0.1% Tween 20

and 5% nonfat dry milk. Immunodetection was accomplished with horseradish-conjugated secondary antibodies, followed by ECL detection system. Immunoblots with anti- β -tubulin antibody (Santa Cruz Biotechnology) were used to confirm that an equal amount of proteins was loaded onto each lane.

2.3.3.7 $[Ca^{2+}]_i$ measurement

$[Ca^{2+}]_i$ was measured as described in Chapter 2 Section 2.2.4.1 with slight modification. Briefly, cells were seeded onto poly-L-lysine-coated glass discs one day before intracellular Ca^{2+} measurement. The cells were loaded for 1 h in dark with 5 μ M Fluo-3/AM and 0.02% pluronic F-127 in culture media, before mounting onto a microscope chamber containing bath solution. Isotonic bath solution (300 mOsm) contained (mM): 65 NaCl, 5 KCl, 1 $CaCl_2$, 1 $MgCl_2$, 10 HEPES (pH7.4); osmolarity calibrated to 300 mOsm with around 140 mM mannitol. Hypotonic bath solution and hypertonic bath solutions contained identical ionic concentrations to isotonic bath solution, and the osmolarity calibrated to different values by varying the concentration of mannitol. In experiments with nodose ganglion cells, the bath solutions contained 2 mM $CaCl_2$. Normal physiological saline solution (NPSS) contained in mM: 140 NaCl, 5 KCl, 2 $MgCl_2$, 1 $CaCl_2$, 10 Glucose, 10 HEPES, pH 7.4. Fluorescence $[Ca^{2+}]_i$ signals was recorded by InCyt Basic Fluorescence Imaging System or FV1000 confocal system (in experiments with nodose ganglion cells). Changes in $[Ca^{2+}]_i$ were displayed as a ratio of real-time fluorescence (F_t) relative to the intensity at the beginning (F_0) of the experiment (F_t/F_0). Maximal change in $[Ca^{2+}]_i$ was presented as ratio F_{max}/F_0 . In some

experiments, cells were loaded with Fura-2/AM for ratiometric Ca^{2+} -fluorescent measurement, and the data are presented as ratio of the fluorescence signal from excitation at 340nm to that at 380nm (F_{340}/F_{380}). Two-tailed Student's t-test was used for statistical evaluation, with “*p*” at 0.05 as the level of significance. All experiments were performed at room temperature ($\sim 23\text{ }^{\circ}\text{C}$).

2.3.3.8 Electrophysiology

Single-channel activity was recorded at cell-attached configuration using an EPC9 patch clamp amplifier (HEKA) controlled by Pulse software (HEKA). Patch pipettes (resistance at 6–9 M Ω for single channel recording) were filled with pipette solution, which contained (mM): Cs-aspartate 140, CsCl 5, MgCl₂ 1, CaCl₂ 1, HEPES 10, pH 7.4 with CsOH. Bath solution was NPSS used in $[\text{Ca}^{2+}]_i$ measurement. Currents were sampled at 50 kHz and filtered at 5 kHz, and the data were analyzed with PulseFit 8.7 (HEKA) and Clampfit 9 (Axon). Experiments were performed at room temperature ($\sim 23\text{ }^{\circ}\text{C}$).

2.3.3.9 Arterial blood pressure and baroreceptor activity recording *in vivo*

On day 6 after lentiviral transduction, the rat was anaesthetized with 100 mg/kg pentobarbital sodium. The right common carotid artery was cannulated and the blood pressure was detected by a pressure transducer connected to an amplifier (ML221, ADInstruments, USA). Blood pressure was continuously recorded by Chart 5.0 (ADInstruments). The abdomen was opened and a segment of abdominal aorta above the two renal arteries

was detached from surrounding tissues, and gripped by an inflatable cuff. The abdominal aorta was gradually clamped by inflating the cuff with a pump, and the arterial blood pressure was elevated from basal in around 20 seconds. The left aortic depressor nerve was gently isolated from its junction with the left recurrent laryngeal nerve inferiorly by blunt dissection. The left aortic depressor nerve was gently placed on a bipolar silver electrode which was connected to an amplifier (Model 1700 Differential AC Amplifier, A-M Systems Inc., USA). The nerve activity was amplified 10,000 times and filtered through a bandpass of 100 to 5,000 Hz. The signal was continuously measured and the data was analyzed by Clampfit 9.0 software (Axon Instruments, USA). Simultaneous recordings of the arterial blood pressure and depressor nerve firing were performed when the cuff was inflated to clamp the abdominal aorta. Rat was sacrificed at the end of the experiment by blood loss from a cut at abdominal aorta.

2.3.3.10 Data analysis and presentation

Data from $[Ca^{2+}]_i$ measurement were plotted as traces and expressed as mean \pm SEM of cells in one experiment. Bar charts show data in mean \pm SEM of individual experiments. Current-voltage curves in electrophysiology and baroreceptor activity curve were mean \pm SEM of individual experiments. Number of individual recordings “n” is given in parenthesis. Student’s t-test was used for statistical comparison, with probability $p < 0.05$ (*) as a significant difference.

3 Chapter 3 TRPC5 is not stimulated by nitric oxide

3.1 Introduction

Nitric oxide (NO) is a short-lived, reactive molecule that can serve as an important cellular signal (Snyder, 1994). NO signaling is involved in endothelial-dependent vascular relaxation, cell motility, immune defense and neurite outgrowth (Bicker, 2005; Chung *et al.*, 2008; Ignarro, 2002). While many NO-elicited responses are mediated by cGMP, which is produced from the activity of NO-stimulated guanylate cyclase (Snyder, 1994), NO can also act independent of cGMP (Hess *et al.*, 2005). A well documented NO action independent of cGMP is S-nitrosylation. In S-nitrosylation, a nitric oxide moiety is covalently attached to cysteine residues of a protein, resulting in an alteration in protein function. S-nitrosylation serves as a type of posttranslational modification analogous to phosphorylation and acetylation. While some substrate proteins are constitutively S-nitrosylated (Jaffrey *et al.*, 2001), other proteins can be reversibly S-nitrosylated dependent upon the concentration of NO and the accessibility of the NO radicals to the cysteine residues (Hess *et al.*, 2005).

A wide spectrum of proteins including metabolic, structural and signaling proteins can be S-nitrosylated (Hess *et al.*, 2005; Jaffrey *et al.*, 2001). S-nitrosylation is reported to modulate the activity of a number of ion channels including calcium-activated potassium channels, ryanodine receptors, hyperpolarization-activated cation channels, cyclic nucleotide-gate channels and N-methyl-D-aspartate receptors (Hess *et al.*, 2005; Jaffrey *et al.*, 2001;

Stamler *et al.*, 1997).

Recently, Yoshida *et al.* reported an interesting finding that S-nitrosylation can activate TRPC5 (26). TRPC5 is a non-selective cation channel, playing an important functional role in neurons and vascular cells (Yoshida *et al.*, 2006). Yoshida *et al.* found that NO S-nitrosylates on Cys553 and Cys558 to activate TRPC5 in TRPC5-overexpressing HEK cells. They also demonstrated that, TRPV1, TRPV3 and TRPV4, which contain these two conserved cysteines, were also activated by NO donors through a similar mechanism. In addition, the authors showed that NO donor SNAP could activate TRPC5 in the primary cultured bovine aortic endothelial cells (BAECs), resulting in an enhanced Ca^{2+} influx. Because TRPC5 is known to play a key functional role in neurons and vascular cells (Beech, 2007b), Yoshida's model that TRPC5 acts as an NO sensor is of high interest.

In the present study, the issue of TRPC5 activation by NO donors was revisited. Live-cell cytosolic calcium imaging techniques was used to examine the action of NO donors on TRPC5 over-expressed in HEK cells and in the primary cultured BAECs. The results demonstrated that NO donors, at the concentration range that is needed to induce vascular relaxation, were unable to activate TRPC5.

3.2 Results

3.2.1 SNAP and DEA-NONOate induce vasorelaxation

To test the efficacy of the NO donors and to determine the relevant concentration range to induce vasorelaxation, SNAP and DEA-NONOate were applied to isolated arteries, and the vessel tension was measured by isometric wire-myography. Endothelial-denuded mice aortic segments were pre-constricted with 10 μM phenylephrine. After a stable vessel tension was achieved, cumulatively-increasing concentrations of SNAP (from 100 nM, to 300 nM, 1 μM and 300 μM) and DEA-NONOate (from 10 nM, to 100 nM, 1 μM , 10 μM and 100 μM) were applied to the bath solution. 100 nM SNAP induced $\sim 50\%$ relaxation, and 1 μM SNAP completely relaxed the vessels (Figure 3.1A). DEA-NONOate induced $\sim 50\%$ relaxation at 10 μM and complete relaxation at 100 μM (Figure 3.1B).

3.2.2 Lack of action of SNAP on TRPC5-mediated Ca^{2+} influx

HEK cells were transfected with TRPC5 cDNA or pCDNA3 empty vector. Stable expression of TRPC5 protein was confirmed by immunoblot (Figure 3.2A). In Ca^{2+} -imaging experiments, cells were bathed in NPSS. 300 μM SNAP was applied to determine whether it could stimulate a $[\text{Ca}^{2+}]_i$ rise. Among 23 batches of TRPC5-expressing cells tested, SNAP at 300 μM failed to elicit any $[\text{Ca}^{2+}]_i$ rise in 18 batches (Figure 3.2B&D). In the rest 5 batches, SNAP at 300 μM caused a small rise in $[\text{Ca}^{2+}]_i$ (Figure 3.3A). However, this SNAP effect could also be observed in some batches of vector-transfected control cells (4 in 32 batches, Figure 3.3B). In contrast, a well-documented TRPC5 potentiator La^{3+} at (Jung *et al.*, 2003) was able

to stimulate Ca^{2+} influx in all batches of TRPC5-overexpressing cells but not in vector-transfected cells (Figure 3.2B-D). Furthermore, this $[\text{Ca}^{2+}]_i$ rise was inhibited by 75 μM 2-APB (Fig 3.2B), which is a TRPC5 inhibitor (22). In addition, the magnitude of carbachol (100 μM)-induced $[\text{Ca}^{2+}]_i$ rise is much higher in TRPC5-expressing cells than that in vector-transfected cells (Figure 3.2B-D). These results indicate that TRPC5 channels expressed in HEK cells are fully functional, and that the ineffectiveness of SNAP action could not be attributed to a malfunctioned TRPC5.

3.2.3 Lack of action of SNAP DEA-NONOate on TRPC5-mediated Ca^{2+} influx

Another class of NO donor, DEA-NONOate, was also tested. DEA-NONOate, at 10 μM and 100 μM , failed to elicit any observable $[\text{Ca}^{2+}]_i$ rise in TRPC5-expressing cells (Fig. 3.4A-C).

3.2.4 Mouse TRPC5 clone from other lab was not activated by SNAP

The mouse TRPC5 cDNAs were cloned independently by two groups, ours by Dr L. Birnbaumer's group (NIH) and that used by Yoshida et al. by Dr Y. Mori's group (Kyoto University). To address if the difference in cDNA results in the discrepancy of findings, the mouse TRPC5 cDNA clone was given by Dr Y. Mori for the Ca^{2+} -imaging experiments. The experimental procedures were strictly followed as described in Yoshida et al. (Yoshida *et al.*, 2006). In HEK cells transiently transfected with this TRPC5 construct, TRPC5-mediated $[\text{Ca}^{2+}]_i$ was observed after stimulation with carbachol and La^{3+} , the effect of which was absent in vector-transfected cells (Figure 3.5A&B). 300 μM SNAP was, however, unable to stimulate $[\text{Ca}^{2+}]_i$

increase in TRPC5-transfected cells (Figure 3.5A).

3.2.5 Inhibitory effect of T5E3 antibody on TRPC5 function

Ca²⁺ influx through TRPC5 can be induced by micromolar LaCl₃ or muscarinic receptor agonist carbachol (Jung *et al.*, 2003; Schaefer *et al.*, 2000). TRPC5-expressing cells showed increased [Ca²⁺]_i in response to 100 μM LaCl₃ and sustained elevated [Ca²⁺]_i level after 100 μM carbachol application (Figure 3.6A&C). In contrast, in cells pre-incubated with 4 μg/ml T5E3, [Ca²⁺]_i decreased after 100 μM LaCl₃ application and a transient [Ca²⁺]_i increase in response to 100 μM carbachol (Figure 3.6B&C). Previous studies reveal that the transient [Ca²⁺]_i increase after carbachol application is likely due to Ca²⁺-store release and independent of Ca²⁺ influx through TRPC5 (Schaefer *et al.*, 2000). The results show that T5E3 effectively inhibits both the direct stimulation (by La³⁺) and receptor-activation of TRPC5.

3.2.6 Inhibition of Ca²⁺-entry in endothelial cells (BAECs)

Effect of SNAP was also tested in the primary cultured BAECs. Similar to Yoshida's *et al.*'s protocol (26), the cells were first bathed in a Ca²⁺-free physiological medium. Extracellular Ca²⁺ was then added to induce a [Ca²⁺]_i rise. But instead of using TRPC5-specific siRNA or TRPC5-dominant negative constructs as reported by Yoshida *et al.* (26), we used a TRPC5-specific blocking antibody T5E3 to inhibit TRPC5 activity (Xu *et al.*, 2006a; Xu *et al.*, 2005b). As shown in Figure 3.7A, re-addition of extracellular Ca²⁺ to the bath evoked a robust [Ca²⁺]_i rise in control cells that were pretreated with vehicle 0.1% DMSO. In comparison, this [Ca²⁺]_i

rise was much smaller in cells that were pretreated with SNAP (300 μM) (Figure 3.7C&D). In addition, application of T5E3 (4 $\mu\text{g/ml}$), an antibody that can specifically block TRPC5 channels (Xu *et al.*, 2006a; Xu *et al.*, 2005b), significantly reduced this $[\text{Ca}^{2+}]_i$ rise in response to Ca^{2+} re-addition (Figure 3.7B&D). The magnitude of $[\text{Ca}^{2+}]_i$ rise in response to Ca^{2+} re-addition was similar in T5E3-pretreated and SNAP-pretreated cells (Figure 3.7B-D).

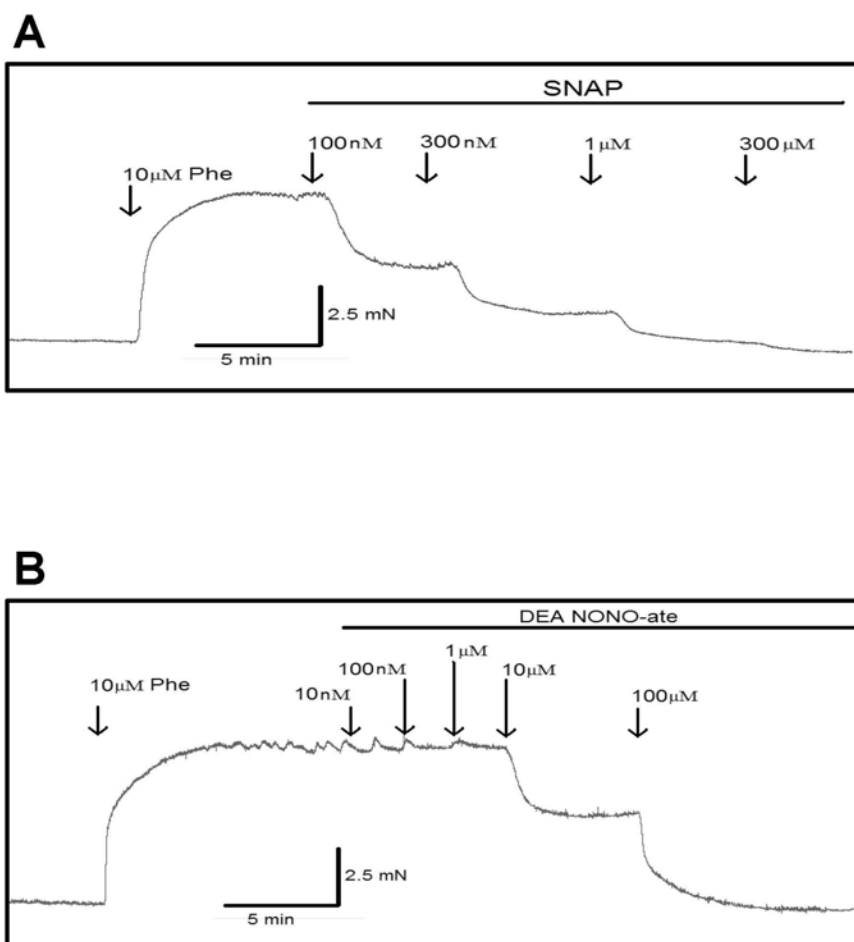


Figure 3.1 Relaxation to SNAP or DEA-NONOate in mice aortic segments. Shown were representative time courses of isometric tension in isolated mouse aortic segments in response to cumulatively-increasing concentrations of SNAP (A) and DEA-NONOate (B) applied to the bath ($n=4$). The aortic segments (~ 2 mm in length) were denuded of the endothelial layer and pre-constricted with 10 μM phenylephrine (Phe).

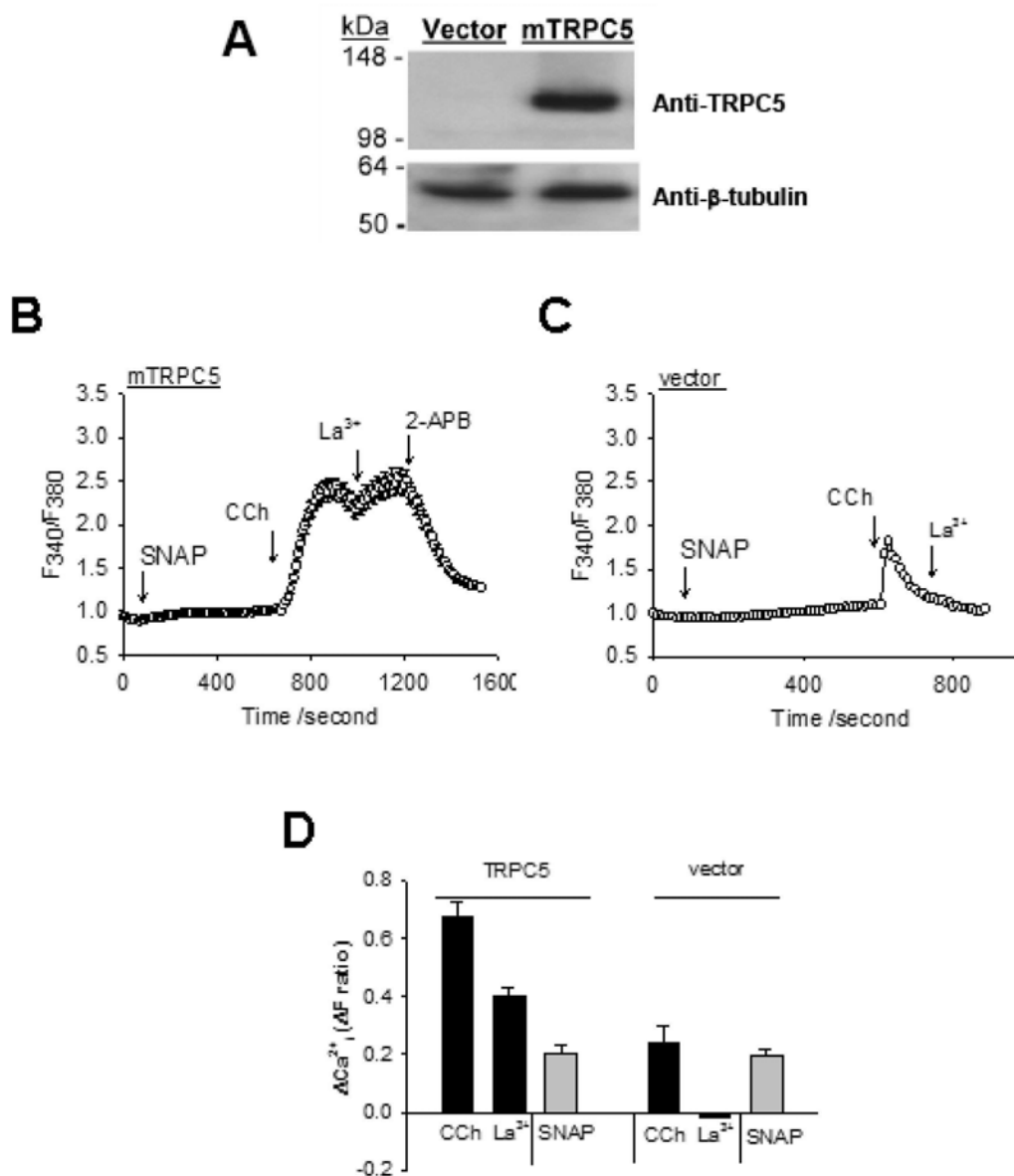


Figure 3.2 SNAP on TRPC5-dependent Ca²⁺-entry in HEK293 cells.

A, Representative image of an immunoblot comparing protein lysates for HEK cells transfected with pCDNA3 (vector) or vector containing TRPC5 (mTRPC5) (upper panel). The blot was also probed with anti-β-tubulin antibody to confirm equal loading of lanes (lower panel). Masses of protein markers are indicated on the left. B-D, shown are representative time courses of [Ca²⁺]_i change in vector-transfected (C) and TRPC5-transfected HEK cells (B). Bath contained NPSS. Arrows indicate the time points when chemicals were added. Each trace represents mean ± SEM of at least 20 cells in one representative experiment (n=7). C, summary of data showing the [Ca²⁺]_i response 1 min after application (CCh) or the maximal [Ca²⁺]_i change as in B and C. Mean ± SEM (n=7). SNAP, 300 μM; carbachol (CCh) 100 μM, 1 min; LaCl₃ (La³⁺) 100 μM; 2-APB, 75 μM.

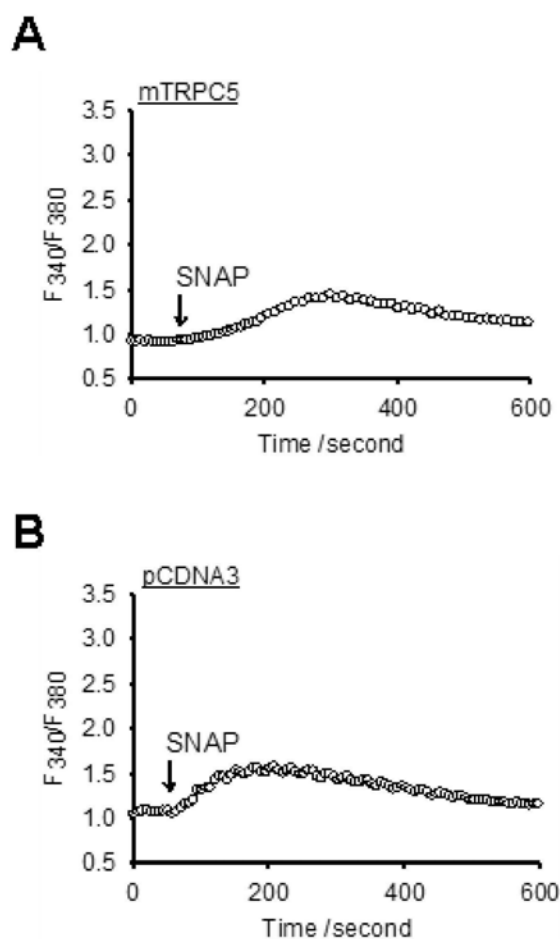


Figure 3.3 Comparable effects SNAP on HEK cells transfected with TRPC5 or vector control.

A-B, representative time courses of $[Ca^{2+}]_i$ changes in paired batches of cells that showed responses to SNAP (300 μ M) in TRPC5-expressing cells (A) and control cells (B). Each trace represents the mean \pm SEM data of ≥ 20 cells. Such responses were observed in 5 out of 23 batches of mTRPC5-transfected and 4 out of 32 batches of vector (pCDNA3)-transfected cells.

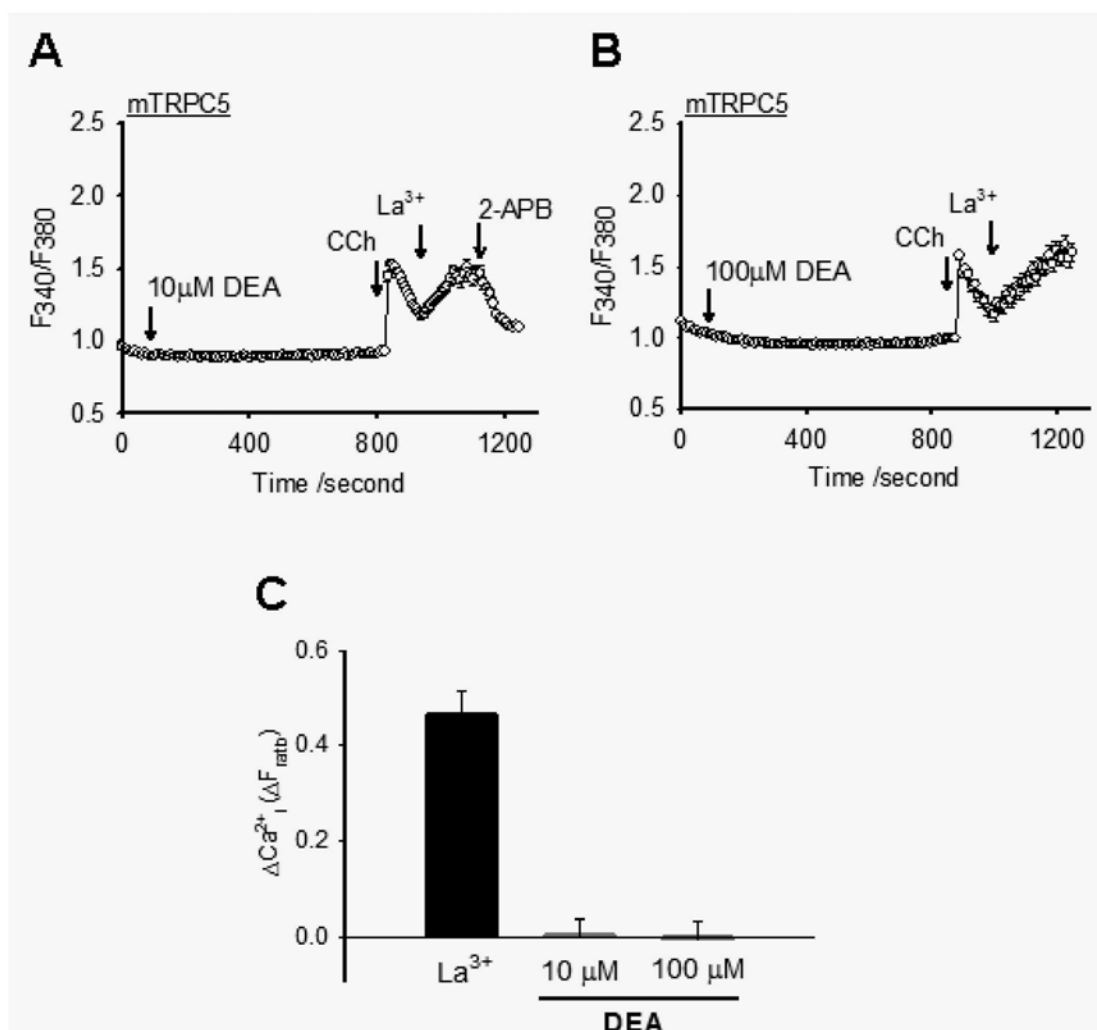


Figure 3.4 DEA-NONOate on TRPC5-dependent Ca²⁺-entry.

A and B, representative time-series graphs for [Ca²⁺]_i in TRPC5-expressing HEK cells in response to DEA-NONOate at 10 μM (A) or 100 μM (B) (n=8). The data points represents the mean ± SEM for ≥20 cells. Carbachol (CCh), 100 μM; LaCl₃ (La³⁺), 100 μM; DEA-NONOate (DEA), as indicated; 2-APB, 75 μM. C, summary of data (mean ± SEM) for the maximum [Ca²⁺]_i change in response to LaCl₃ and DEA-NONOate as in A&B (n=8).

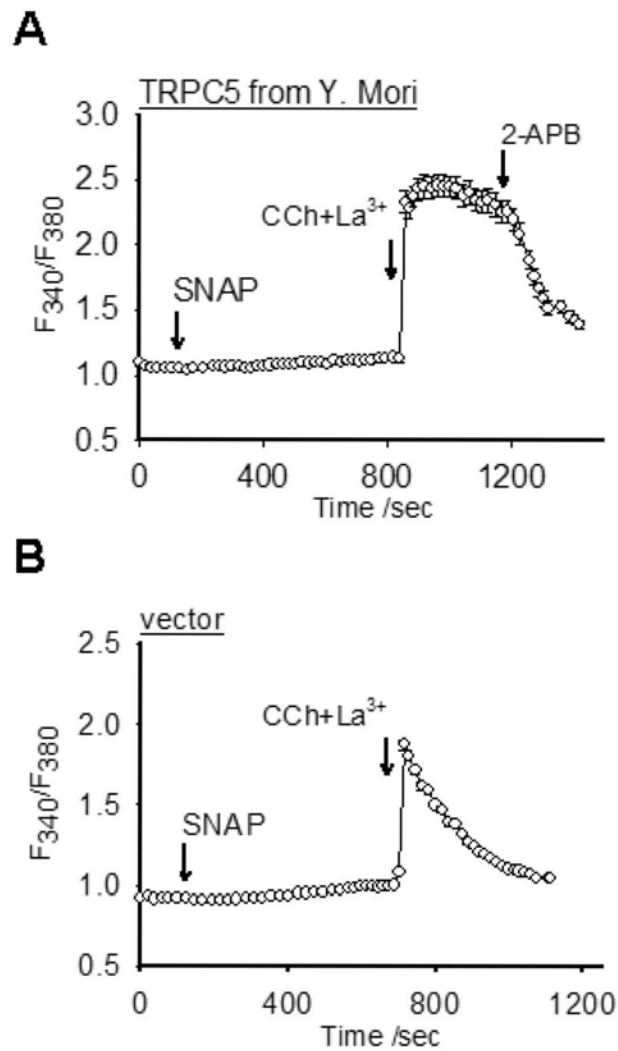


Figure 3.5 Ca^{2+} -imaging experiments with TRPC5 and SNAP from Dr Y. Mori

A-B, Ca^{2+} -imaging data obtained using mouse TRPC5 (kindly provided by Y. Mori) and vector (pCDNA3) and a transient transfection protocol from Yoshida et al. (Yoshida *et al.*, 2006). In brief, transfected cells were trypsinized after 16 hours and seeded and cultured on coverslip for 24 hours before recordings. The bath solution was HBS and $[\text{Ca}^{2+}]_i$ was detected by Ca^{2+} -imaging system. Arrows indicate the time points when chemicals were added. Each trace represents the mean \pm SEM from ≥ 20 cells in one representative experiment ($n=4-6$). SNAP (provided by Y. Mori), 300 μM ; carbachol (CCh), 100 μM ; LaCl_3 (La^{3+}), 100 μM ; 2-APB, 75 μM .

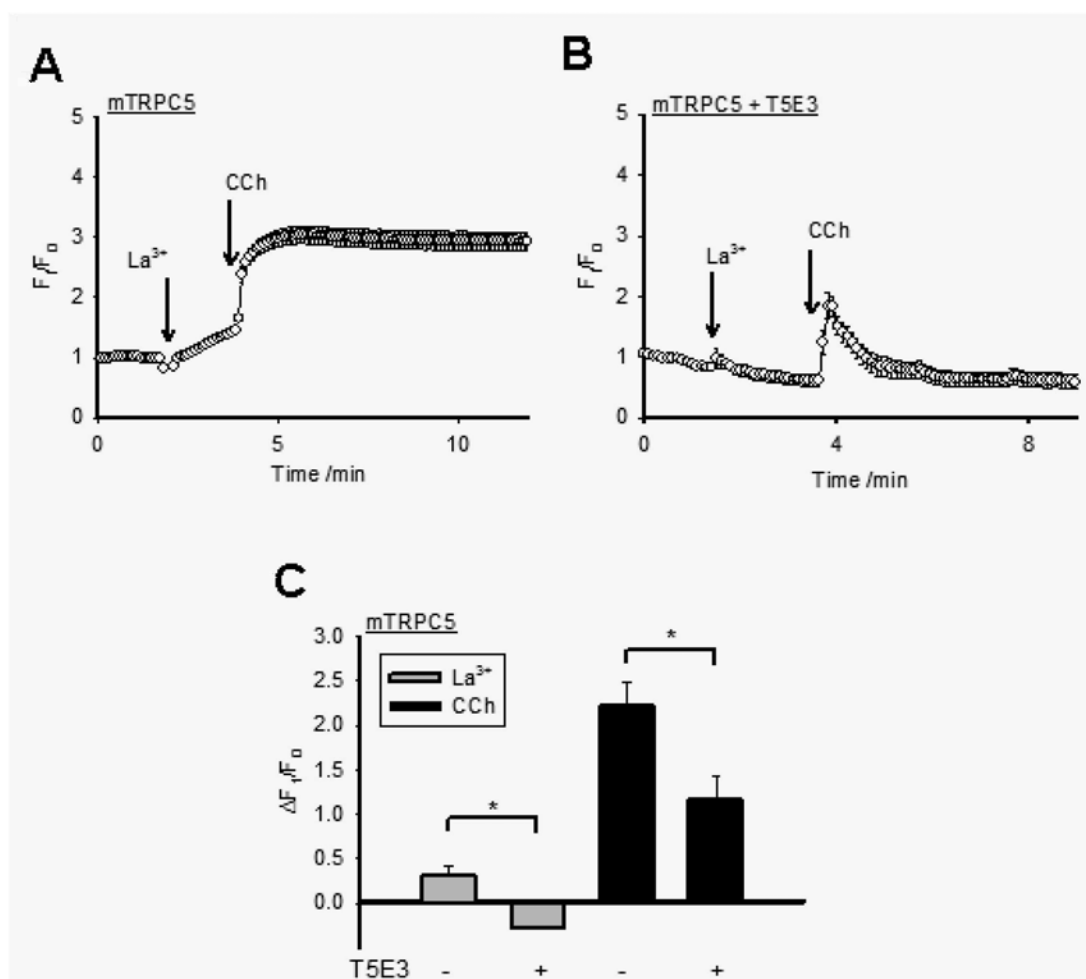


Figure 3.6 T5E3 antibody blocked Ca^{2+} influx through TRPC5.

A-B, representative time courses of $[Ca^{2+}]_i$ changes in TRPC5-expressing HEK cells, with (B) or without (A) 4 μ g/ml T5E3 in the bath solution. $[Ca^{2+}]_i$ was detected by calcium-sensitive dye Fluo-3 as describe in Chapter 2 Section 2.2.4.1, with the real time fluorescence normalized to initial fluorescence (F_v/F_0). Arrows indicate the time points when chemicals were added. Each trace represents the mean \pm SEM of ≥ 20 cells in a representative experiment ($n=3$). C, summary of data showing the $[Ca^{2+}]_i$ change (mean \pm SEM) in response to 100 μ M $LaCl_3$ (La^{3+}) and 100 μ M carbachol (CCh) as in A and B. * $p < 0.05$.

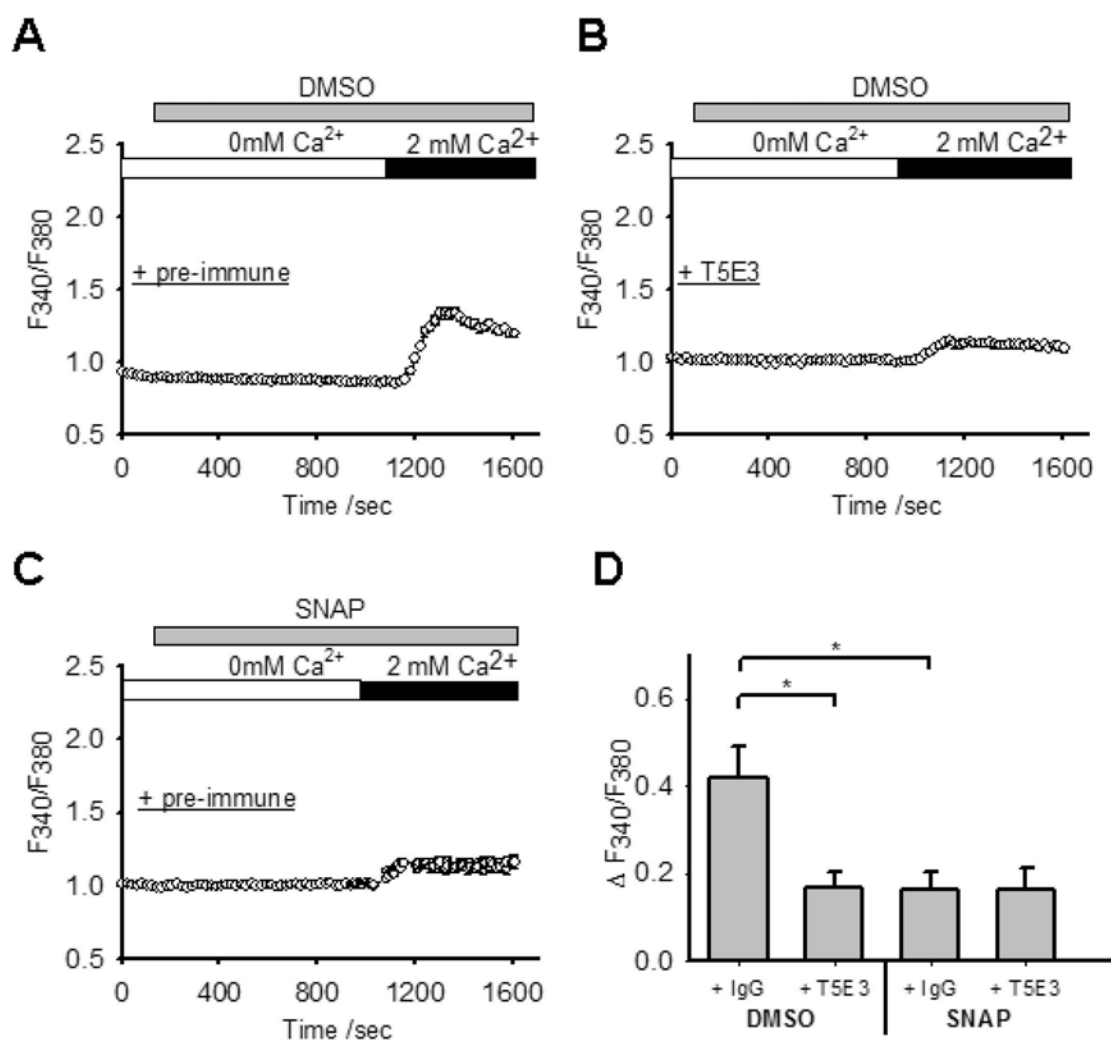


Figure 3.7 Inhibition of Ca²⁺-entry by SNAP in endothelial cells

A-C, representative time courses of [Ca²⁺]_i change in BAECs in response to extracellular Ca²⁺ re-addition. BAECs were bathed in HBS containing 4 μ g/ml T5E3 (B) or pre-immune IgG (A, C) for 20-30 minutes at room temperature prior to Ca²⁺-imaging. Bath solution was changed to HBS-EGTA containing IgG or T5E3 at the beginning of recording. 300 μ M SNAP (C) or 0.1% DMSO (A, B) was added to the bath for ~15 minutes, followed by changing the bath solution to HBS containing DMSO or SNAP with/without T5E3/pre-immune IgG. Each trace represents mean \pm SEM of at least 15 cells in one representative experiment (n=4). D, summary of data for all independent experiments of the type shown in (A-C), showing the maximal [Ca²⁺]_i change after restoring Ca²⁺ in bath. Mean \pm SEM (n=4). *, *p*<0.05.

3.3 Discussion

In the present study, the effect of NO donors on TRPC5 activity was revisited. Two NO donors, SNAP and DEA-NONOate, were used in the study. Both NO donors, even when applied at a concentration two log orders higher than that required for vascular relaxation, failed to activate Ca^{2+} influx in TRPC5-expressing HEK cells. In addition, SNAP application inhibits, instead of activating as reported previously (Yoshida *et al.*, 2006), the TRPC5-mediated Ca^{2+} influx in BAECs. These data argue against the previously reported stimulating action of NO on TRPC5. The results indicate that the previous proposed scheme of TRPC5 activation by S-nitrosylation needs to be re-evaluated.

In order to reproduce the original findings that an NO donor SNAP can stimulate TRPC5-mediated Ca^{2+} influx in HEK cells, Ca^{2+} -imaging experiments with TRPC5-expressing HEK cells were performed as reported by Yoshida *et al.* (Yoshida *et al.*, 2006). In contrast to Yoshida *et al.*, we found that SNAP at 300 μM failed to induce any $[\text{Ca}^{2+}]_i$ rise in majority batches (18 out of 23) of TRPC5-overexpressing HEK cells. Two lines of evidence indicate that TRPC5 is fully functional in these cells. 1) Carbachol-induced $[\text{Ca}^{2+}]_i$ rise in these cells is much higher than that in vector-transfected HEK cells (Schaefer *et al.*, 2000). 2) La^{3+} , a well-documented potentiator of TRPC5 (Zeng *et al.*, 2004), was able to stimulate Ca^{2+} rise in these cells. And furthermore, this La^{3+} -induced Ca^{2+} rise was rapidly attenuated after application of 2-APB, which is a TRPC5 inhibitor. Based on these evidences, inability of SNAP to elicit any $[\text{Ca}^{2+}]_i$ response in the present study cannot be attributed to an inadequate expression of TRPC5. However, we did observe that, in limited

batches of TRPC5-expressing cells (5 of 23), SNAP was able to induce a small $[Ca^{2+}]_i$ rise. Nevertheless, the magnitude of this SNAP-induced $[Ca^{2+}]_i$ rise in the minority batches of TRPC5-expressing cells was much lower than those reported by Yoshida et al.. Importantly, such a small $[Ca^{2+}]_i$ rise in response to SNAP could also be observed in vector-transfected HEK cells, suggesting that this $[Ca^{2+}]_i$ rise was independent of TRPC5. In fact, Yoshida et al. also observed a small $[Ca^{2+}]_i$ rise in response to 300 μ M SNAP in vector-transfected cells (~0.3 unit of change in F340/F380 ratio) (Yoshida *et al.*, 2006).

300 μ M SNAP is a very high concentration which may release supra-physiological concentration of NO, because the effective range of SNAP that can induce vascular relaxation is between 100 nM - 1 μ M. SNAP belongs to the nitroso-amine class of NO donor, which spontaneously releases NO (Feelisch, 1998). Hence, TRPC5 was exposed to ample amount of NO released from SNAP, but still was not stimulated. To confirm this finding, another class of NO donor DEA-NONOate which decomposes at physiological pH to liberate NO (Feelisch, 1998), was also tested. DEA-NONOate, at the physiologically relevant concentration of 10 and 100 μ M, again failed to induce a $[Ca^{2+}]_i$ rise in TRPC5-expressing cells.

In some experiments reported by Yoshida et al., SNAP concentration was used as high as 1 mM. It is possible that SNAP at a concentration higher than 300 μ M could stimulate TRPC5 activity. But even if such stimulation exists, it may not be directly related to NO. Oxidation of NO by endogenous reactive species yields other NO-related species at higher oxidation states, e.g. N_2O_3 and $ONOO^-$ (Espey *et al.*, 2002; Feelisch, 1998). In addition, toxic side-effect has

been reported for some NO donors at excessive concentration (Rindone *et al.*, 1992). One cannot exclude possible side-effect caused by SNAP metabolites or its backbone NAP at high concentration. High dose of SNAP has been reported to generate free radicals (Zhang *et al.*, 2003), which could result in oxidation of free thiol on cysteines (Espey *et al.*, 2002; Stamler *et al.*, 1997). Notably, Yoshida *et al.* also demonstrated that H₂O₂, a reactive oxygen species, was capable of stimulating TRPC5, giving rise to the possibility that TRPC5 is sensitive to redox reaction other than S-nitrosylation of the cysteine residues.

Yoshida *et al.* suggest that NO nitrosylates Cysteine 553 (C553) and Cysteine 558 (C558) of TRPC5 from intracellular side (Yoshida *et al.*, 2006). However, the two cysteines lay on the loop between the predicted transmembrane segment S5 and S6 (Vannier *et al.*, 1998; Yoshida *et al.*, 2006). C553 is 9 amino acids downstream of the E543, which is responsible for the extracellular action of La³⁺ on TRPC5 (Jung *et al.*, 2003), and C558 is 16 amino acids upstream of the highly conserved LFW residues in the pore region (Hofmann *et al.*, 2002; Strubing *et al.*, 2003). C553 also lies on the region where binding of antibody leads to channel blockade (Xu *et al.*, 2006a; Xu *et al.*, 2005b). Thus, it is conceivable that C553 and C558 locate on the extracellular loop. Another group reported that substitutions of these two cysteines with other amino acids result in constitutively robust channel with the native voltage dependence abolished (Xu *et al.*, 2008). Regarding the sensitivity of TRPC5 to reducing agents, these two cysteines are thus suggested to be natively engaged in disulphide bridge (Xu *et al.*, 2008). In summary, sufficient evidence support that the two cysteines are located at extracellular side, and are unavailable for S-nitrosylation from the cytosolic side.

More importantly, the SNAP experiments have been performed as reported by Yoshida et al. using the same mouse TRPC5 clone and the same SNAP, which were kindly provided by Dr. Y. Mori. The experimental protocols were followed as described in the report by Yoshida et al.: 1) HEK cells were transiently transfected with mouse TRPC5, and the experiments were performed 2 days post-transfection; 2) The composition of bath solution was exactly the same as that of Yoshida et al (26). However, application of 300 μ M SNAP again failed to induce any significant Ca^{2+} rise in these cells, whereas carbachol plus La^{3+} application can induce a $[\text{Ca}^{2+}]_i$ rise in these cells, an indication for the presence of functional TRPC5. These results suggest that the contrasting results to that by Yoshida et al. may not be resulted from the difference in TRPC5 cDNA clones, SNAP, or experimental media.

TRPC5 is expressed in vascular endothelial cells (Yao *et al.*, 2005a). Yoshida et al. investigated possible SNAP effect on TRPC5 in the primary cultured BAECs (Yoshida *et al.*, 2006). In their experiments, they first incubated the endothelial cells in a Ca^{2+} -free physiological medium containing SNAP. They found that re-addition of extracellular Ca^{2+} induce a $[\text{Ca}^{2+}]_i$ rise in normal BAECs but not in those cells that expressed either dominant-negative TRPC5 or TRPC5-specific siRNA. However, these data could be interpreted in two different ways. 1) One interpretation, as has been proposed by Yoshida et al., is that a lower expression of TRPC5 reduced the SNAP response in these cells. 2) However, an alternative explanation of the data is that a lowered expression of TRPC5, which is known to contribute to basal Ca^{2+} influx (Beech, 2007b; Yamada *et al.*, 2000), reduced the basal Ca^{2+} influx in response to Ca^{2+}

re-addition. In the present study, SNAP treatment actually caused a reduction in Ca^{2+} re-addition-induced Ca^{2+} influx in BAECs, which agrees with the results from several previous reports (Dedkova *et al.*, 2002; Kwan *et al.*, 2000; Takeuchi *et al.*, 2004). Further, this Ca^{2+} influx was reduced by T5E3, a blocking antibody that can plug the pore of TRPC5 (Xu *et al.*, 2006a; Xu *et al.*, 2005b). The result demonstrates that TRPC5 contributes to basal Ca^{2+} influx in the primary cultured BAECs.

In conclusion, NO donors failed to stimulate both exogenously expressed TRPC5 and native TRPC5 in the primary cultured endothelial cells. The data argue against any stimulatory effect of NO on TRPC5 activity. The results are consistent with NO having inhibitory effect to endothelial Ca^{2+} influx, and TRPC5 as a component of Ca^{2+} influx pathway in endothelial cells.

4 Chapter 4 Stimulation of TRPC5 by genistein

4.1 Introduction

TRPC5 is a widely-expressed Ca^{2+} -permeable non-selective cation channel that mediates a variety of physiological process (Chapter 1 Section 1.2; (Beech, 2007b)). There are diverse modes of activation for TRPC5 (Zeng *et al.*, 2004). The channel can be activated by Ca^{2+} store depletion, lanthanides, lysophosphatidylcholine, extracellular thioredoxin and vesicular trafficking (Beech, 2007b; Xu *et al.*, 2008; Zeng *et al.*, 2004). The channel activity is also stimulated following the activation of G-protein-coupled receptors and/or receptor tyrosine kinases (Schaefer *et al.*, 2000). Although TRPC5 can be activated by multiple factors, there is still insufficient knowledge on the specific signaling molecule(s) that directly open the channel. In this regard, a recent study suggests that reduced thioredoxin may directly activate TRPC5 by breaking a disulphide bridge in the predicted extracellular loop adjacent to the ion-selectivity filter of the channel (Xu *et al.*, 2008). There is also evidence that lysophospholipids can activate TRPC5 through a relatively direct action, probably by causing a physical distortion of lipid bilayer (Xu *et al.*, 2006a).

Plant-derived isoflavones receive great attention for their potential health beneficial properties in protecting against cancer, heart diseases, rheumatoid arthritis, Alzheimer's disease and other pathological conditions (Altavilla *et al.*, 2004; Si *et al.*, 2007). Dietary isoflavones can be found in soybeans and soy foods (Messina, 1999). The primary soy-derived isoflavones are genistein, daidzein and their respective β -glycosides. Among them, genistein is the most

widely studied isoflavones. Genistein is a phytoestrogen that can act on estrogen receptors at nanomolar level (Escande *et al.*, 2006). At the concentration range of 10-100 micromolar, it also inhibits tyrosine kinases (Barnes *et al.*, 2000). In addition, genistein may exert a direct, noncatalytic blocking effect on ion channels, including L-type Ca^{2+} channel (Belevych *et al.*, 2002; Chiang *et al.*, 1996), voltage-gated Na^+ channel (Paillart *et al.*, 1997), voltage-gated K^+ channel (Smirnov *et al.*, 1995) and inward rectifying K^+ channel (Chiang *et al.*, 2002), in a tyrosine kinase-independent manner.

In the present study, I used the live cell fluorescent calcium imaging and patch clamping technique to study the effect of genistein on TRPC5. We found that genistein was capable of stimulating TRPC5 activity in heterologously expressed HEK cells. The stimulatory effect was independent of tyrosine kinase activity and estrogen receptors. Genistein also increased TRPC5 channel open probability as recorded in excised membrane patches, suggesting a relatively direct action. Furthermore, genistein also potentiated the stimulating action of La^{3+} on TRPC5 activity. This is the first study showing an action of genistein on a TRP channel.

There are accumulating reports demonstrating a direct vascular relaxant effect by genistein (Cruz *et al.*, 2008; Cruz *et al.*, 2006; Mishra *et al.*, 2000; Nevala *et al.*, 2001; Si *et al.*, 2007; Valero *et al.*, 2006). It is evident that the genistein-induced vasorelaxation involves vascular ion channels, for instance Ca^{2+} -sensitive K^+ channels and cystic fibrosis transmembrane conductance regulator (Nevala *et al.*, 2001; Valero *et al.*, 2006). In addition, at micromolar concentrations, genistein acutely dilates arteries in an endothelium- and/or

nitric oxide-dependent mechanism (Mishra *et al.*, 2000; Si *et al.*, 2007). Endothelial-dependent vasorelaxation is regulated, in part, by cytosolic Ca^{2+} level in endothelial cells (Vanhoutte, 1992). Given that TRPC5 is expressed in endothelial cells, it was therefore hypothesized that genistein stimulates endothelial TRPC5 channel to elevate cytosolic Ca^{2+} level. Using live cell fluorescent calcium imaging and TRPC5-blocking antibody, it is found that genistein induces Ca^{2+} influx through TRPC5 in bovine aortic endothelial cells and rat mesenteric artery endothelial cells.

4.2 Results

4.2.1 Effect of genistein on TRPC5-mediated $[Ca^{2+}]_i$ rise

TRPC5 was stably transfected into HEK293 cells. Compared to wild type HEK cells, these TRPC5-transfected cells expressed TRPC5 proteins at a much higher level (Figure 4.1A). Fluorescence Ca^{2+} imaging was used to test the effect of genistein on TRPC5 activity. In one protocol, cells bathed in $0Ca^{2+}$ -PSS were first treated with a muscarinic agonist carbachol (100 μ M), which initiated a $[Ca^{2+}]_i$ rise (Figure 4.1B&C) due to Ca^{2+} release from intracellular Ca^{2+} stores (Schaefer *et al.*, 2000). Subsequent addition of extracellular Ca^{2+} (1 mM) evoked another $[Ca^{2+}]_i$ rise in TRPC5-transfected (Figure 4.1B) but not in vector-transfected HEK cells (Figure 4.1C). This is consistent with previous reports that showed a stimulating action of carbachol on TRPC5 via receptor-operated mechanism (Schaefer *et al.*, 2000). Interestingly, addition of genistein (50 μ M) into the bath caused a further rise in $[Ca^{2+}]_i$ (Figure 4.1B). In another protocol, cells bathed in $0Ca^{2+}$ -PSS were pretreated with genistein (50 μ M) for 10 min, followed by addition of extracellular Ca^{2+} , which elicited a marked rise in $[Ca^{2+}]_i$ in TRPC5-expressing cells (Figure 4.2A), but not in cells that were transfected with vector plasmid (Figure 4.2B). Because genistein stock was prepared in DMSO, another control experiment was performed, in which the cells were pretreated with 0.1% DMSO (vehicle) (Figure 4.2A&B). As expected, the $[Ca^{2+}]_i$ rise in response to extracellular Ca^{2+} addition was also much smaller in vehicle-pretreated cells than in genistein-pretreated cells (Figure 4.2A&C).

4.2.2 Synergistic action of genistein and La^{3+} on TRPC5

Direct application of genistein (50 and 100 μM) in the absence of bath La^{3+} elicited a $[\text{Ca}^{2+}]_i$ rise in TRPC5-expressing HEK cells (Figure 4.3A&C), but the magnitude of $[\text{Ca}^{2+}]_i$ rise was small. However, if the cells were bathed in a La^{3+} (100 μM)-containing physiological solution, the $[\text{Ca}^{2+}]_i$ rise in response to genistein became much larger (Figure 4.3B&C). In reverse, presence of genistein (50 and 100 μM) in bath solution also potentiated the $[\text{Ca}^{2+}]_i$ rise in response to extracellular La^{3+} (Figure 4.4A&B). These experiments show that genistein and La^{3+} acted synergistically to stimulate TRPC5.

4.2.3 Concentration-dependent stimulation of TRPC5 by genistein

We further tested a range of genistein concentrations (10 to 200 μM) on TRPC5 stimulation. Bath application of genistein elicited $[\text{Ca}^{2+}]_i$ rise on TRPC5-expressing cells in a concentration-dependent manner (Figure 4.5A). Fitting of the concentration-response curve yielded a half-maximal response (EC_{50}) at ~ 93 μM (Figure 4.5C). La^{3+} shifted the dose-response curve of genistein to the left, resulting a lower EC_{50} at ~ 51 μM (Figure 4.5C).

4.2.4 Effect of tyrosine kinase inhibitors and daidzein on TRPC5-mediated $[\text{Ca}^{2+}]_i$ rise

To determine if the genistein effect is related to its inhibitory action on tyrosine kinases, a panel of tyrosine kinase inhibitors was tested. These include a wide spectrum tyrosine kinase inhibitor herbimycin, a src family tyrosine kinase inhibitor PP2, and an inhibitor for epidermal growth factor receptor tyrosine kinase lavendustin A. Unlike genistein, herbimycin (2

μM), PP2 (20 μM) and lavendustin A (10 μM) all failed to stimulate TRPC5 (Figure 4.6A-C and Figure 4.7). In contrast, daidzein, which is a genistein analog inactive towards tyrosine kinases (Akiyama *et al.*, 1987), was capable of stimulating TRPC5 (Figure 4.6D and Figure 4.7).

4.2.5 Independent of estrogen receptors and phospholipase C (PLC) activity

An estrogen receptor antagonist ICI-182780 was used to determine if the genistein effect is mediated through classic estrogen receptor α or β . As shown in Figure 4.8, a pre-incubation of cells with ICI-182780 (50 μM) had no effect on genistein (100 μM)-induced Ca^{2+} influx in TRPC5 expressing cells (Figure 4.8A). Previous reports have shown that receptor activation of TRPC5 relies on phospholipase C activity (Beech, 2007b; Schaefer *et al.*, 2000). However, pretreatment of cells with a phospholipase C inhibitor U73122 (10 μM) did not affect the $[\text{Ca}^{2+}]_i$ response to genistein (Figure 4.9B). U73343 (10 μM), an inactive analog of U73122, also had no effect (Figure 4.9A). These data suggest that the genistein effect on TRPC5 is not mediated through estrogen receptors or phospholipase C.

4.2.6 Action of genistein on TRPC5 current

Whole cell patch clamp was used to verify the stimulating action of genistein on TRPC5. Application of genistein (50 μM) increased whole-cell cation current in TRPC5-overexpressing cells (Figure 4.10 and Figure 4.11A), but not in wild-type HEK cells (Figure 4.11C). Vehicle control experiments were also performed, in which addition of vehicle (DMSO, 0.1%) had no effect on whole cell current in TRPC5-overexpressing cells (Figure 4.11B). Current-voltage relationship

of genistein-stimulated current displays double rectification (Figure 4.11A), which is characteristic of TRPC5 channels (Beech, 2007b). Single channel recordings were made in inside-out membrane patches excised from TRPC5-expressing cells. A low level of basal channel activity could be observed (Figure 4.12A). Application of genistein (50 μM) caused a significant increase in channel activity (Figure 4.12B&D-F). The channel activity was blocked by 75 μM 2-APB (Figure 4.12C), which is a known blocker for TRPC5 (Beech, 2007b). Single channel current voltage relationship was obtained (Figure 4.13B), and the single channel slope conductance was estimated to be ~ 46 pS, which matched the reported values (Alfonso *et al.*, 2008; Jung *et al.*, 2003; Strubing *et al.*, 2001; Yamada *et al.*, 2000).

4.2.7 Effect of genistein on TRPC5 in native endothelial cells

TRPC5 is known to be expressed in the primary cultured BAECs (Yao *et al.*, 2005a). Protein lysate from BAECs showed immuno-reactivity to a protein with similar molecular mass as over-expressed TRPC5 (Figure 4.14A). The immuno-fluorescent signal of TRPC5 proteins was detected in cultured BAECs. The TRPC5 proteins were probed by two TRPC5-specific antibodies: anti-TRPC5 antibody against cytosolic C-terminus (Alomone Lab, 1:100) and T5E3 antibody against extracellular turret (homemade, 1:50) (Figure 4.14B&C).

In functional study, bath application of 100 μM genistein stimulated a $[\text{Ca}^{2+}]_i$ rise in BAECs (Figure 4.15A). This $[\text{Ca}^{2+}]_i$ rise was mostly due to Ca^{2+} influx because it was almost absent in cells that were bathed in a

Ca²⁺-free medium (Figure 4.15B). Incubation of the cells with a TRPC5 blocking antibody T5E3 diminished this genistein-induced [Ca²⁺]_i rise (Figure 4.15A&B), suggesting an involvement of TRPC5.

In addition to BAECs, the effect of genistein on [Ca²⁺]_i in rat mesenteric artery endothelial cells (RMECs) was tested. Primary cultured RMECs show positive immuno-fluorescent signal to TRPC5, which was separately detected by anti-TRPC5 (Alomone Lab) and T5E3 (Figure 4.16A&B). Bath application of 10 μM genistein elicited a [Ca²⁺]_i rise in the cells, which was inhibited by TRPC5 blocking antibody T5E3 (Figure 4.16C&D). The results suggest that TRPC5 on RMECs is stimulated by genistein to increase [Ca²⁺]_i.

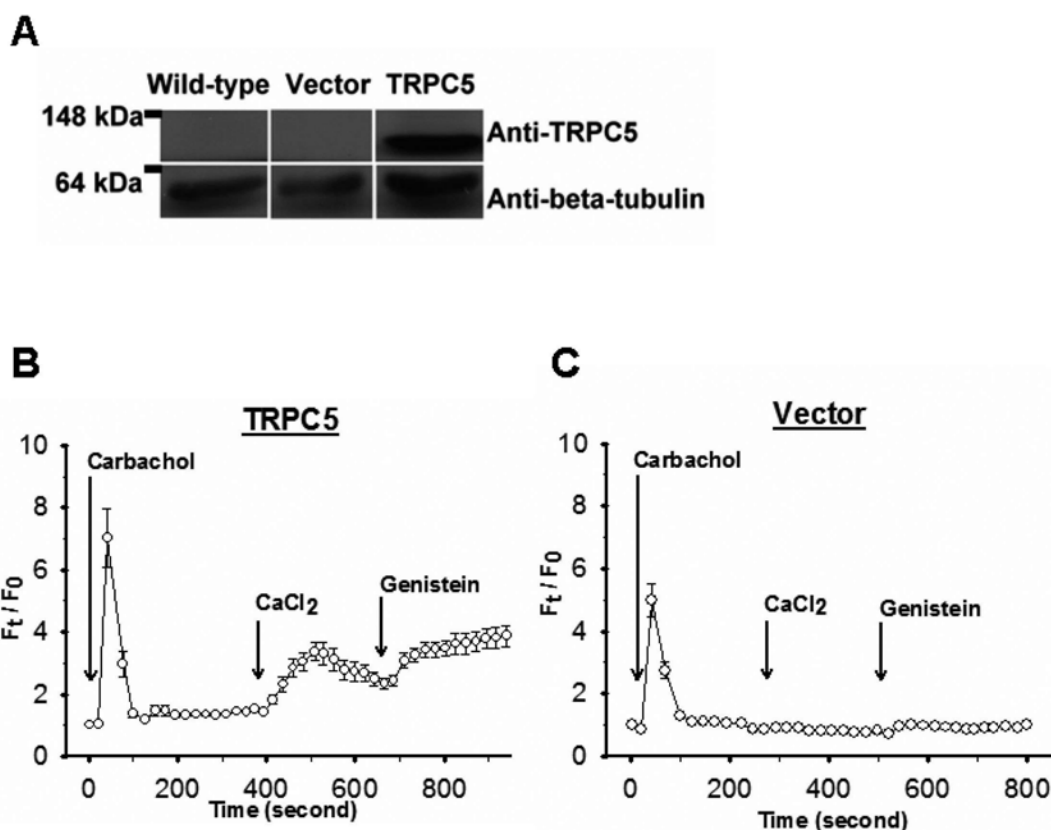


Figure 4.1 Expression of TRPC5 in HEK cells and elevation of $[Ca^{2+}]_i$ by genistein

A, representative image of immunoblot experiments ($n = 3$). TRPC5 protein level was compared between wild-type (Wild-type), pcDNA3-transfected (vector) and TRPC5-transfected (TRPC5) HEK cells. The blot was probed with anti- β -tubulin antibody to confirm equal loading of lanes (lower panel). Molecular weights of protein markers are indicated on the left. B and C, representative time course of $[Ca^{2+}]_i$ change in vector-transfected (C) and TRPC5-transfected HEK cells (B). 100 μ M La^{3+} was included in the bath to block other non-selective cation channels and to select for TRPC5-mediated Ca^{2+} influx. Each trace represents Mean \pm SEM of at least 20 cells in one representative experiment ($n=4$).

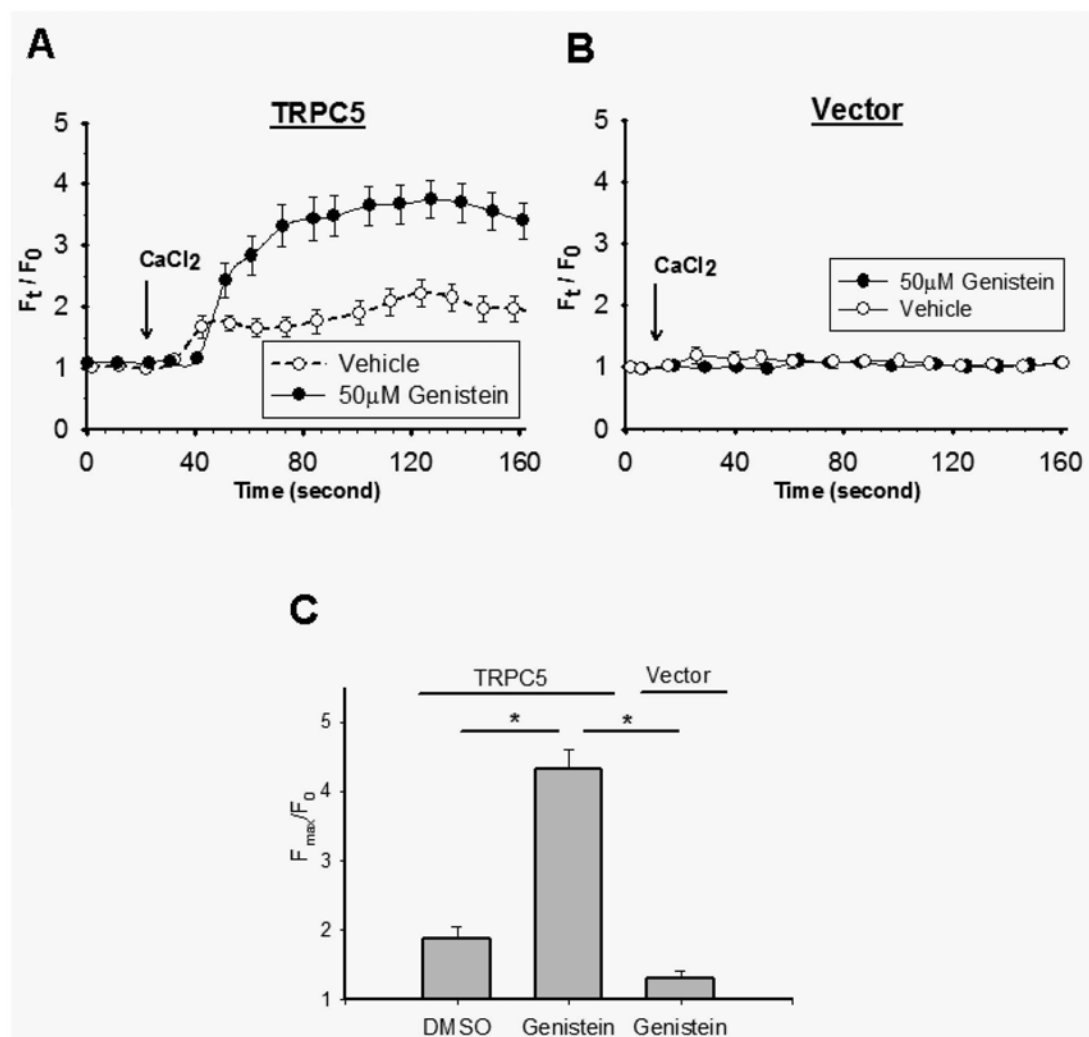


Figure 4.2 TRPC5-mediated Ca^{2+} influx after genistein pretreatment
A and B, representative time course of $[Ca^{2+}]_i$ change in vector-transfected (B) and TRPC5-transfected HEK cells (A); cells were pretreated with genistein (50 μ M) or vehicle (0.1% DMSO) for 10 min in $0Ca^{2+}$ -PSS. Each trace represents Mean \pm SEM of at least 20 cells in one representative experiment (n=4-7). C, summary of data as in A and B, showing mean \pm SEM of the maximal $[Ca^{2+}]_i$ change (n=4-7). * $p < 0.05$.

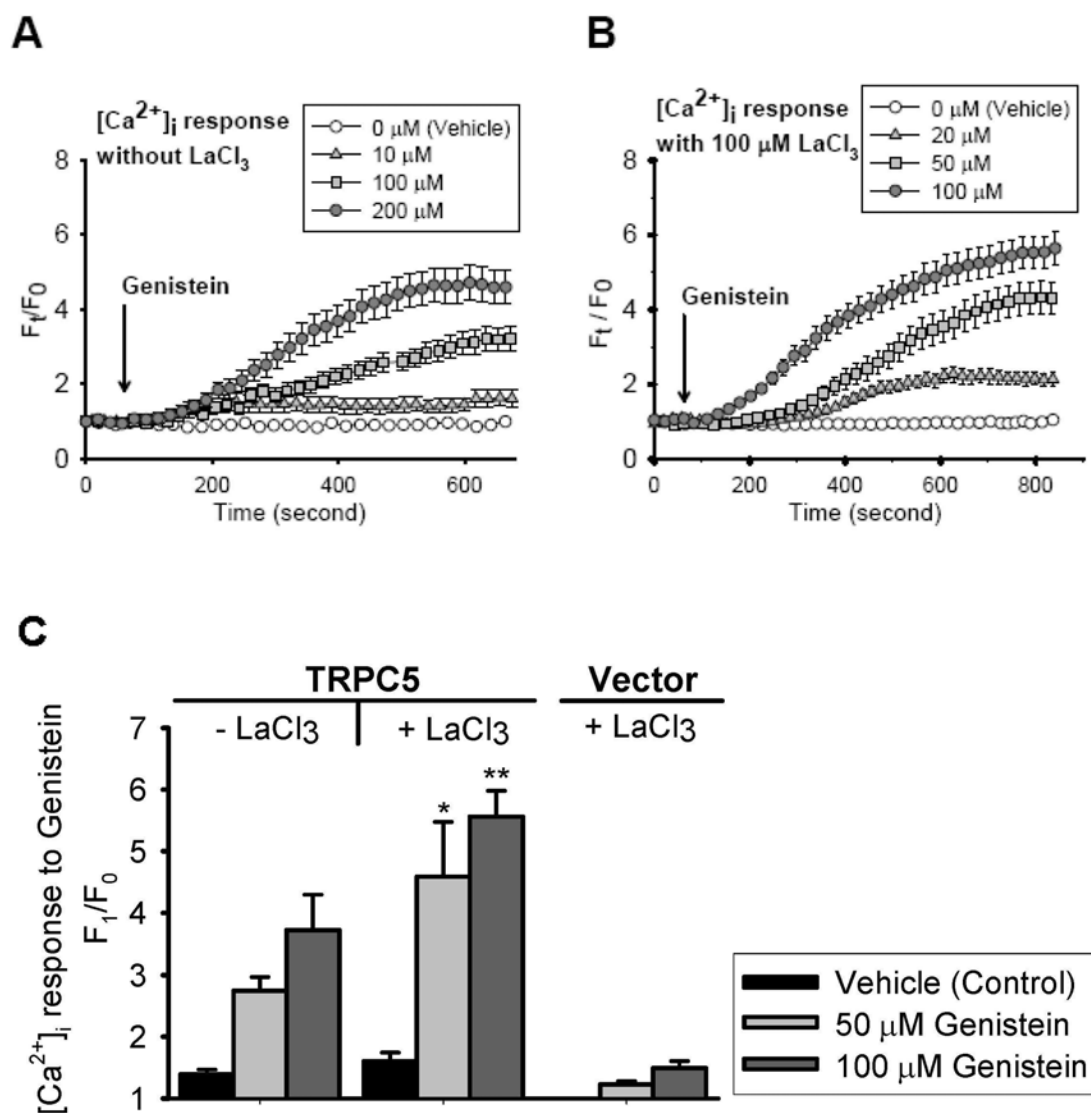


Figure 4.3 Potentiation effect of La³⁺ on genistein-induced TRPC5 activation. A and B, representative time course of [Ca²⁺]_i change in TRPC5-transfected HEK cells in response to different concentrations of genistein. Cells were bathed in NPSS (A) or NPSS+100 μM LaCl₃ (B). Each trace represents mean ± SEM of at least 20 cells from one representative experiment (*n* = 4-10). Vehicle contained 0.1% DMSO. C, summary of data showing the peak [Ca²⁺]_i rise in response to genistein in the absence or the presence of 100 μM LaCl₃. Mean ± SEM (*n* = 3-8). *, *p*<0.05; **, *p*<0.01 compared to vehicle.

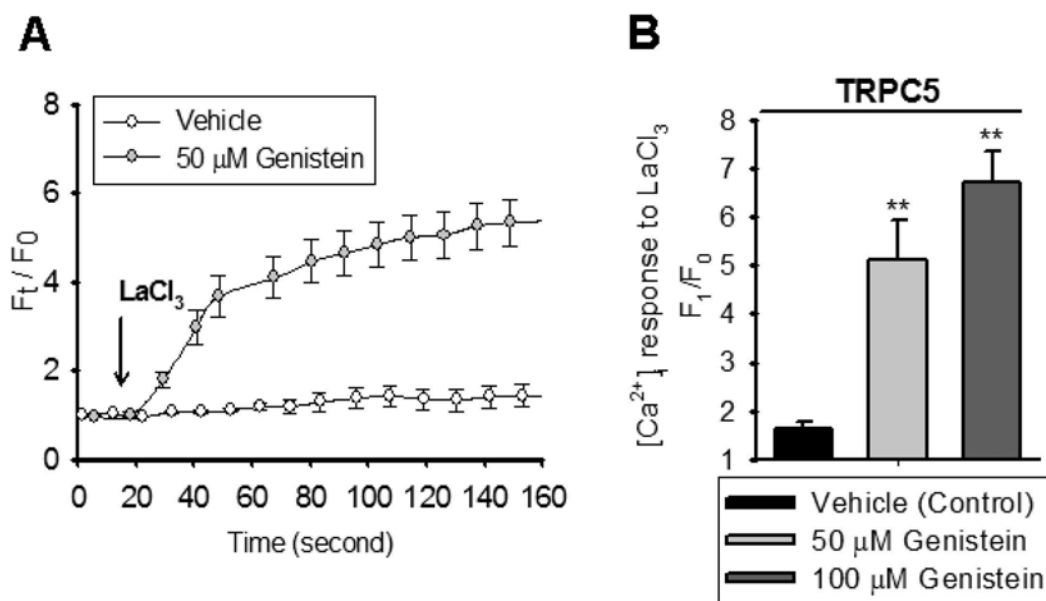


Figure 4.4 Potentiation effect of genistein on La^{3+} -induced TRPC5 activation. A, representative time course of La^{3+} (100 μ M)-induced $[Ca^{2+}]_i$ change in TRPC5-transfected HEK cells in the absence or the presence of 50 μ M genistein. Vehicle contained 0.1% DMSO. Cells were bathed in NPSS. Each trace represents Mean \pm SEM of at least 20 cells from one representative experiment. B, summary of data showing the peak $[Ca^{2+}]_i$ rise in response to 100 μ M La^{3+} . Mean \pm SEM ($n = 4-8$). **, $p < 0.01$ compared to vehicle.

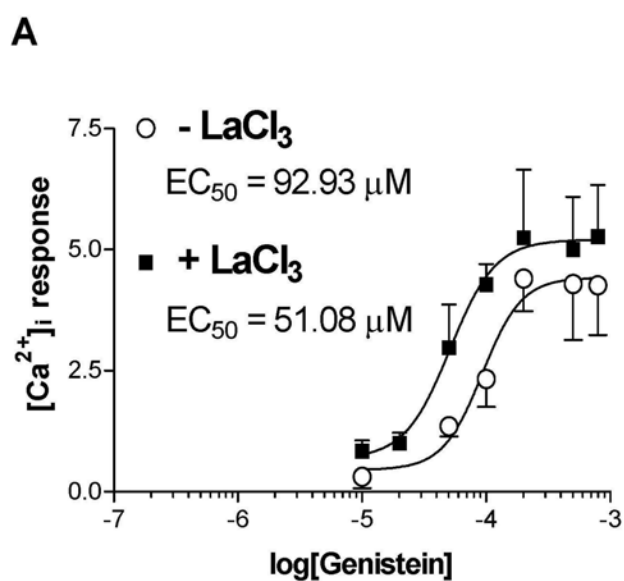


Figure 4.5 Concentration-dependent stimulation of TRPC5 by genistein.

A, plot of concentration-response with curve-fitting to determine the genistein concentration for half-maximal response (EC₅₀). [Ca²⁺]_i response at each concentration was subtracted by the background given by vehicle control. Mean ± SEM (*n* = 4-12).

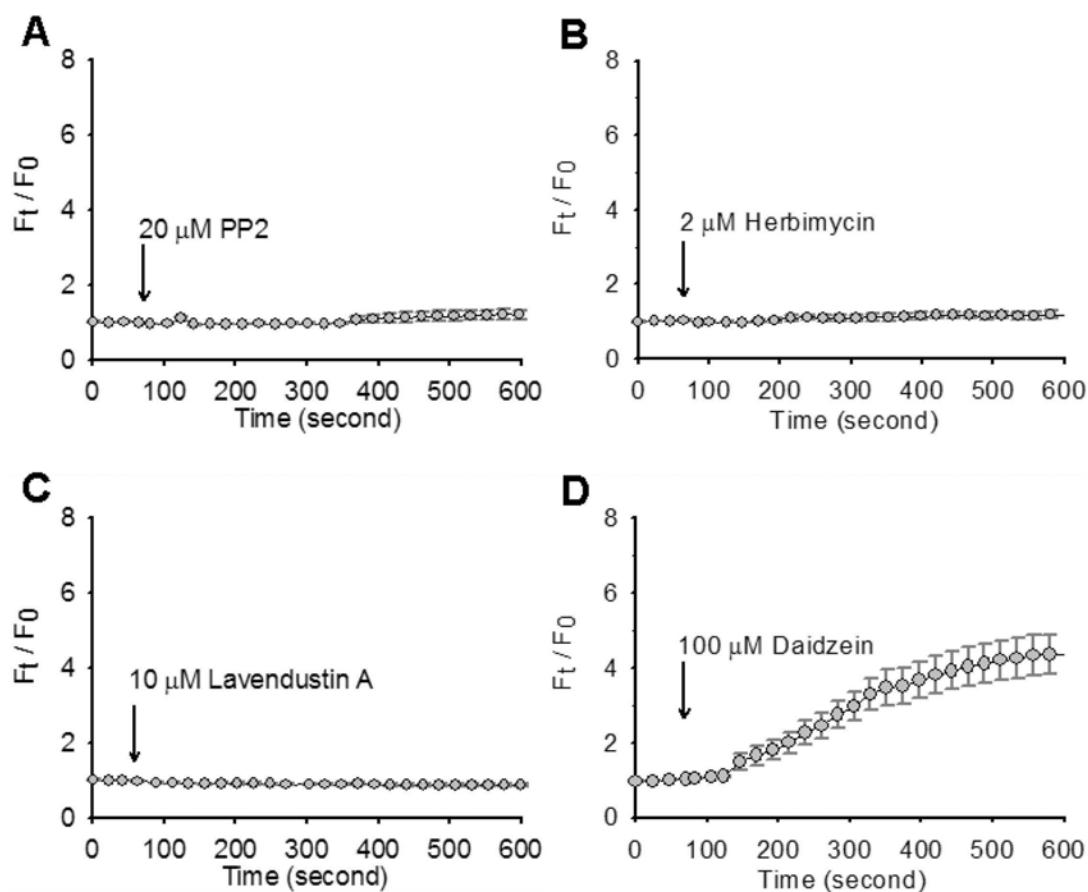


Figure 4.6 Effect of a panel of tyrosine kinase inhibitors and inactive genistein analog daidzein on TRPC5-mediated $[Ca^{2+}]_i$ rise.

A-D, representative time course of $[Ca^{2+}]_i$ change in response to 20 μ M PP2 (A), 2 μ M herbimycin (B), 10 μ M lavendustin A (C), or 100 μ M daidzein (D) in TRPC5-transfected HEK cells. Each trace represents Mean \pm SEM of at least 20 cells from one representative experiment. Cells were bathed in NPSS in the presence of 100 μ M $LaCl_3$.

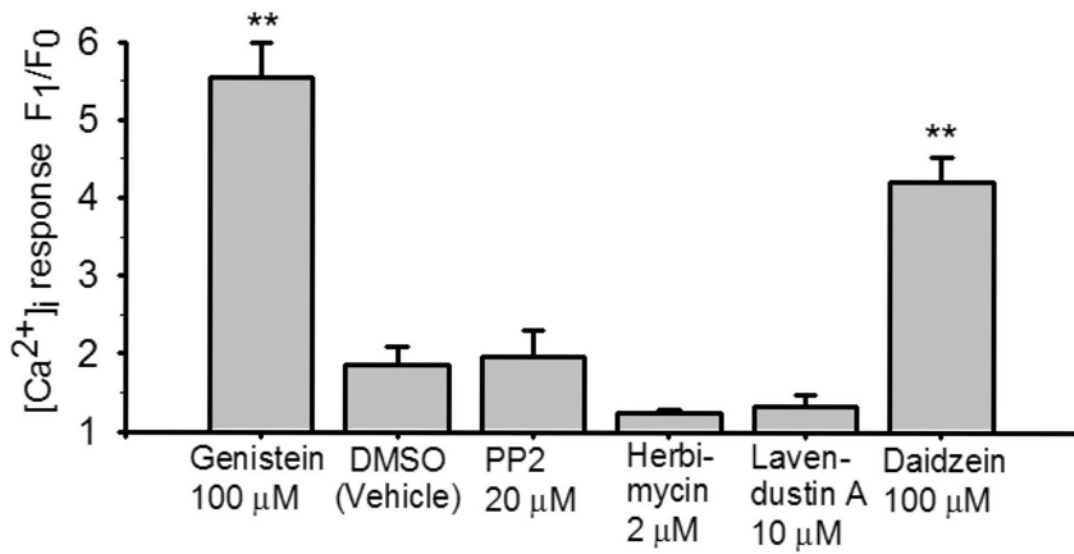


Figure 4.7 Summary of the effect of tyrosine kinase inhibitors and inactive genistein analog daidzein on TRPC5-mediated $[Ca^{2+}]_i$ rise.

Summary of data showing the maximal $[Ca^{2+}]_i$ rise as in Figure 4.6. Mean \pm SEM ($n = 3-8$ experiments). **, $p < 0.01$ compared to vehicle.

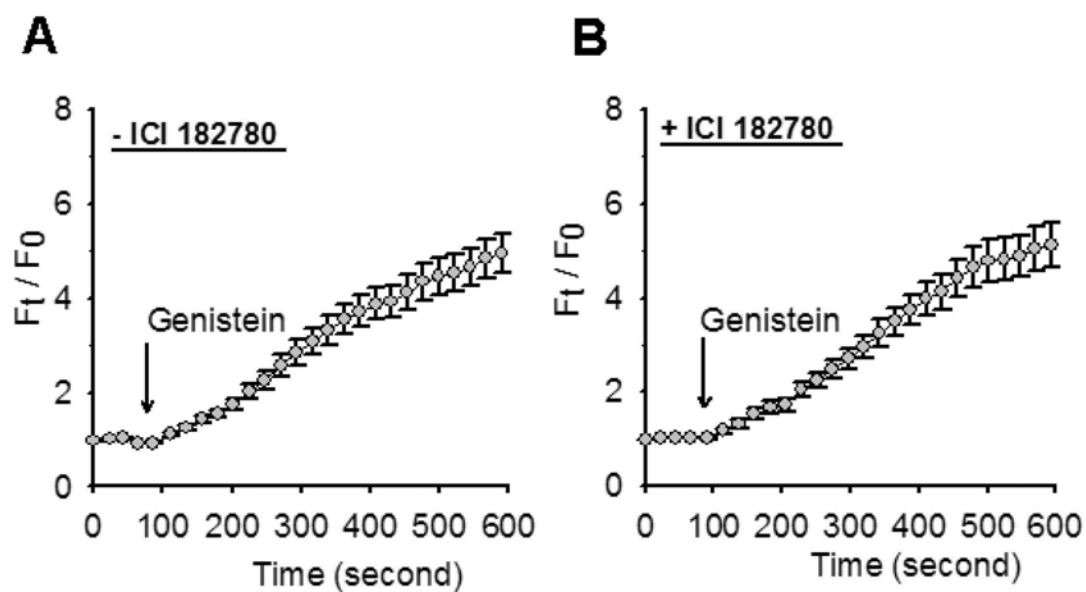


Figure 4.8 Effects of estrogen receptor antagonist ICI-182780 on TRPC5-mediated $[Ca^{2+}]_i$ rise.

Shown were representative time course of $[Ca^{2+}]_i$ change in response to 100 μ M genistein in TRPC5-transfected HEK cells in the absence (A) or the presence (B) of 50 μ M ICI-182780. Cells were pretreated with ICI-182780 for 5 min. Each trace represents Mean \pm SEM of at least 20 cells in one representative experiment ($n=3-5$).

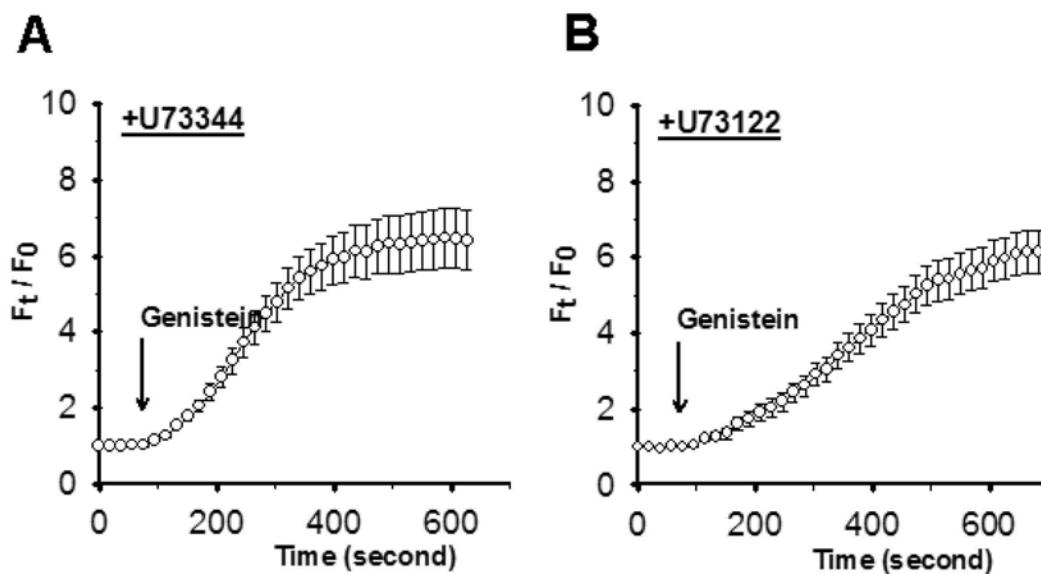


Figure 4.9 Effects of phospholipase C inhibitor U73122 on TRPC5-mediated $[Ca^{2+}]_i$ rise.

Shown were representative time course of $[Ca^{2+}]_i$ change in response to 100 μ M genistein in TRPC5-transfected HEK cells in the presence of 10 μ M U73343 (A) or 10 μ M U73122 (B). Cells were pretreated with U73122 or U73343 for 30 min. Each trace represents Mean \pm SEM of at least 20 cells in one representative experiment ($n=4$).

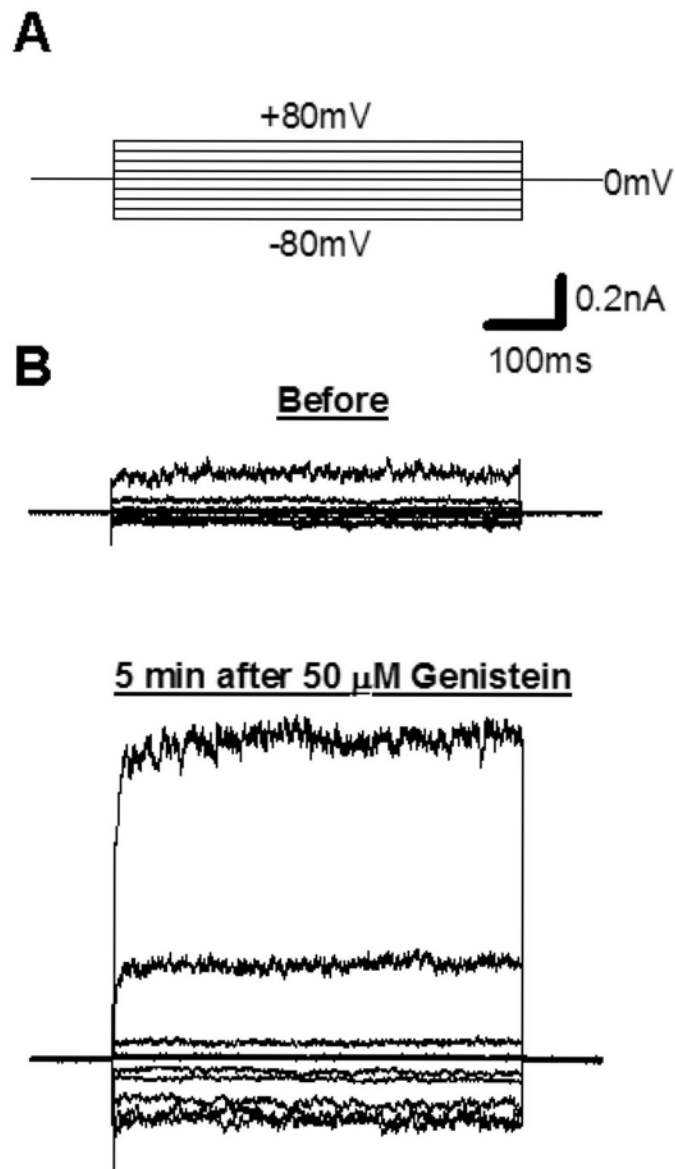


Figure 4.10 Stimulating action of genistein on the whole-cell currents in TRPC5-expressing HEK cells.

A and B, representative traces showing voltage protocol (A) and corresponding whole-cell currents (B) immediately before and 5 min after bath application of 50 μ M genistein in TRPC5-transfected HEK cells.

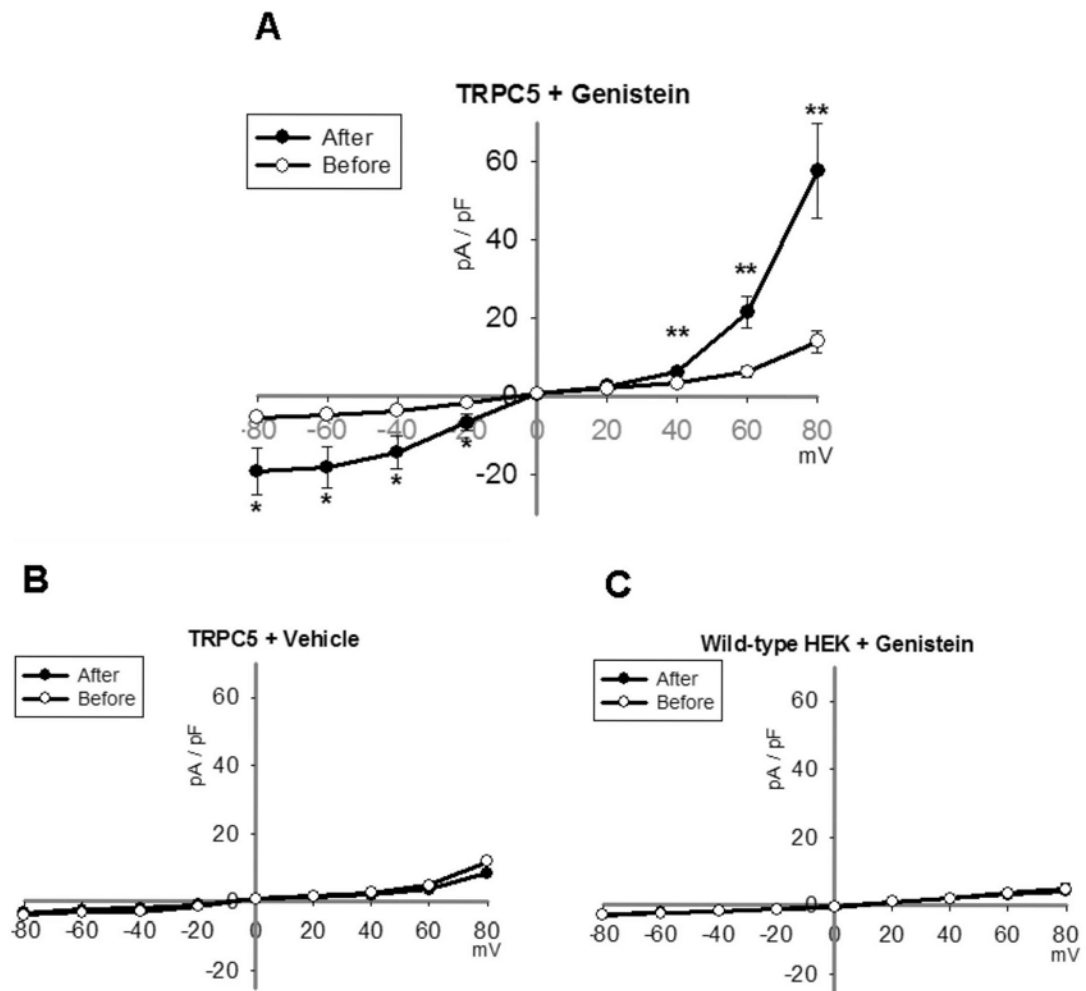


Figure 4.11 Stimulating action of genistein on the whole-cell currents due to TRPC5.

A-C, current-voltage relationships for TRPC5-transfected (A and B) or wild-type HEK cells (C) immediately before (open circles) and 5 min after (solid black circles) bath application of 50 μ M genistein (A and C) or 0.1% DMSO (B). Mean \pm SEM ($n = 3-8$). *, $p < 0.05$; **, $p < 0.01$ compared to “Before”.

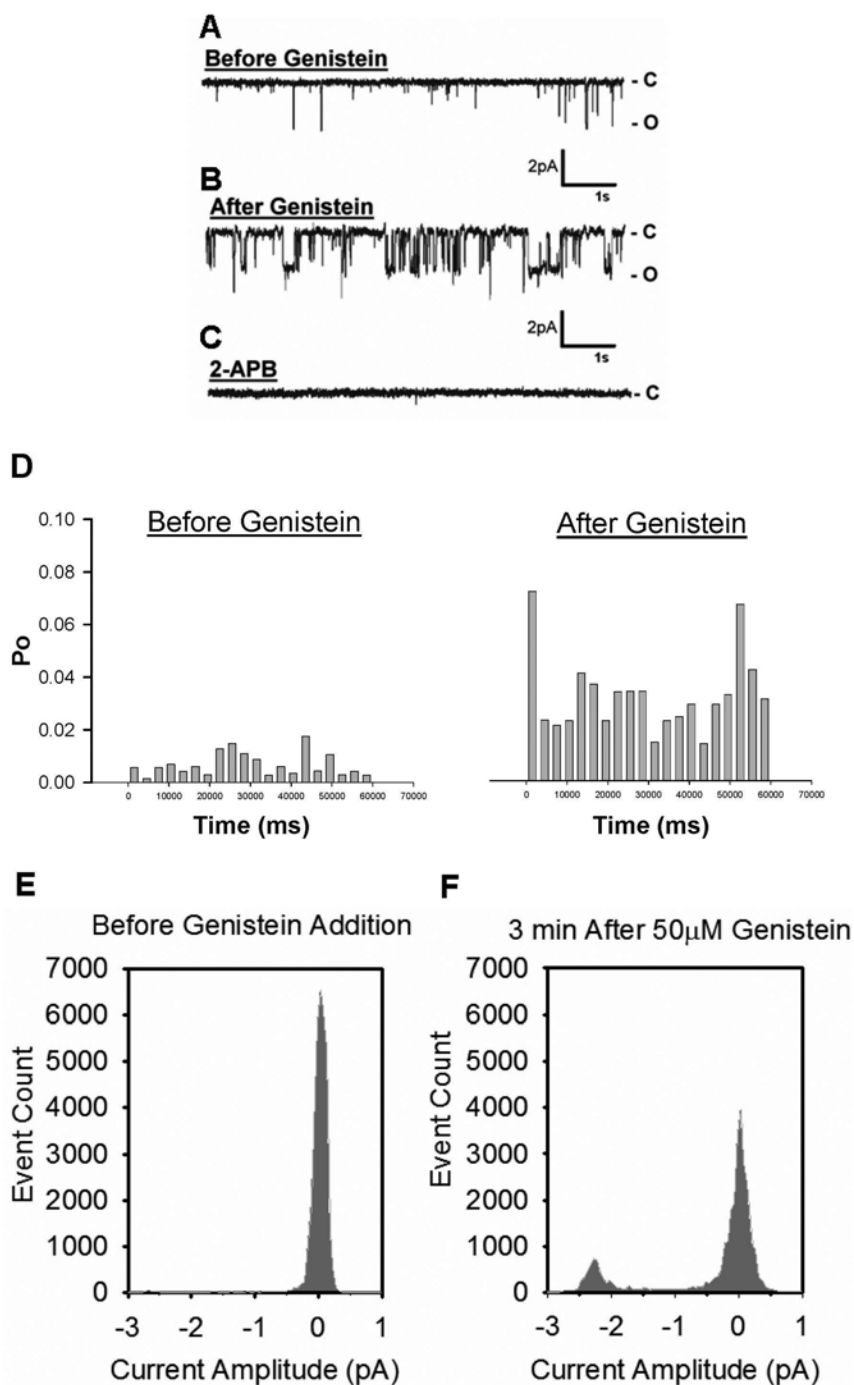


Figure 4.12 Single channel recording of genistein-modulated channels in excised inside-out patches from TRPC5-transfected HEK cells.

A-C, representative single channel traces in the absence (A) or the presence (B and C) of 50 μM genistein. Addition of 75 μM 2-APB abolished the current (C). The patch potential was held at -60 mV. **C**: Close state; **O**: Open state. D, channel open probability (P_o) changes over time during the patch recording as in A and B, before and after application of 50 μM genistein to the intracellular side of the membrane patch, calculated for each consecutive 3 sec interval. E and F, event histogram of a representative experiment before (E) and after (F) 50 μM genistein application at -60 mV. ($n = 3-5$)

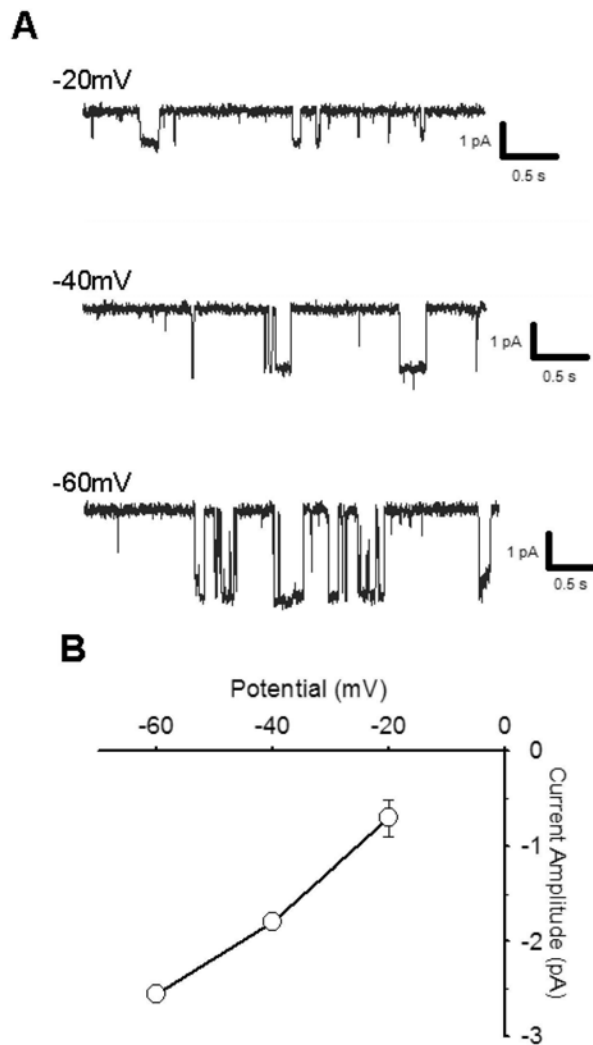


Figure 4.13 Single channel conductance of the genistein-sensitive channel

A, single channel traces of an inside-out patch from TRPC5-expressing HEK cells during incubation with 50 μ M genistein; membrane patches were clamped at -20 mV, -40 mV and -60 mV potentials. B, single channel current-voltage relationship of the genistein-sensitive channel recorded on TRPC5-expressing HEK cells. Mean \pm SEM ($n = 3-5$).

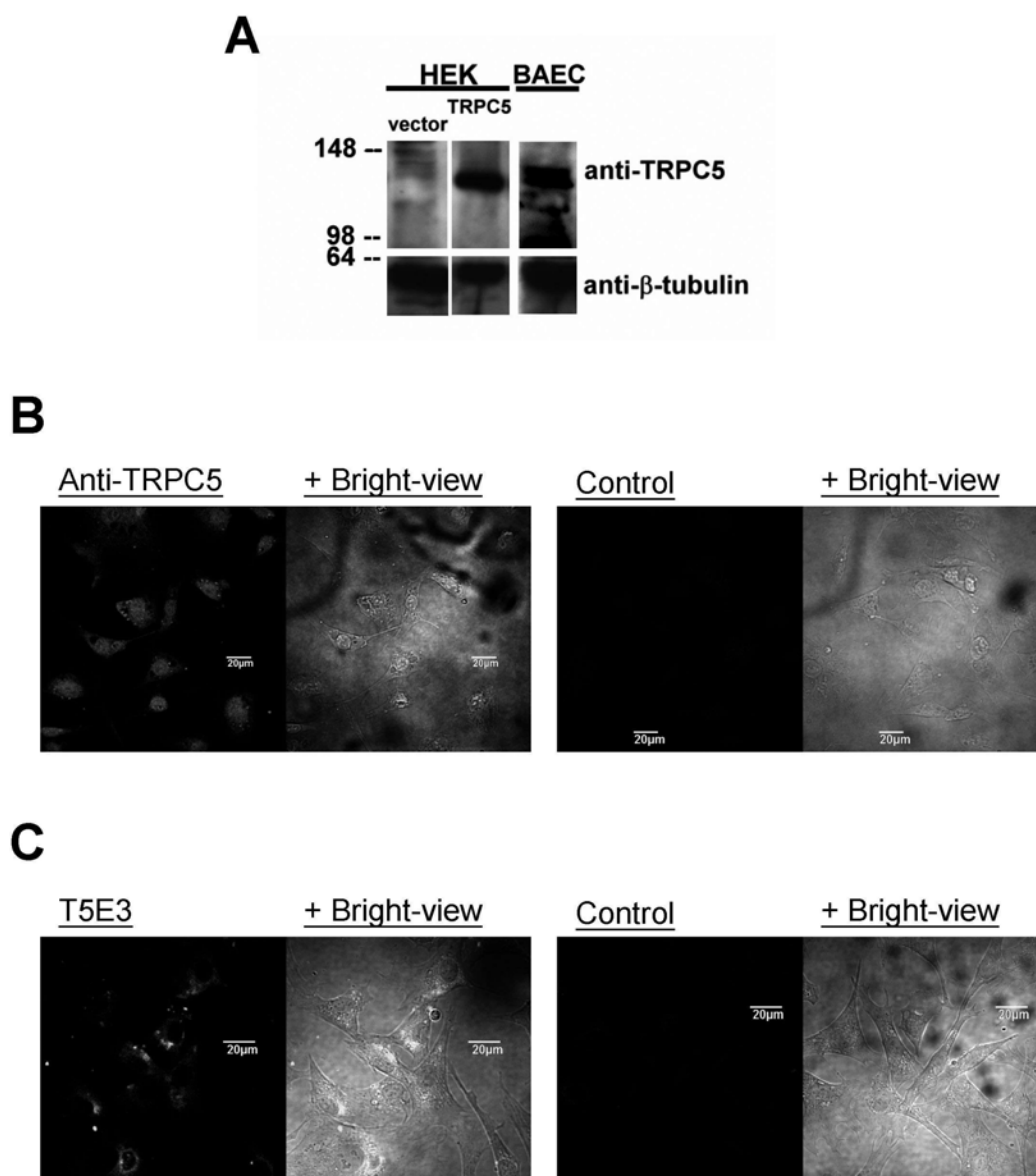


Figure 4.14 Expression of TRPC5 protein in primary cultured bovine aortic endothelial cells (BAECs)

A, representative image of immunoblot probed with anti-TRPC5 (Alomone Lab) and anti- β -tubulin ($n = 3$). TRPC5 protein levels were compared between the lysates from: (left panel) vector-transfected HEK cells (vector); (middle panel) TRPC5-transfected HEK cells; and (right panel) BAECs. The blot was probed with anti- β -tubulin antibody to confirm equal loading of lanes (lower panel). Molecular weights (kDa) of protein markers are indicated on the left. B and C, immunocytochemical detection of TRPC5 in BAECs by confocal microscopy. Immuno-reactivity to TRPC5 detected by anti-TRPC5 antibody (B, left panel) and T5E3 antibody (C, left panel). The paired images show TRPC5 fluorescent signal (left) and the bright-view image merged with fluorescent signal (right). The control images (right panel) were from sections without addition of primary antibodies.

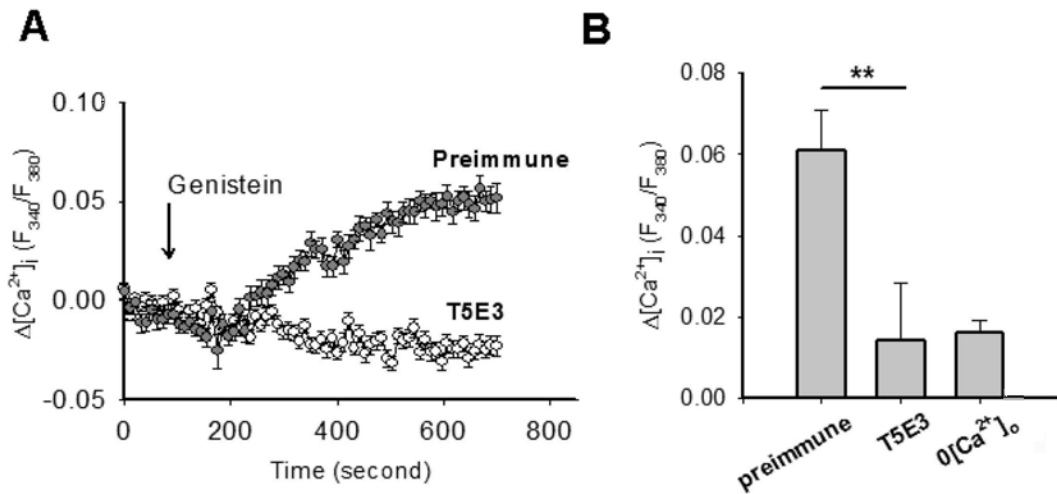


Figure 4.15 Effect of genistein on TRPC5-mediated $[Ca^{2+}]_i$ rise in bovine aortic endothelial cells (BAECs)

A, representative time course of $[Ca^{2+}]_i$ change in response to 100 μ M genistein in BAECs that were pre-incubated with T5E3 (4 μ g/ml) or pre-immune IgG (4 μ g/ml, labeled as “preimmune”) for 10 minutes. Each trace represents Mean \pm SEM of at least 15 cells from one representative experiment ($n=6-8$). B, summary of data showing $[Ca^{2+}]_i$ changes 10 minutes after application of genistein. $0[Ca^{2+}]_o$, Ca^{2+} -free HBS bath solution. Mean \pm SEM ($n = 3$ for $0[Ca^{2+}]_o$; $n = 6$ for T5E3; $n = 8$ for preimmune). **, $p < 0.01$

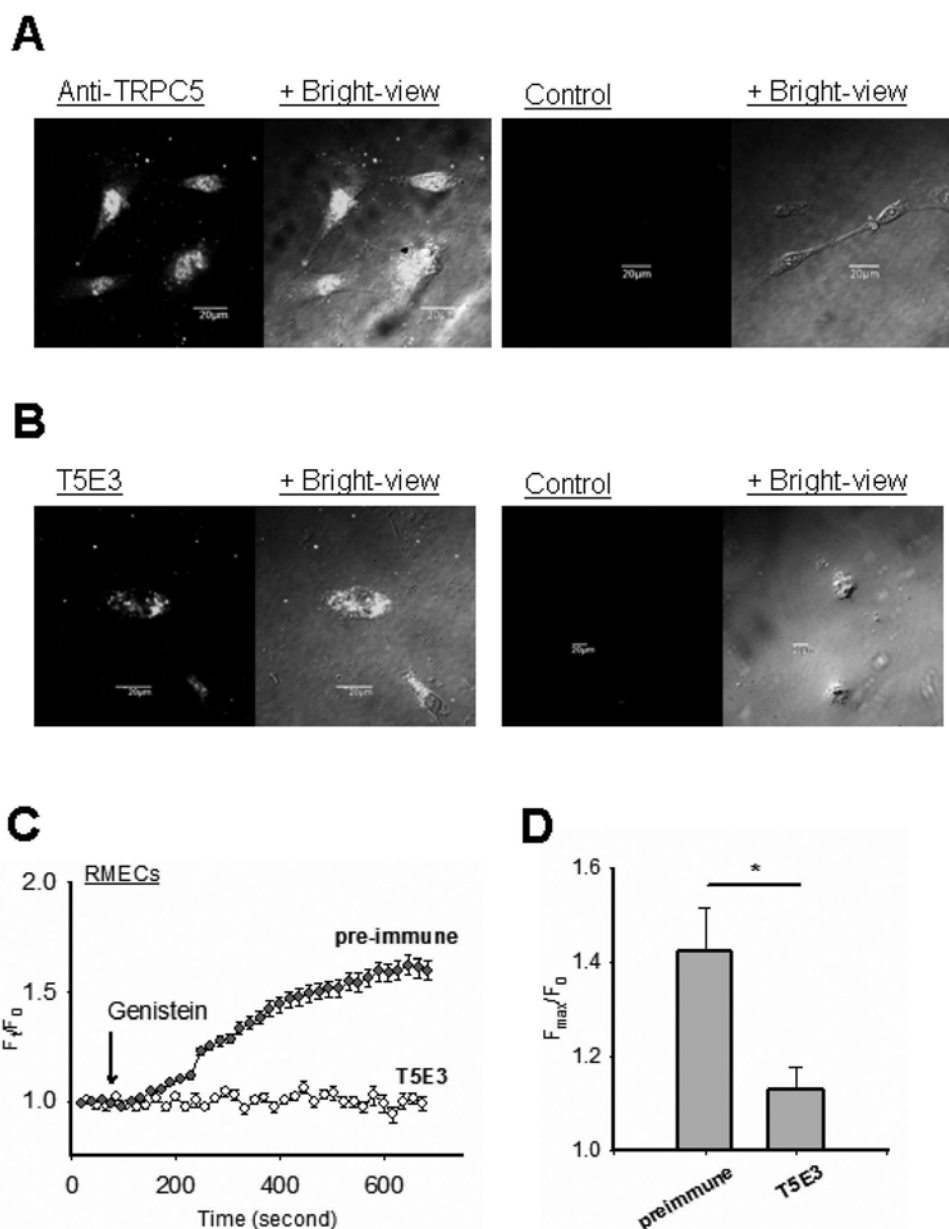


Figure 4.16 Effect of genistein on TRPC5-mediated $[Ca^{2+}]_i$ rise in rat mesenteric artery endothelial cells (RMECs)

A and B, immunocytochemical detection of TRPC5 in BAECs by confocal microscopy. Immuno-reactivity to TRPC5 detected by anti-TRPC5 antibody (A, left panel) and T5E3 antibody (B, left panel). The paired images show TRPC5 fluorescent signal (left) and the bright-view image merged with fluorescent signal (right). The control images (right panel) were from sections without addition of primary antibodies. C, representative time course of $[Ca^{2+}]_i$ change in response to 10 μ M genistein in RMECs that were pre-incubated with T5E3 (4 μ g/ml) or pre-immune IgG (4 μ g/ml, labeled as “preimmune”) for 15 minutes. Each trace represents Mean \pm SEM of at least 8 cells from one representative experiment ($n=5-7$). D, summary of data showing maximal $[Ca^{2+}]_i$ changes after application of genistein. Mean \pm SEM ($n=5-7$). *, $p<0.05$

4.3 Discussion

In the present study, we found that genistein augmented TRPC5-mediated Ca^{2+} influx in both the heterologously expressed HEK cells and the primary cultured bovine aortic endothelial cells. Genistein also enhanced TRPC5-mediated cation current. The stimulating effect of genistein synergized with La^{3+} , which is a well documented potentiator for TRPC5. The effect of genistein could not be mimicked by several other tyrosine kinase inhibitors, but it could be mimicked by daidzein, which is inactive for tyrosine kinase inhibition. The action by genistein was not mediated through estrogen receptors or phospholipase C, because selective inhibitors against these targets had no effect. Importantly, the stimulating action of genistein on TRPC5 could be demonstrated on excised inside-out patches. Taken together, these data suggest that the action of genistein on TRPC5 is relatively direct.

Several different protocols were used to determine whether genistein could indeed enhance TRPC5 activity in heterologously expressed HEK293 cells. In the first protocol, the TRPC5-expressing cells were treated with carbachol in a Ca^{2+} -free medium, followed by extracellular Ca^{2+} addition, which initiated a Ca^{2+} influx. Genistein was then added. It was found that the genistein application elicited a further Ca^{2+} rise. In the second protocol, cells were pretreated with genistein in a Ca^{2+} -free medium, followed by extracellular Ca^{2+} addition, which elicited a $[\text{Ca}^{2+}]_i$ rise. It was found that the magnitude of this $[\text{Ca}^{2+}]_i$ rise was much larger in genistein-pretreated cells than those without genistein pretreatment. In the third protocol, direct addition of genistein caused a $[\text{Ca}^{2+}]_i$ rise in cells bathed in Ca^{2+} -containing physiological solution. Furthermore, in patch clamp studies, genistein stimulated TRPC5-mediated

cation current in whole cell patches and in excised inside-out patches. These data confirmed a stimulating action of genistein on TRPC5 activity. Interestingly, we observed that lanthanum and genistein act synergistically on TRPC5. Lanthanum is previously known to interact with the negatively-charged amino acid residues near the extracellular pore region of TRPC5 proteins, thereby potentiating the channel opening (Jung *et al.*, 2003). In the present study, lanthanum was able to potentiate the stimulating action of genistein on TRPC5. Conversely, genistein was also capable of potentiating the lanthanum action on TRPC5.

Genistein is a phytoestrogen that can act on estrogen receptors at nanomolar level (Escande *et al.*, 2006). Activity of estrogen receptors can alter ion homeostasis in a variety of tissues and cells including central nervous system, vascular system, and pancreatic endocrine cells (Kelly *et al.*, 2001; Nadal *et al.*, 2004; Raz *et al.*, 2008). In the present study, an estrogen receptor antagonist ICI82780 had no effect on the stimulating action of genistein on TRPC5, suggesting that the action is independent of classical estrogen receptors. Genistein is also commonly used as tyrosine kinase inhibitors. At the concentration range of 10-100 micromolar, genistein inhibits tyrosine kinases (Barnes *et al.*, 2000). Indeed, genistein was found to inhibit ATP-sensitive K⁺ channel, N-type Ca²⁺ channels, T-type channels, TRPC3, and TRPM2, via a tyrosine kinase-dependent mechanism (Kawasaki *et al.*, 2006; Morikawa *et al.*, 1998; Ogata *et al.*, 1997; Zhang *et al.*, 2007). However, in the present study, we found that the genistein action could not be mimicked by other tyrosine kinase inhibitors including herbimycin, PP2 and lavendustin A. On the other hand, the genistein action could be mimicked by daidzein, which is inactive for tyrosine

kinase inhibition. Therefore, the genistein effect on TRPC5 is independent of tyrosine kinases. It has been reported that the membrane-anchored phospholipase C is critical to the receptor-operated TRPC5 activation (Schaefer *et al.*, 2000). However, in the present study, inhibition of phospholipase C by U73122 had no effect on the genistein action on TRPC5, suggesting that the genistein action on TRPC5 is not mediated through phospholipase C.

Evidence shows that genistein may inhibit multiple ion channels via a relatively direct mechanism. These include L-type Ca^{2+} channel (Belevych *et al.*, 2002; Chiang *et al.*, 1996), voltage-gated Na^{+} channel (Paillart *et al.*, 1997), voltage-gated K^{+} channel (Smirnov *et al.*, 1995) and inward rectifying K^{+} channel (Chiang *et al.*, 2002). Unlike most of other studies, we found that genistein stimulates TRPC5 activity. Furthermore, the effect of genistein can be demonstrated on excised inside-out patches, suggesting that the action is relatively direct and does not require a cytosolic factor. However, it is unclear how genistein modulates TRPC5 exactly. One possibility is that genistein may alter lipid layer properties. It is reported that genistein can be adsorbed and partitioned onto the plasma membrane, thus altering elastic properties of lipid bilayer (Arora *et al.*, 2000; Hwang *et al.*, 2003; Whaley *et al.*, 2006). Such an alteration in lipid environment may cause a change in gating properties of some ion channels. This model has been previously used to explain the genistein-induced activation of gramicidin A channels (Hwang *et al.*, 2003), which are a group of short antibiotic peptides produced by *Bacillus brevis*. We speculate that a similar mechanism may underlie the stimulating action of genistein on TRPC5. To our support, genistein applied from either side of the membrane was found to stimulate TRPC5 (Fig. 4.10-4.13). In addition,

daidzein, which only differs from genistein by having one less -OH and is also incorporated into lipid bilayer (Whaley *et al.*, 2006), exerts similar stimulatory action on TRPC5. Interestingly, several reports have shown that TRPC5 activity could be modulated by phosphatidylinositol-4,5-bisphosphate (Trebak *et al.*, 2008), lysophosphatidylcholine (Flemming *et al.*, 2006), and sphingosine 1-phosphate (from the intracellular side) (Beech, 2007a), all of which are capable of inserting into bilayer. Indeed, TRPC5 has been proposed as a sensor for endogenous phospholipids (Beech, 2007a; Beech, 2007b; Flemming *et al.*, 2006). Therefore, it is likely that natural isoflavones, i.e. genistein and daidzein, may stimulate TRPC5 by altering channel-lipid interaction. The present study is the first to demonstrate the ability of isoflavones to stimulate a TRP channel.

Plant-derived estrogenic molecules and isoflavones have received a great deal of attention over the past decade because of their potentially preventive roles against cardiovascular diseases (Si *et al.*, 2007). Among these compounds, genistein in particular has been shown to be the most efficacious in animal models and experimental studies. Genistein *in vitro* relaxes rat arteries by a nitric oxide- and/or endothelium-dependent mechanism (Altavilla *et al.*, 2004; Mishra *et al.*, 2000). Results from the experiments with primary cultured endothelial cells suggest that genistein is capable of stimulating native TRPC5 to increase $[Ca^{2+}]_i$, which is a precedent signal to nitric oxide (NO) production and subsequent vasorelaxation. Results from Chapter 2 reveal that NO is unlikely to mediate the stimulation of TRPC5 by genistein. In addition, data from the functional studies with expression system supports a direct action of genistein on TRPC5. The results indicate TRPC5 as one of the NO-independent mediators accounting for the previously recognized acute vasorelaxation by

genistein. On the other hand, the present study focused on endothelial TRPC5 only. It is notable that vascular smooth muscle cells also expressed functional TRPC5 (Beech, 2007b). Further investigation is needed to address the effect of genistein on TRPC5 in the intact vasculature.

In conclusion, genistein stimulates the activity of TRPC5. The action was neither related to tyrosine kinase phosphorylation nor related to estrogen receptors. Genistein and lanthanum act synergistically to stimulate TRPC5-mediated Ca^{2+} influx. The stimulating action of genistein on TRPC5 can be mimicked by daidzein, which can also be partitioned into lipid bilayer. Furthermore, the stimulation can be recorded on excised inside-out patches. These data suggest that the genistein action is relatively direct. It is possible that genistein enhances TRPC5 activity by modifying the channel-lipid interaction in the bilayer. Finally, native TRPC5 expressed in vascular endothelial cells is stimulated by genistein to increase cytosolic Ca^{2+} level.

5 Chapter 5

TRPC5 mechanosensitivity and functional role in arterial baroreceptor

5.1 Introduction

Channels embedded in the lipid bilayer are constantly exposed to the negative and positive mechanical forces exerted on the bilayer (Cantor, 1997). External mechanical forces acting on the bilayer change the transverse pressure profile, and directly transduce the pressure to the embedded protein by lipid-protein interactions (Figure 5.1). In this case, force is delivered to the channel by surface tension or bending of the lipid bilayer, causing a hydrophobic mismatch that favours opening (Hamill *et al.*, 2001). The channel opening decreases the energy stored in surface tension (Figure 5.1). In another scenario, the primary force sensors could be the cytoskeletons or extracellular matrix proteins (Hamill *et al.*, 2001). Cytoskeletal proteins thus can act as force transducer to the tethered channel protein, and gate the channel by inducing conformational change (Figure 5.1). In addition, a channel can be considered mechanically sensitive but not mechanically gated. Force sensing enzymes may generate second messengers to gate the channel, thus conferring the channel responsiveness to mechanical force (Figure 5.1).

TRP channels are regarded as cellular sensors, which detect a wide variety of stimuli including mechanical forces and changes in cell volume (Lin *et al.*, 2005; Pedersen *et al.*, 2007). Several TRPs have been implicated to possess such features, including: TRPC1, TRPC6, TRPM3, TRPM4, TRPV1, TRPV2,

TRPV4 and TRPA1. However, there is controversy as to whether some of these TRPs such as TRPC1 and TRPC6 can serve as a direct mechano-sensor (Gottlieb *et al.*, 2008; Yamamoto *et al.*, 2006). On the other hand, membrane stretch or cell swelling/shrinkage concomitantly alters metabolism of signaling molecules which may affect the activity of downstream TRP channels (Pedersen *et al.*, 2007; Vriens *et al.*, 2004; Yamamoto *et al.*, 2006). Thus, comprehensive methods have to be applied in order to define a TRP channel as mechanosensitive. Most importantly, demonstrating the channel mechanosensitivity on physiological context is crucial to substantiate the definition.

A recent report demonstrated that TRPC5 is activated upon hypo-osmotic and pressure-induced cell swelling (Gomis *et al.*, 2008). Although the data do not appear to be sufficient to define TRPC5 as a mechanosensor, TRPC5 is indeed found to be expressed in many kinds of cells with inherit mechanosensitive Ca^{2+} influx including endothelial cells, smooth muscle cells, cardiac myocytes and arterial baroreceptor neurons (Bush *et al.*, 2006; Flemming *et al.*, 2006; Glazebrook *et al.*, 2005; Yip *et al.*, 2004). The functional role of TRPC5 at baroreceptor is of high interest since it is believed that the mechanosensors are cation channels (Chapleau *et al.*, 1995a; Chapleau *et al.*, 2001).

Arterial baroreceptors are nerve termini that innervate adventitia of arterial wall (Figure 5.2). The baroreceptors at aortic arch and carotid sinus respond to stretching of vessel wall as a result of alteration in arterial blood pressure (Kirchheim, 1976). The mechanical signal is transduced to electrical signal by mechanosensitive channels that depolarize the membrane upon stimulation.

Subsequent opening of voltage-gated channels in response to depolarization generates action potentials. Action potentials are transmitted along the fibers to the cell bodies at frequencies related to the magnitude of depolarization (Figure 5.2). The baroreceptor discharge is interpreted by the central nervous system to trigger reflex adjustments that oppose the change in blood pressure (Kirchheim, 1976).

Evidence suggests that these mechanosensitive channels are permeable to Na^+ and Ca^{2+} , and the elevated cation influx upon increased arterial pressure is responsible for inducing membrane depolarization (Chapleau *et al.*, 1995a; Chapleau *et al.*, 2001). Extracellular gadolinium, but not lanthanum, has been known to block the mechanically induced Ca^{2+} influx (Cunningham *et al.*, 1997; Cunningham *et al.*, 1995; Ditting *et al.*, 2003; Hajduczuk *et al.*, 1994; Sharma *et al.*, 1995; Sullivan *et al.*, 1997). It has been shown that the Ca^{2+} influx is not mediated by voltage-gated channel (Sullivan *et al.*, 1997). The identity of the mechanosensitive channels at baroreceptor was not known until the discovery of the degenerin/epithelial Na^+ channel (DEG/ENaC) subunits at aortic baroreceptor (Drummond *et al.*, 2001). Nevertheless, the mechanosensitive Ca^{2+} channel(s) remains elusive. A recent study revealing the expression of TRPC proteins in aortic baroreceptor hints that TRP channel may play the role (Glazebrook *et al.*, 2005).

In the present study, the mechanosensitivity of TRPC5 is characterized by fluorescent Ca^{2+} imaging and electrophysiological techniques. In addition, functional role of native TRPC5 expressed at aortic baroreceptor neurons is demonstrated by both *in vitro* and *in vivo* studies.

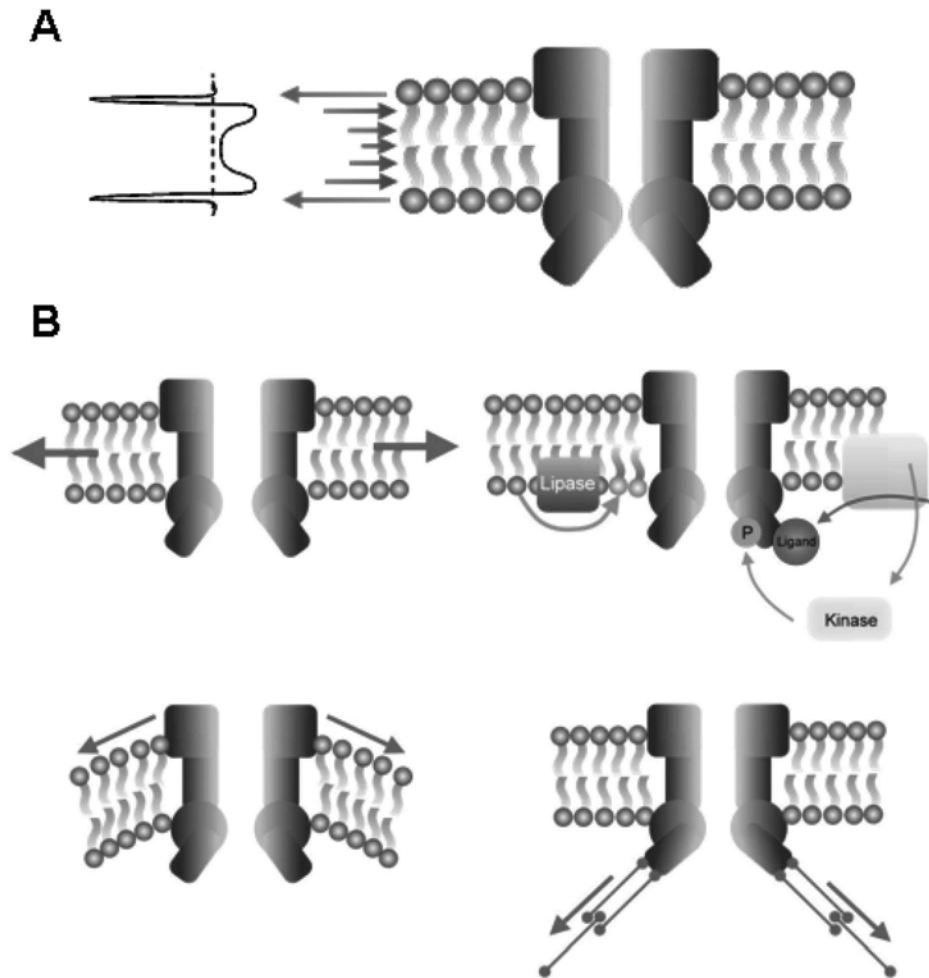


Figure 5.1 Gating modes of mechanosensitive channel

A, Pressure profile of a membrane-embedded channel. Channel in a plasma membrane is exposed to lateral forces from the lipid bilayer, indicated by the pressure profile at the left-hand side, which create positive or negative forces (arrows) acting on the channel. In equilibrium, the conformational energy of the channel matches this pressure profile. Any changes in this equilibrium may cause modulation of channel activity. B, Potential gating mechanisms for mechanically sensitive ion channels. Force is delivered to the channel by surface tension or bending of the lipid bilayer, causing a hydrophobic mismatch that favours opening. Opening decreases the energy stored in surface tension (*upper & lower left*); channel gating can be a consequence of regulation by signaling events initiated by a distant mechano-sensor, e.g. membrane-bound mechanosensitive lipase (*upper right*); another model supposes that specific accessory proteins such as cytoskeletal proteins and/or extracellular matrix molecules are bound to channel, and that the stimulus force is conveyed by these tethers to induce a conformational change (*lower right*). Adapted and modified from Pedersen and Nilius (2007).

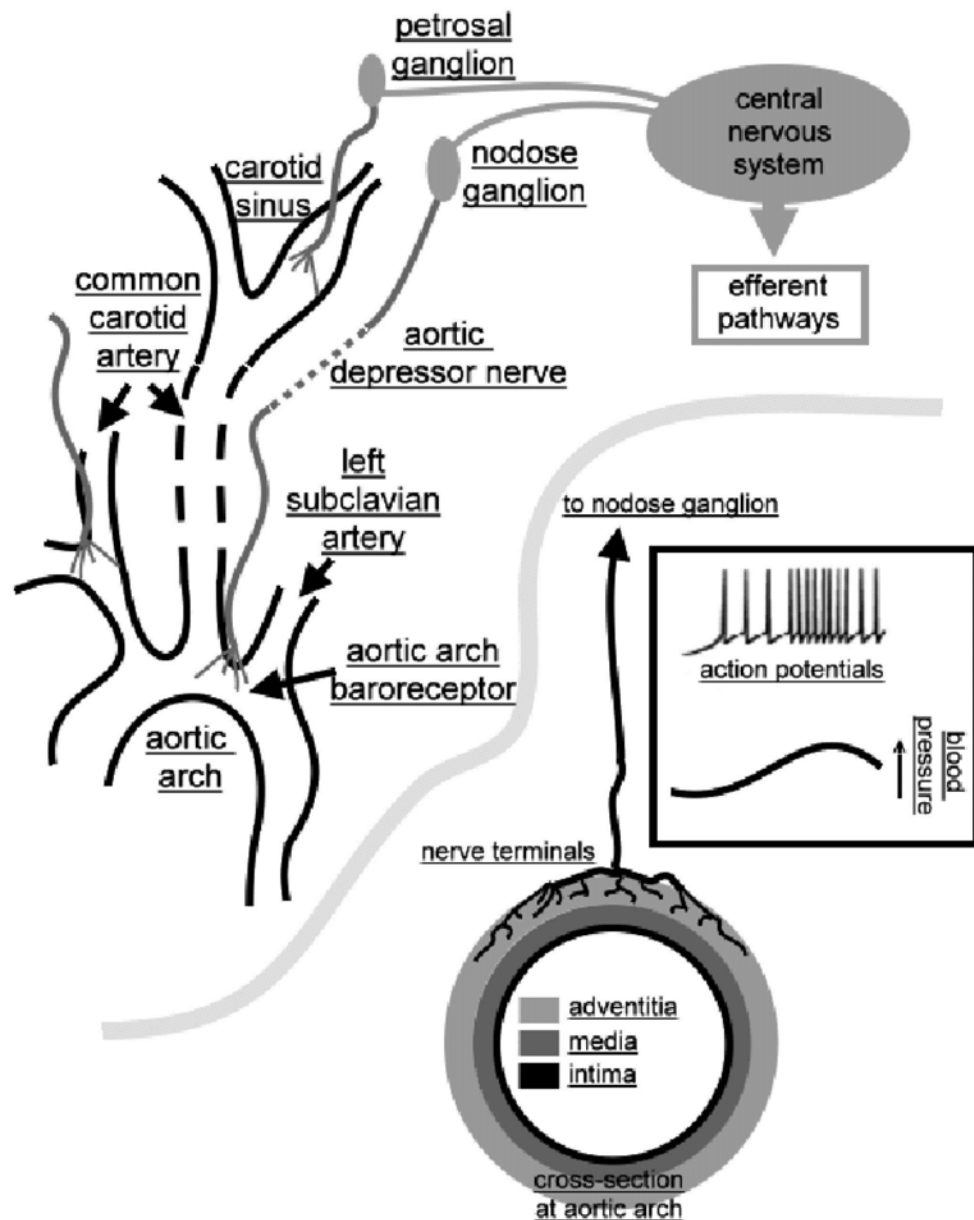


Figure 5.2 Schematic depiction of arterial baroreceptors anatomy and activation mechanism.

Arterial baroreceptors are nerve endings from sensory cells located at ganglions. Blood pressure elevation causes vessel distension and stimulates the stretch-sensitive nerve terminals that innervate the adventitia. Mechano-electrical transduction involves opening of mechanosensitive ion channels on the nerve endings that depolarize the terminals in relation to the magnitude of deformation. Sufficient depolarization evokes action potentials that are transmitted along the depressor nerve at frequencies related to the magnitude of depolarization. Cell bodies at ganglions receive and relay the signals to central nervous system to elicit reflex through efferent pathways.

5.2 Results

5.2.1 Cell swelling at hypotonicity induces Ca^{2+} influx via TRPC5

HEK cells stably expressing TRPC5 were exposed to bath solutions that were calibrated at different osmolarities. At 360 mOsm, hypertonic bath solution caused shrinkage of the cells (Figure 5.3A). On the contrary, hypotonic bath solution (210 mOsm) caused cell swelling (Figure 5.3A). The cells swelled and did not burst, maintained the morphology until the bath solution was exchanged into isotonic at 300 mOsm, at which point the cells restored normal shape. When TRPC5-expressing cells were loaded with Ca^{2+} sensitive dye Fluo-3 and viewed by fluorescent microscope, the cell fluorescent signals elevated when external osmolarity was changed from isotonic to hypotonic (Figure 5.3B). This indicates that the $[\text{Ca}^{2+}]_i$ was elevated, and the $[\text{Ca}^{2+}]_i$ rise could be restored by changing the bath back to isotonic and hypertonic solution (Figure 5.4A). The $[\text{Ca}^{2+}]_i$ rise was absent when bath Ca^{2+} was omitted at hypotonicity (Figure 5.4A,C), indicating a Ca^{2+} influx rather than Ca^{2+} store release was responsible for the $[\text{Ca}^{2+}]_i$ rise. Lanthanum, a potentiator of TRPC5 and blocker of many non-selective cation channels, did not abolish but rather enhanced the hypotonic $[\text{Ca}^{2+}]_i$ rise (Figure 5.4A). Pretreatment of cells with U73122, a specific inhibitor to phospholipase C (PLC), did not affect the hypotonic $[\text{Ca}^{2+}]_i$ rise (Figure 5.4B,C). The $[\text{Ca}^{2+}]_i$ rise at hypotonicity was only observed in TRPC5-expressing cells, but not in control cells transfected with empty vector (Figure 5.5A,B,D). Hypotonicity did not induce $[\text{Ca}^{2+}]_i$ rise in TRPC6-overexpressing cells, which could respond to OAG in functional studies (Figure 5.5C,D).

To further confirm that TRPC5 is activated by hypotonicity, I applied two types of TRPC5 blockers, 2-APB and T5E3. 2-APB is a pharmacological blocker that has been shown to effectively abolish TRPC5 activity (Xu *et al.*, 2005a). When the bath solution contained 75 μM 2-APB, hypotonicity did not induce $[\text{Ca}^{2+}]_i$ (Figure 5.6A,C). T5E3 is a rabbit IgG antibody specifically raised to block TRPC5 at pore region (Xu *et al.*, 2006a). The preparation and effectiveness of T5E3 were described in Chapter 2 Section 2.2.5 and Chapter 3 Section 3.3.5 respectively. As expected, 4 $\mu\text{g}/\text{ml}$ T5E3 effectively blocked the hypotonic $[\text{Ca}^{2+}]_i$ rise (Figure 5.6B,C).

$[\text{Ca}^{2+}]_i$ change in response to different osmolarity steps was studied. The $[\text{Ca}^{2+}]_i$ did not increase significantly when external osmolarity decreased from 270 mOsm to 255mOsm (Figure 5.7A,B). A dramatic increase in the Ca^{2+} response occurred at 240 mOsm and 210 mOsm (Figure 5.7A,B), suggesting that TRPC5 activity is enhanced only when the external osmolarity reaches a threshold between 240 and 210 mOsm.

5.2.2 Intact cytoskeletal function is critical to cell swelling-activation of TRPC5

Another factor that is involved in the membrane dynamics during cell swelling is the cortical cytoskeletal proteins (Hamill *et al.*, 2001). Mechanical force can be transmitted through the cytoskeletal proteins to the tethered membrane proteins (Pedersen *et al.*, 2007). Upon treatment of the cells with cytochalasin D, a barbed end blocker that inhibits actin polymerization, hypotonic treatment failed to elicit the previously observed $[\text{Ca}^{2+}]_i$ rise (Figure 5.8A,B). The data indicate that membrane tension may

not be the sole factor affecting TRPC5 activity, and cytoskeletal protein(s) also participates in the activation. Previous reports have shown that TRPC5 is physically coupled to the cytoskeletal-anchoring protein NHERF via the C-terminal PDZ-binding domain (Tang *et al.*, 2000). A truncated TRPC5 mutant (Δ C-TRPC5), which lacks the last 9 amino acid residues that compose the PDZ-binding motif, was tested for its sensitivity to hypotonicity. Similarly to wild-type TRPC5, $[Ca^{2+}]_i$ in Δ C-TRPC5 cells increased as external osmolarity decreased (Figure 5.9A,B). The data suggest that the hypotonicity activation of TRPC5 is not mediated by the PDZ-binding domain.

5.2.3 Membrane stretch stimulate single TRPC5 channels on membrane

Cell swelling is accompanied by stretching of the cell membrane and increasing the tension of the bilayer (Hamill *et al.*, 2001). TRPC5 responsiveness to cell swelling suggests that TRPC5 may sense the membrane tension. To complement the results from the hypotonic treatment experiments, the TRPC5 protein at membrane patch was challenged by negative pressure applied via the patch pipette, and the channel activity was recorded by electrophysiology. It has been reported that endogenous stretch-sensitive channels are much more abundant in HEK cells than in Chinese hamster ovarian (CHO) cells (Maroto *et al.*, 2005). I therefore prepared the TRPC5-expressing CHO cells. The TRPC5-IRES-GFP construct that allows simultaneous expression of TRPC5 and GFP was prepared as described in Chapter 2 Section 2.2.3.1. The CHO cells were transfected with the construct and cultured under stable selection. GFP positive cells were isolated under fluorescence

microscope (Figure 5.10B). These cells showed the expression of TRPC5 proteins as determined by western-blot analysis (Figure 5.10A).

Cell-attached patch clamp experiment was performed to study TRPC5 at single channel level in CHO cells. Pipette solution contained low concentration of chloride ion to reduce interference of chloride channel activity. At cell-attached configuration, tonic channel activity with current amplitude ~ 2.7 pA at -60 mV could be observed in TRPC5-expressing CHO cells (Figure 5.11A). This value matches the reported TRPC5 single channel amplitude (Jung *et al.*, 2003). Membrane stretch was induced by applying negative pressure through the patch pipette. Negative pressure at -40 mmHg enhanced the opening of the channel (Figure 5.11A,C). In control cells transfected with IRES-GFP, no stretch-sensitive TRPC5-like current was detected (Figure 5.11B). The current amplitudes of the stretch-sensitive channel recorded in TRPC5-expressing CHO cells had an I-V relationship that gave the channel conductance as 40.28 pS (Figure 5.12A,B). The single channel conductance of TRPC5 reported by others ranges from 38 to 47.6 pS.

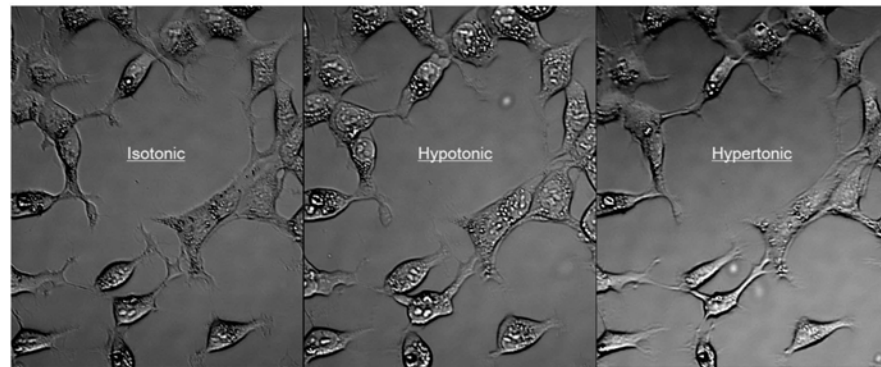
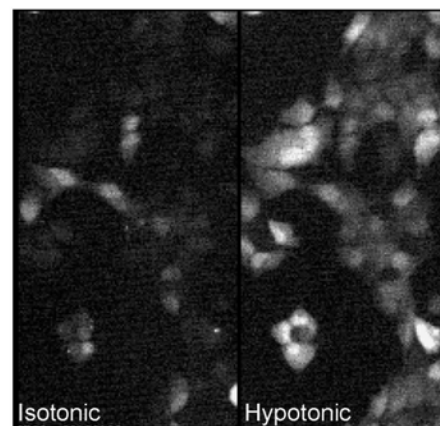
A**B**

Figure 5.3 Hypotonicity-induced cell swelling and $[Ca^{2+}]_i$ rise in TRPC5-expressing HEK cells

A, Cell morphology in isotonic, hypotonic and hypertonic bath solutions. Shown are bright-view images captured by confocal microscopy. B. Cytosolic Ca^{2+} fluorescent signal when cells were bath in isotonic solution and later in hypotonic solution. HEK cells were transfected to stably express TRPC5. Cells were loaded with Ca^{2+} -sensitive dye fluo-3 and viewed by Ca^{2+} -imaging system.

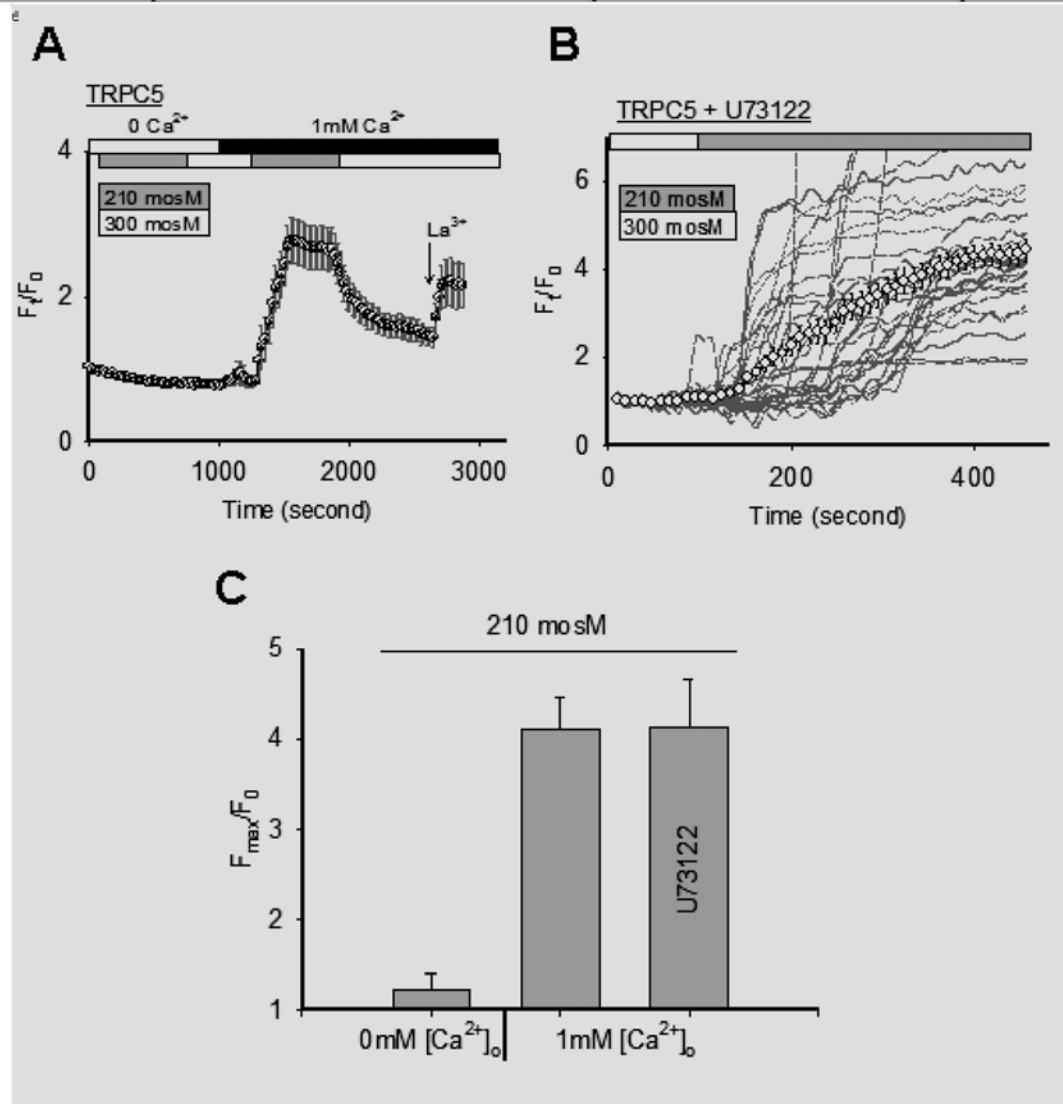


Figure 5.4 Hypotonicity-induced $[Ca^{2+}]_i$ rise is resulted from Ca^{2+} influx and independent of phospholipase C activity

A and B, representative time-series graphs for $[Ca^{2+}]_i$ fluorescent signal in TRPC5-expressing HEK cells in response to hypotonicity at 210 mOsm. A, bath solution osmolarity was lower to 210 mOsm in two steps as indicated: first in the absence of Ca^{2+} ($0 Ca^{2+}$); and latter in bath solution containing 1 mM Ca^{2+} (1 mM Ca^{2+}). $100 \mu M LaCl_3$ (La^{3+}) was bath-applied before the end of the protocol. The data points represent the mean \pm SEM for ≥ 20 cells in a representative experiment ($n=5$). B, cells were pre-incubated with $10 \mu M$ U73122 for 30 min before bath solution changed to hypotonic (210 mOsm). The data points represent the mean \pm SEM for ≥ 20 cells in a representative experiment ($n=4$). Traces of individual cells are shown in grey. C, summarized mean \pm SEM ($n \geq 4$) data for the maximum $[Ca^{2+}]_i$ increase (F_{max}/F_0) in response to hypotonicity (210 mOsm), at zero bath Ca^{2+} , 1 mM bath Ca^{2+} and U73122 treatment.

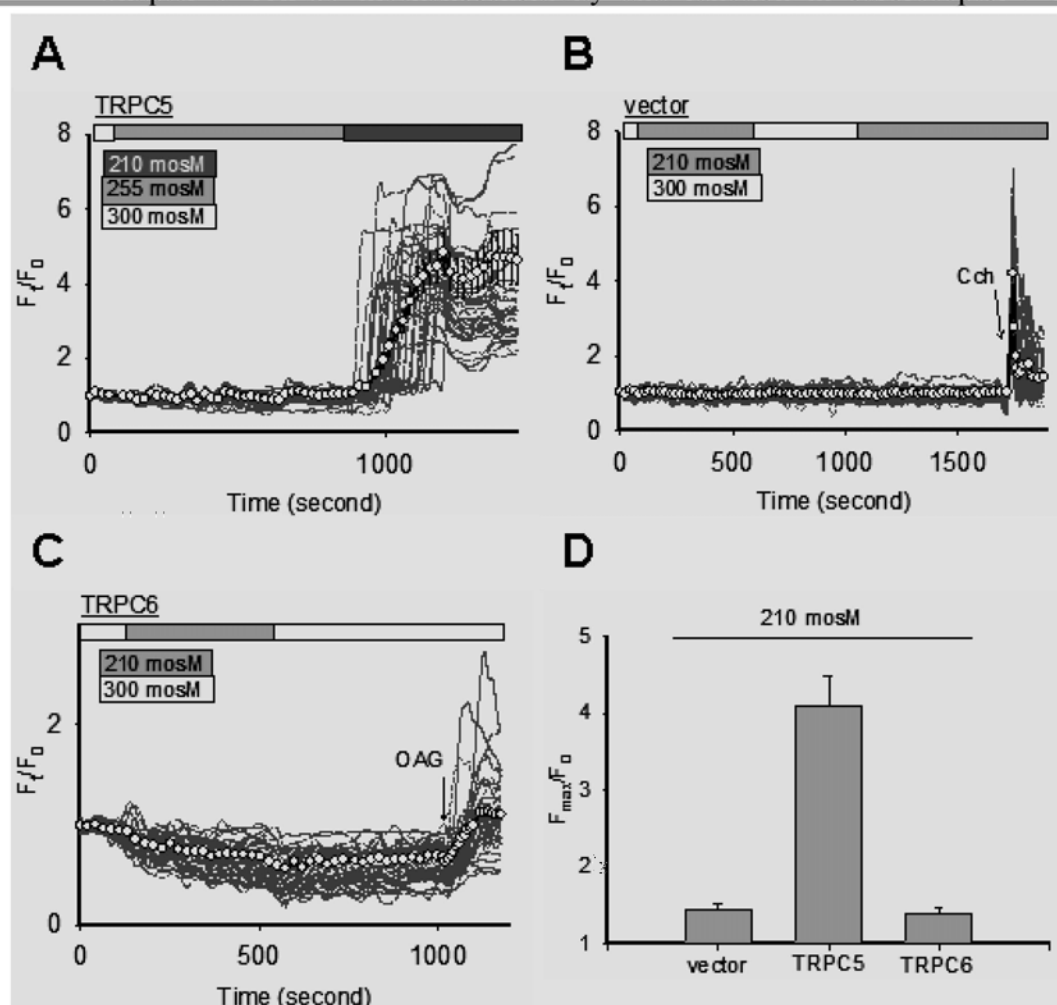


Figure 5.5 TRPC5 mediates hypotonicity-induced Ca^{2+} influx

A-C, representative time-series graphs for $[Ca^{2+}]_i$ fluorescent signal in HEK cells in response to hypotonicity. TRPC5-transfected (A, TRPC5), pCDNA3-transfected (B, vector) and TRPC6-transfected (C, TRPC6) HEK cells were subjected to hypotonic bath solution as indicated by the grey bars. 100 μ M carbachol (CCh) and 100 μ M 1-oleoyl-2-acetyl-sn-glycerol (OAG) were bath applied as indicated in B and C respectively. The data points represent the mean \pm SEM for ≥ 20 cells in a representative experiment ($n \geq 4$). Traces of individual cells are shown in grey. D, summarized mean \pm SEM ($n \geq 4$) data for the maximum $[Ca^{2+}]_i$ increase (F_{max}/F_0) in response to hypotonicity (210 mOsm) as in A, B and C.

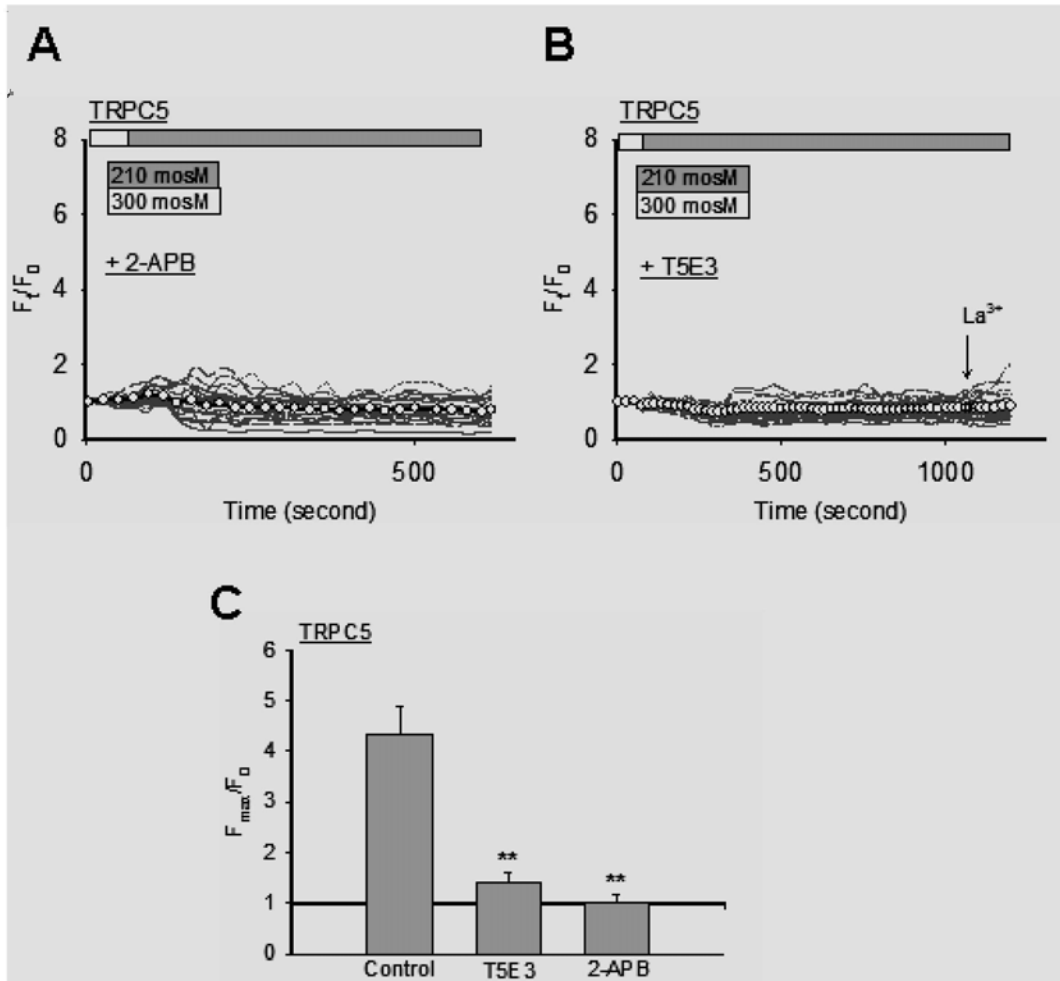


Figure 5.6 TRPC5-blockade abolished hypotonic $[Ca^{2+}]_i$ rise

A and B, representative time-series graphs for $[Ca^{2+}]_i$ fluorescent signal in TRPC5-expressing HEK cells in response to hypotonicity. A ($n=5$), bath contained $75 \mu M$ 2-APB. B ($n=12$), cells were pre-incubated with $4 \mu g/ml$ T5E3 antibody for 15 min before recording; $100 \mu M$ $LaCl_3$ (La^{3+}) was added as indicated, and failed to elicit $[Ca^{2+}]_i$ rise. The data points represent the mean \pm SEM for ≥ 20 cells in a representative experiment. Traces of individual cells are shown in grey. C, summarized mean \pm SEM ($n \geq 5$) data for the maximum $[Ca^{2+}]_i$ increase (F_{max}/F_0) in response to hypotonicity (210 mOsm) as in A and B. ** $p < 0.01$.

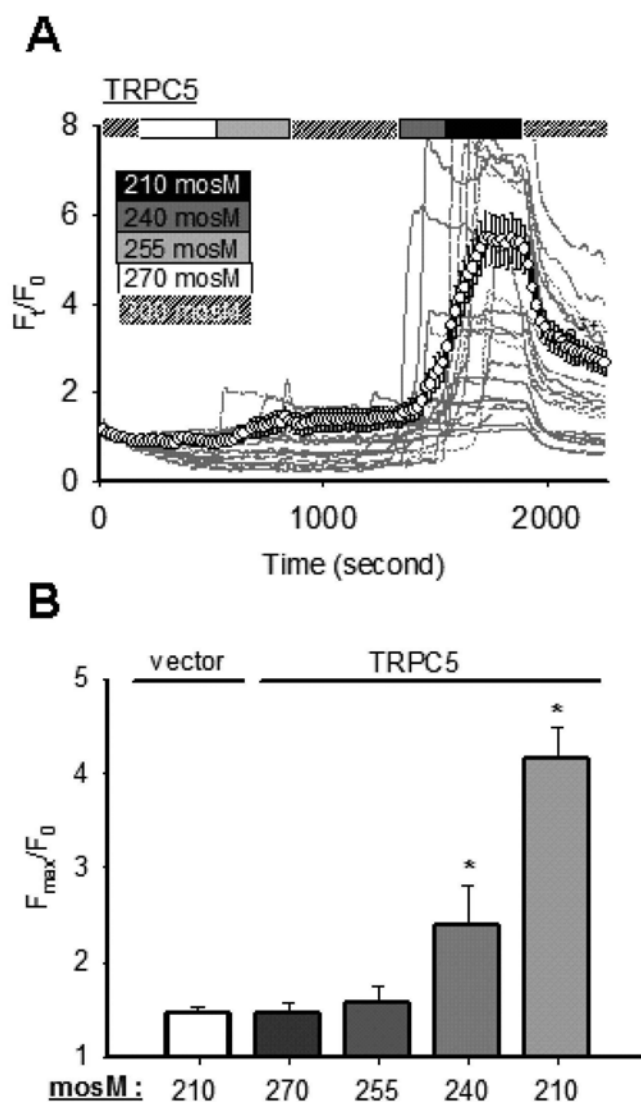


Figure 5.7 The osmolarity threshold to trigger Ca^{2+} influx through TRPC5

A, representative time-series graphs for $[Ca^{2+}]_i$ fluorescent signal in TRPC5-expressing HEK cells in response to bath solutions at different osmolarities. The data points represent the mean \pm SEM for ≥ 20 cells in a representative experiment ($n=7$). Traces of individual cells are shown in grey. B, summarized mean \pm SEM ($n \geq 7$) data for the maximum $[Ca^{2+}]_i$ increase (F_{max}/F_0) in response to different hypotonicities in pCDNA3-transfected cells (vector) and TRPC5-transfected cells (TRPC5). * $p < 0.05$.

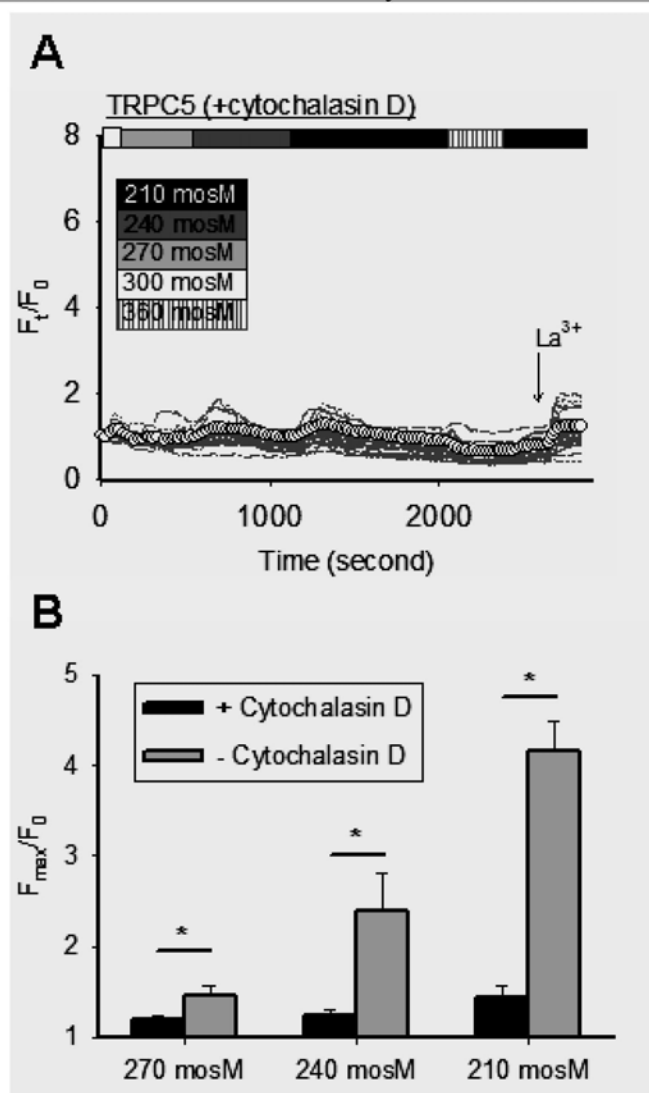


Figure 5.8 Cytoskeletal function is critical to hypotonic activation of TRPC5

A, representative time-series graphs for $[Ca^{2+}]_i$ fluorescent signal in TRPC5-expressing HEK cells treated with cytochalasin D. Cells were pre-incubated with 25 μ M cytochalasin D for 45 min before subjecting to hypotonic treatments; 100 μ M $LaCl_3$ (La^{3+}) was added as indicated to check for the TRPC5 function. The data points represent the mean \pm SEM for ≥ 20 cells in a representative experiment ($n=6$). Traces of individual cells are shown in grey. B, summarized mean \pm SEM ($n \geq 6$) data for the maximum $[Ca^{2+}]_i$ increase (F_{max}/F_0) in response to hypotonicity, comparing cytochalasin D treated and un-treated cells. * $p < 0.05$.

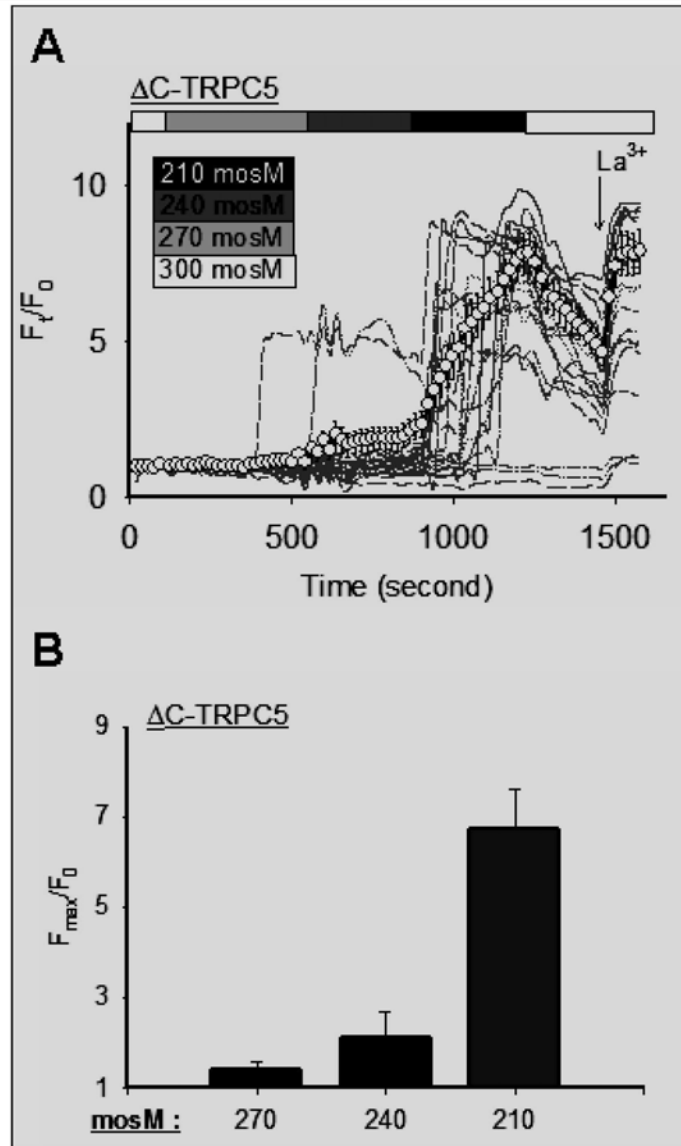


Figure 5.9 The hypotonic activation of TRPC5 is independent of C-terminal PDZ-binding domain

A, representative time-series graphs for $[Ca^{2+}]_i$ fluorescent signal in HEK cells transfected with ΔC -TRPC5, a TRPC5 mutant lacking the last 9 amino acid residues at C-terminus.; hypotonic steps were applied as indicated; 100 μM $LaCl_3$ (La^{3+}) was added at last to check the channel function. The data points represent the mean \pm SEM for ≥ 20 cells in a representative experiment ($n=5$). Traces of individual cells are shown in grey. B, summarized mean \pm SEM ($n=5$) data for the maximum $[Ca^{2+}]_i$ increase (F_{max}/F_0) in response to different hypotonicity as in A.

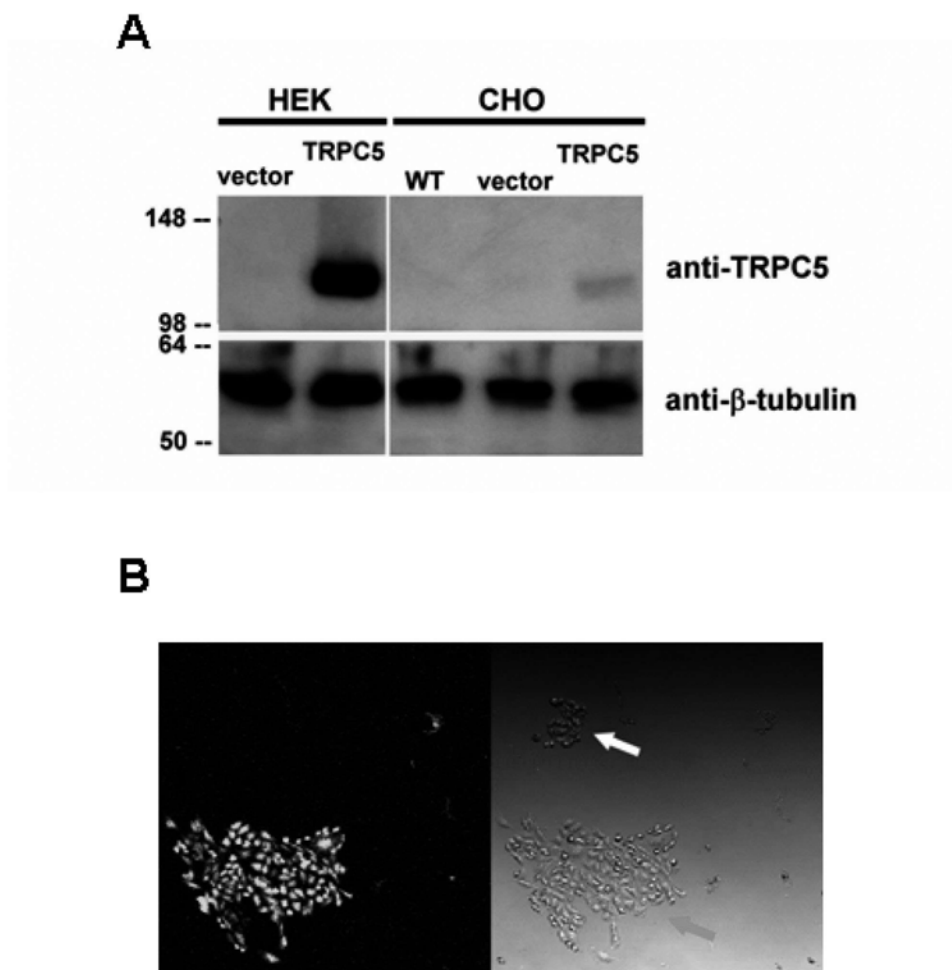


Figure 5.10 Expression of TRPC5 in CHO cells

A, representative image of an immunoblot comparing protein lysates from: (left panel) HEK cells transfected with pCDNA3 (vector) or TRPC5 (TRPC5); and (right panel) CHO cells without transfection (WT), transfected with pCDNA6-IRES-GFP (vector) and TRPC5-IRES-GFP (TRPC5). The blot was also probed with anti- β -tubulin antibody to confirm equal loading of lanes (lower panel). Molecular weights of protein markers are indicated on the left. B, CHO cells after transfection viewed by confocal microscopy. Cells with GFP fluorescence (Green arrow) were picked for stable culture and further experiments.

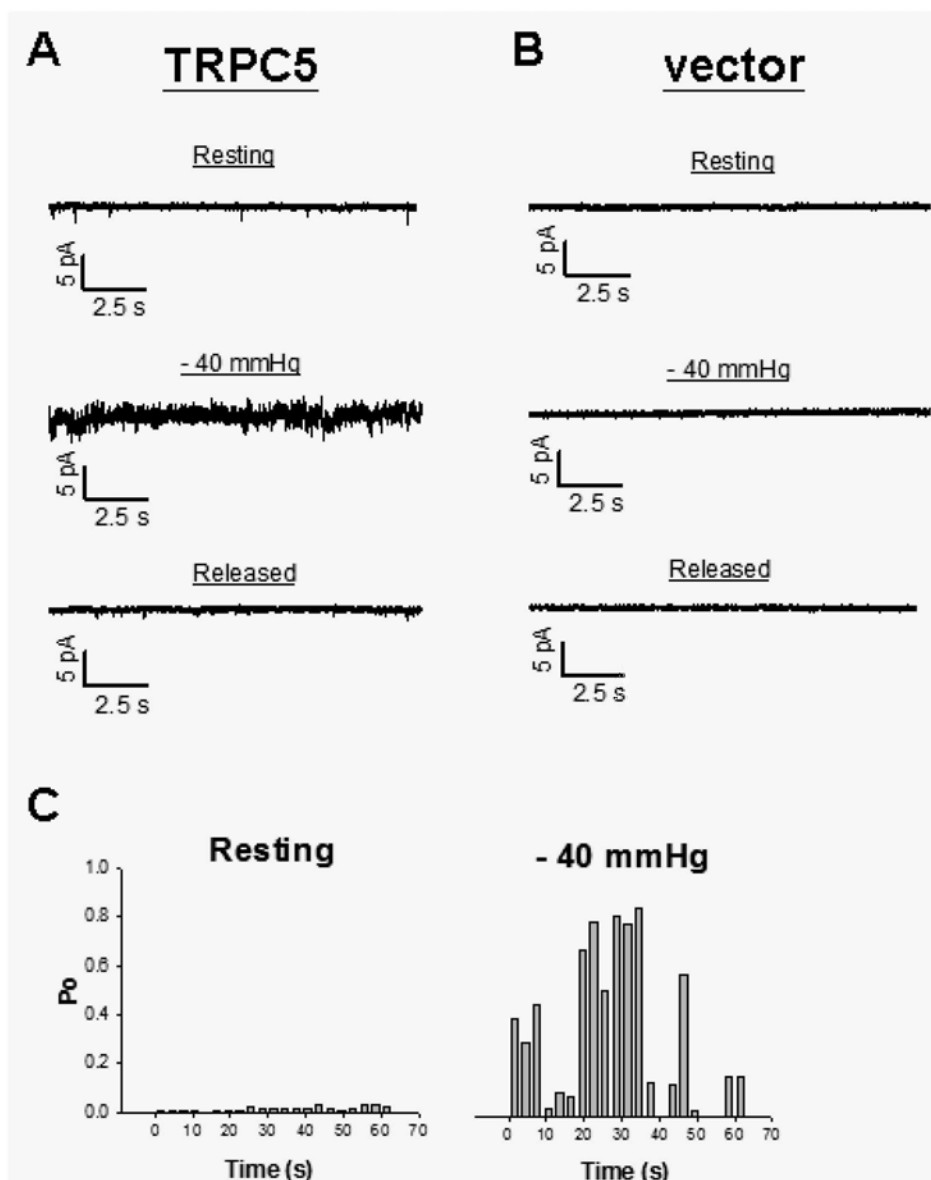


Figure 5.11 Suction induced TRPC5 single channel opening at membrane patch

A-B, single channel traces before (Resting), during (-40 mmHg) and after (Released) application of -40 mmHg pressure in the pipette clamping TRPC5-expressing (A, TRPC5) and control vector-transfected (B, vector) CHO cells. The patch potential was held at -60 mV. C, channel open probability (P_o) changes over time during the patch recording before (Resting) and after (-40 mmHg) application of -40 mmHg pressure to the patch, calculated for each consecutive 3 sec interval.

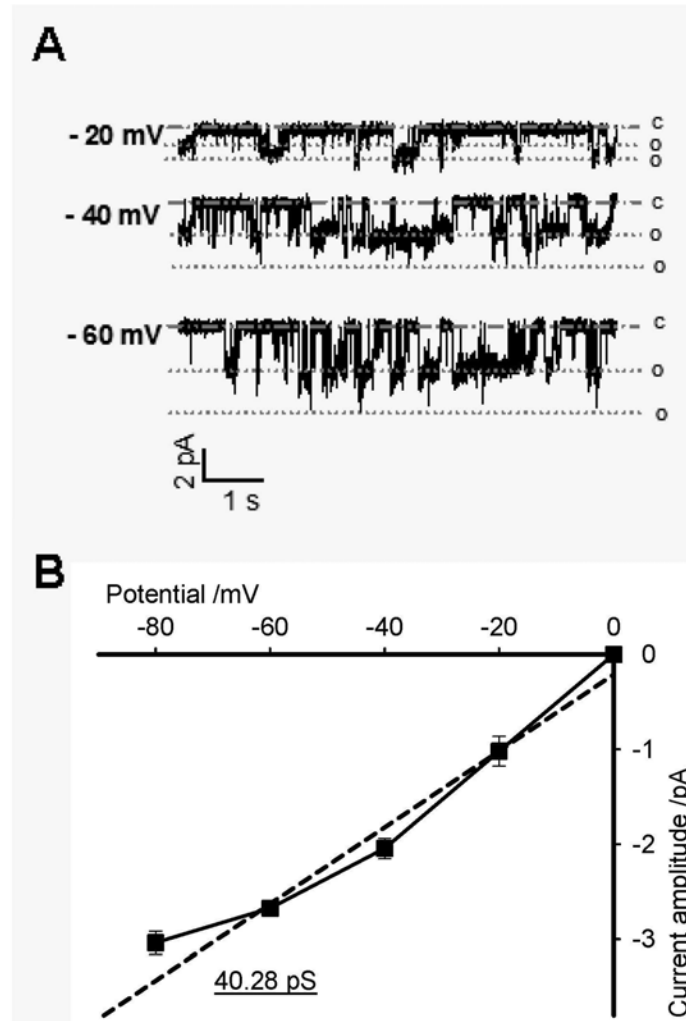


Figure 5.12 Single channel conductance of the stretch-activated channel matches TRPC5 identity

A, single channel traces of TRPC5-expressing CHO cells during application of -40 mmHg pressure to the membrane patch. Membrane patches were clamped at -20 mV, -40 mV and -60 mV potentials. C: Close state; O: Open state. B, single channel current-voltage relationship of the -40 mmHg pressure-sensitive channel recorded on TRPC5-expressing CHO cells.

Collectively, results from the experiments with over-expressed TRPC5 suggest that TRPC5 activity is enhanced in response to membrane stretch. To establish TRPC5 as a mechano-sensor, functional role of TRPC5 in physiologically-relevant mechanosensory system was investigated. Previous study reveals the localization of TRPC5 protein in the nerve termini at the aortic baroreceptor (Glazebrook *et al.*, 2005). Hence, the second part of the study focused on the mechanosensory function of TRPC5 in baroreceptor.

5.2.4 Expression of TRPC5 at rat arterial baroreceptor neurons

Western-blot of lysate from nodose ganglion cells by a specific anti-TRPC5 antibody detected the expression of a protein with similar molecular weight as the TRPC5 expressed in HEK cells (Figure 5.13A), indicating expression of TRPC5 protein by the nodose ganglion neurons. Immunofluorescent staining was used to probe TRPC5 expression in rat baroreceptor neurons *in situ*. As anatomical structure, the cell bodies of the baroreceptor neuron situate in the nodose ganglion, and the axons extend to form a bundle of fibers identified as aortic depressor nerve. The terminals of the nerve innervate the adventitia of the aortic arch. In the present study, the left aortic depressor nerve and the associated baroreceptor neurons were selected as experimental subjects. Cryosections from nodose ganglion and aortic depressor nerve, and the adventitia laid between the left common carotid artery and the left subclavian artery at the aortic arch were prepared and labeled with anti-TRPC5 and anti-PGP-9.5 antibody. PGP-9.5 is an ubiquitin hydrolase abundantly expressed in neuronal cells (Schofield *et al.*, 1995), and served as a neuronal marker in the present study. TRPC5

immunoreactive signals were detected in nodose ganglion cells, and the signals overlapped well with that of anti-PGP-9.5 (Figure 5.13B). There was not a clear membrane-outlined anti-TRPC5 signal, suggesting that the protein is in low concentration at the cell surface. Positive anti-TRPC5 fluorescent signal at the aortic depressor nerve indicates that the channel is trafficked along the fibers and is not confined to the cell bodies (Figure 5.13C). At the aortic arch adventitia, the anti-PGP-9.5 signals reveal the location of neural fibers innervated in the layer (Figure 5.13D). In some fibers, TRPC5 immunoreactive signals were detected (Figure 5.13D). The results suggest that baroreceptor neurons express TRPC5 and deliver the channel to the mechanosensory terminals at aortic arch.

5.2.5 Labeling and Isolation of baroreceptor neurons for in vitro experiments

The small size and complex architecture of the baroreceptor terminals at the aortic arch adventitia prevents the direct measurement on mechanosensitive channel(s). Thus, in vitro preparation of isolated baroreceptor neurons in culture was used for the functional study of the native TRPC5. Previous studies show that not all neurons at nodose ganglion respond to mechanical perturbation (Chapleau *et al.*, 1995b; Cunningham *et al.*, 1995; Sharma *et al.*, 1995). To identify the baroreceptor neurons from the cultured nodose neurons, the sensory neurons were labeled by fluorescent dye DiI before isolation. Application of DiI to the aortic arch adventitia in vivo was performed, followed by recovery of the rat for 6 days (Figure 5.14A). This allows transport of the dye along the depressor nerve and back to the cell bodies at nodose ganglion. Fluorescent

imaging of the isolated nodose neurons shows intense DiI signal in some, but not all, of the cultured cells (Figure 5.14B). These cells also showed immunoreactivity to TRPC5 (Figure 5.14C).

5.2.6 TRPC5 participates in mechanosensitive Ca^{2+} influx pathway in baroreceptor neurons

Hypotonic treatment was applied to the isolated nodose neurons to stimulate the mechanosensitive ion channel(s) (Cunningham *et al.*, 1995). Hypotonicity (210 mOsm) induced $[\text{Ca}^{2+}]_i$ rise in the isolated baroreceptor neurons (Figure 5.15A). Extracellular application of TRPC5-blocking antibody T5E3 significantly inhibited this $[\text{Ca}^{2+}]_i$ rise (Figure 5.15A,B), indicating that TRPC5 is one of the Ca^{2+} entry components in response to hypotonicity. Apart from using blocking antibody, dominant-negative TRPC5 (DN-T5) construct was introduced into the isolated neurons by electroporation to knock-down the function of native TRPC5. Control cells electroporated by empty vector showed robust $[\text{Ca}^{2+}]_i$ rise in response to hypotonicity (Figure 5.16A). On the contrary, the cells electroporated with DN-T5 construct showed significantly diminished hypotonic $[\text{Ca}^{2+}]_i$ rise (Figure 5.16A,B).

5.2.7 TRPC5 contributes to baroreceptor activity *in vivo*

Baroreceptor activity can be measured by recording the frequency of the action potential discharge (spike frequency) from the baroreceptor afferent fibers (aortic depressor nerve) during changes in arterial pressure. To determine the contribution of TRPC5 to the baroreceptor activity, a lentiviral vector that carries dominant-negative TRPC5 construct

(lenti-DN-T5) was used to disrupt native TRPC5 function (Figure 5.17). Viral transduction was performed on the left nodose ganglion, where the cell bodies of the mechanosensory baroreceptor neurons are located. Elevation of arterial blood pressure was elicited by clamping the abdominal aorta with an inflation cuff (Figure 5.18). The pressure ramp enhanced the baroreceptor activity by increasing the spike frequency (Figure 5.19), which was recorded by the electrodes in contact with the whole left aortic depressor nerve (Figure 5.18). In lenti-DN-T5-transduced rats, increase in spike frequency in response to the pressure ramp was significantly less than that in control rats transduced by empty lentivirus (lenti-empty) (Figure 5.20). The results indicate a loss in baroreceptor activity if TRPC5 is functionally compromised.

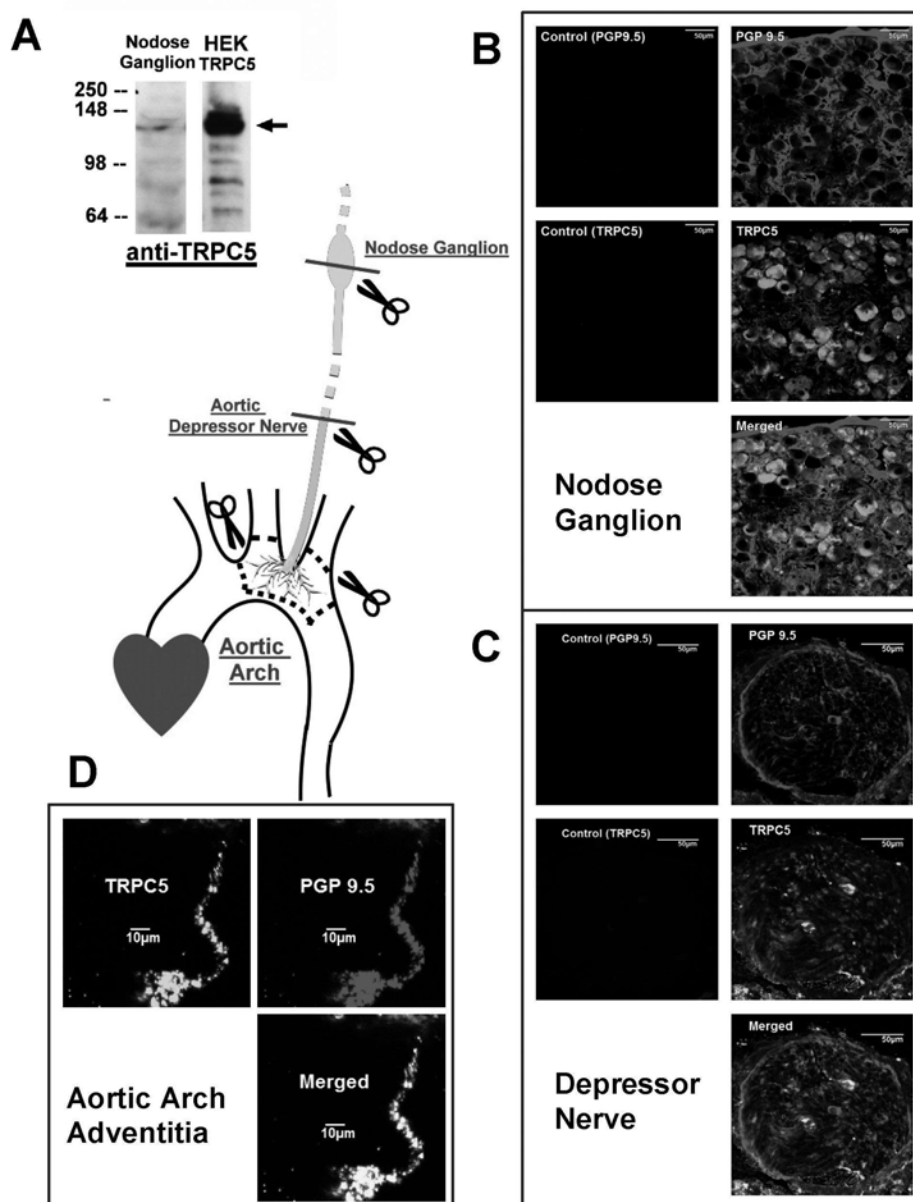


Figure 5.13 Expression of TRPC5 at rat aortic baroreceptor, depressor nerve and nodose ganglia

A, representative image of an immunoblot probed by anti-TRPC5 antibody. Protein lysates were from rat nodose ganglion (left panel) and TRPC5-transfected HEK cells (right panel). Molecular weights (kDa) of protein markers are indicated on the left. B and C, immunoreactivity to TRPC5 and neuronal marker PGP 9.5 of the cryo-sections from rat nodose ganglion (B) and aortic depressor nerve (C). Cryo-sections were obtained at locations as depicted (red dash and scissors). The control images (left panel) were from sections without addition of primary antibodies. D, immunoreactivity to TRPC5 and neuronal marker PGP 9.5 in a whole mount preparation of the aortic arch adventitial layer containing the arterial baroreceptors. The figure presents stacks of Z-series images from a 25-µM thick layer in adventitia.

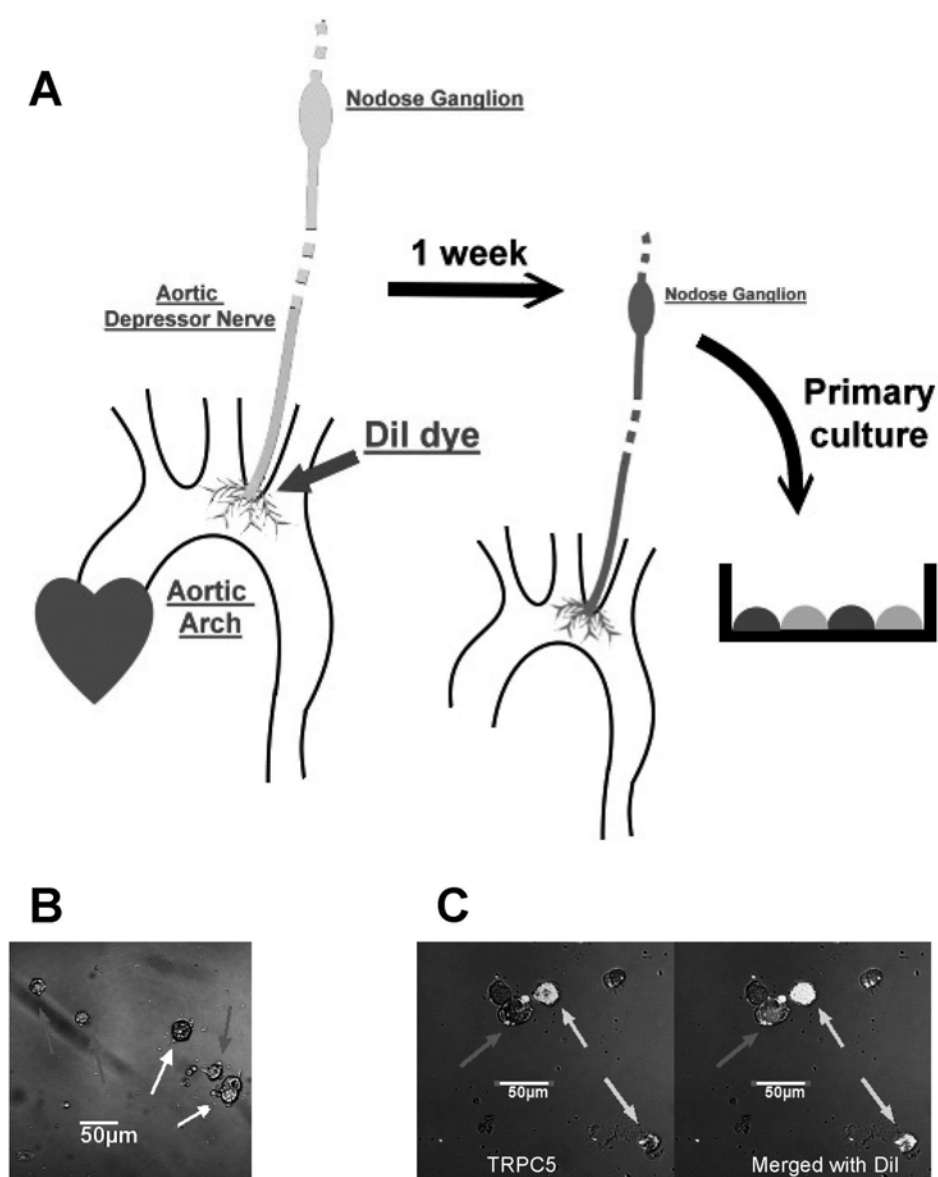


Figure 5.14 DiI-labeling of baroreceptor neurons

A, schematic illustration of the procedures used to label aortic baroreceptor nerves with the fluorescent dye DiI *in vivo*, enabling later identification of the labeled neurons in culture for functional studies. 1-2 μl dye was applied to the aortic arch adventitia in anesthetized rats. The animals are allowed to recover and are maintained for 1 week to allow sufficient time for transport of the DiI along the aortic depressor nerves to the nodose ganglia. Neurons from nodose ganglia were then isolated to primary culture. B, the DiI-labeled neurons are identified by fluorescence at 546 nm excitation (red arrows). These cells were selected for Ca^{2+} studies. C, The DiI-positive neurons express TRPC5. The cells were fixed and probed for TRPC5 immunoreactivity. Green arrows indicate immunoreactive to TRPC5.

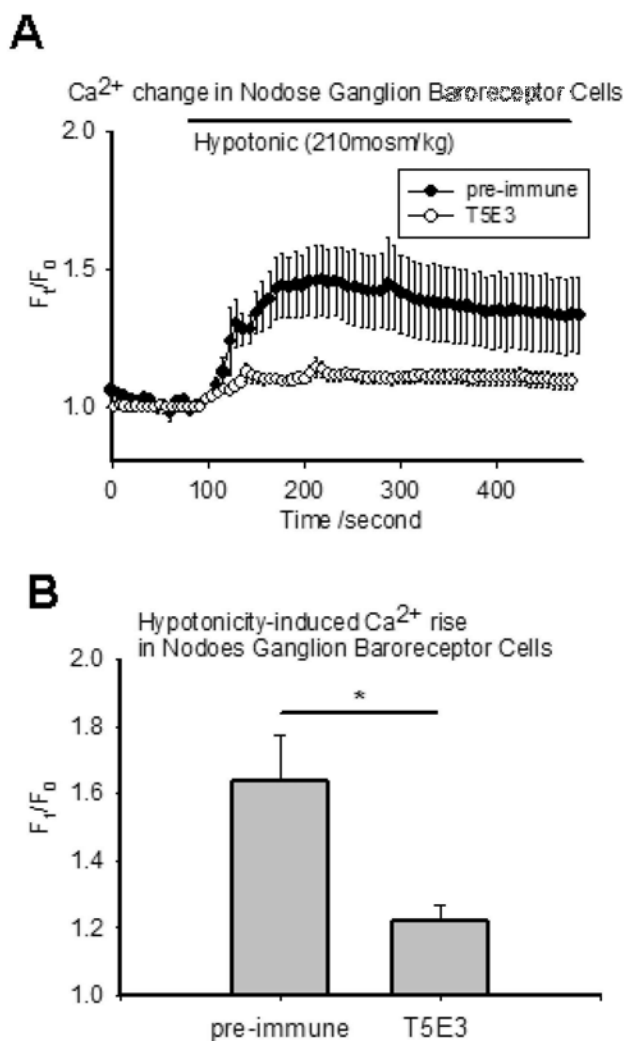


Figure 5.15 Hypotonic [Ca²⁺]_i rise in baroreceptor neurons is inhibited by T5E3

A, representative time-series graphs for [Ca²⁺]_i fluorescent signal in primary cultured DiI-positive neurons from nodose ganglia in response to hypotonicity (210 mOsm). Cells were pre-incubated with T5E3 (4 μg/ml) or pre-immune IgG (4 μg/ml, labeled as “pre-immune”) for 15 min. The data points represents the mean ± SEM for ≥7 cells in a representative experiment (n=6). B, summarized mean ± SEM (n=6) data for the maximum [Ca²⁺]_i increase (F₁/F₀) in response to hypotonicity (210 mOsm) as in A. * *p*<0.5.

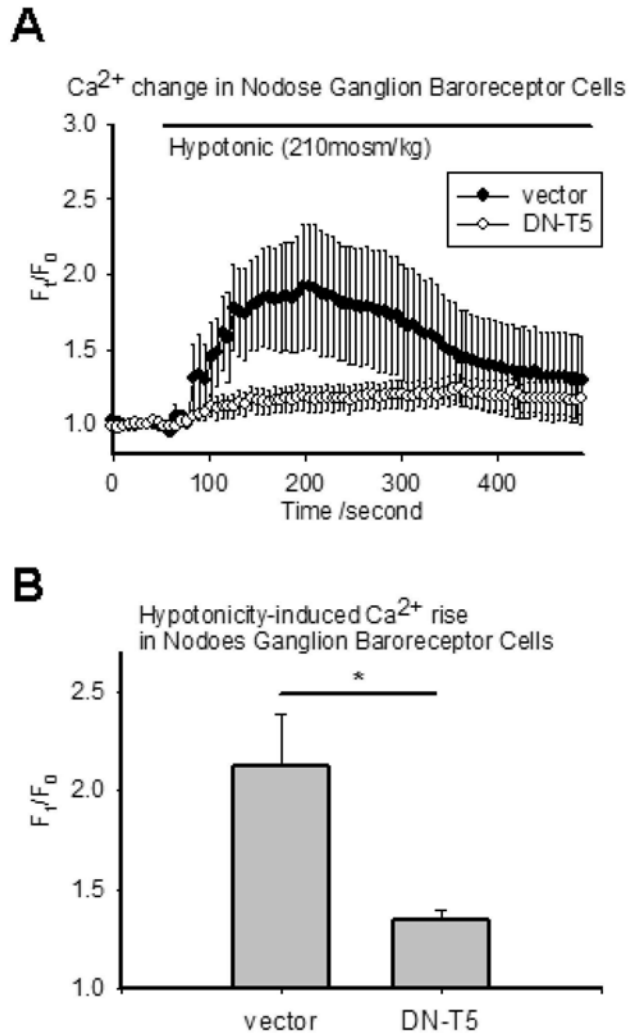


Figure 5.16 Dominant-negative TRPC5 inhibits hypotonic $[Ca^{2+}]_i$ rise in baroreceptor neurons

A, representative time-series graphs for $[Ca^{2+}]_i$ fluorescent signal in primary cultured DiI-positive neurons from nodose ganglia in response to hypotonicity (210 mOsm). Cells were transfected with 5 μ g dominant-negative TRPC5 (DN-T5) or pCDNA6c (vector) by electroporation. The data points represents the mean \pm SEM for ≥ 7 cells in a representative experiment ($n \geq 6$). B, summarized mean \pm SEM ($n \geq 6$) data for the maximum $[Ca^{2+}]_i$ increase (F_1/F_0) in response to hypotonicity (210 mOsm) as in A. * $p < 0.5$.

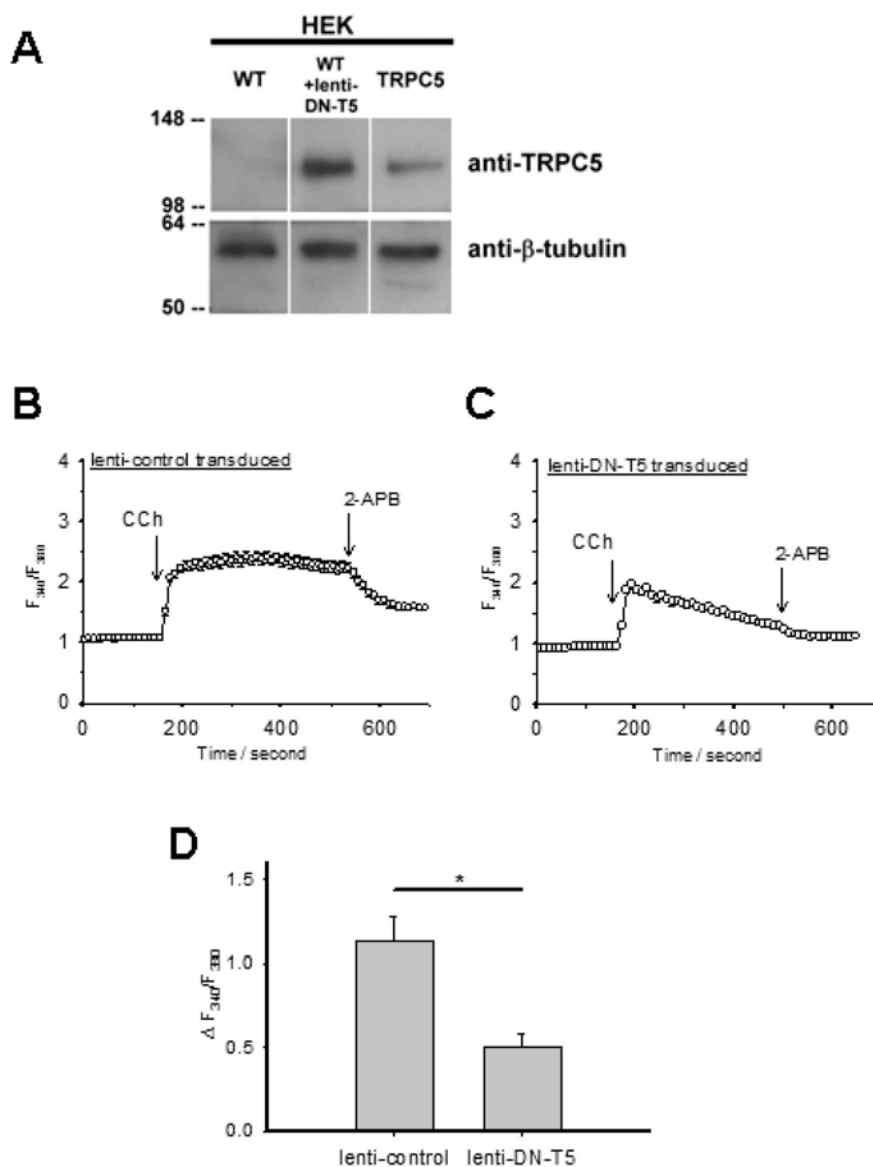


Figure 5.17 DN-TRPC5 carried by lentiviral vector inhibits TRPC5 function

A, representative image of an immunoblot comparing protein lysates from wild-type HEK cells (WT), HEK cells transduced with lentiviral vector carrying dominant-negative TRPC5 (lenti-DN-T5) and HEK cells transfected with TRPC5 (TRPC5). The blot was also probed with anti- β -tubulin antibody to confirm equal loading of lanes (lower panel). Molecular weights of protein markers are indicated on the left. B and C, representative time-series graphs for $[Ca^{2+}]_i$ fluorescent signal in TRPC5-expressing HEK cells transduced with control empty lentiviral vector (B, lenti-control) and lentiviral vector carrying dominant-negative TRPC5 (C, lenti-DN-T5). Bath solution was NPSS. Arrows indicate the time points when 100 μ M carbachol (CCh) and 100 μ M 2-APB (2-APB) were added. Each trace represents the mean \pm SEM of ≥ 20 cells in a representative experiment ($n \geq 6$). D, summary of data (mean \pm SEM) showing the $[Ca^{2+}]_i$ change in response to 100 μ M carbachol (CCh) as in B and C. * $p < 0.05$.

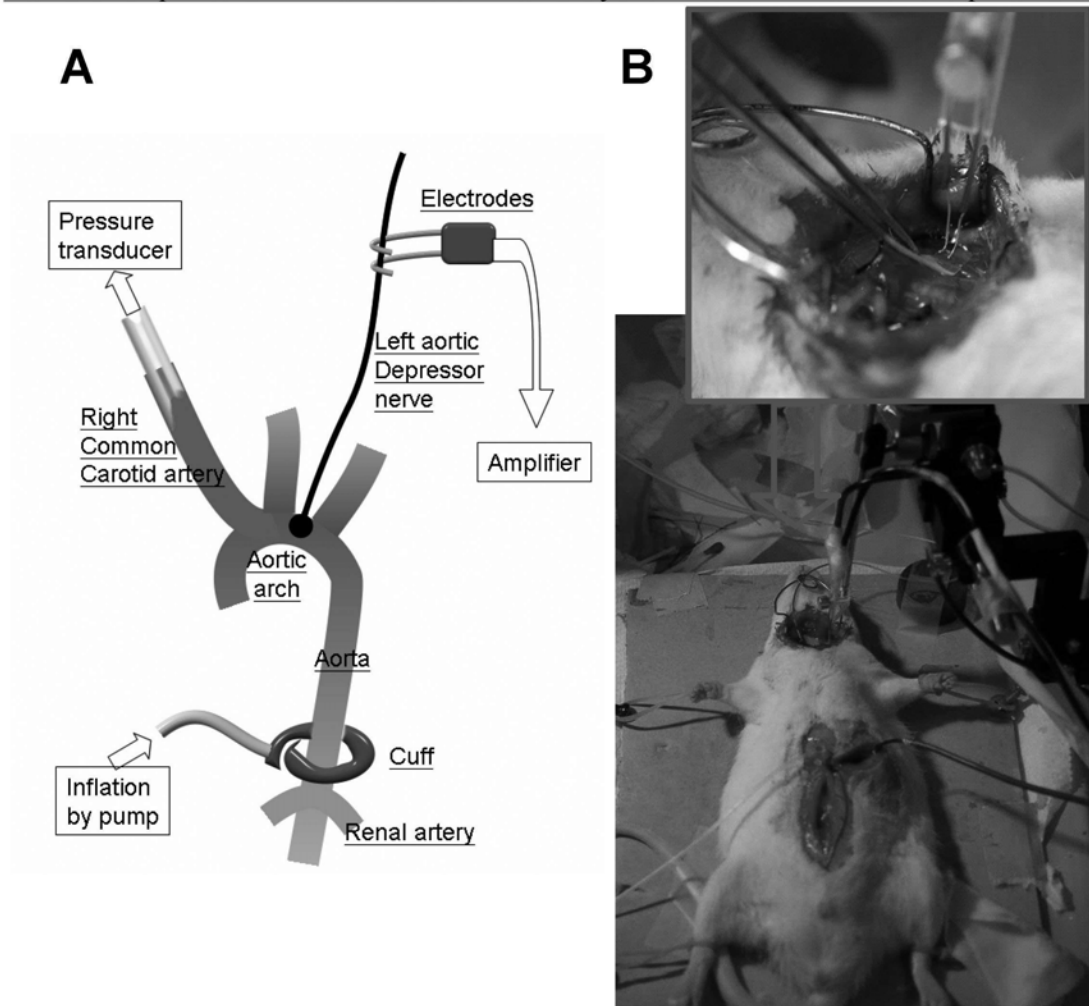


Figure 5.18 *in vivo* measurement of baroreceptor activity

A, schematic depiction of *in vivo* real-time arterial pressure and depressor nerve action potential recording. Rat was anesthetized during the experiment. The right common carotid artery was cannulated and connected to pressure transducer for arterial blood pressure recording. The left aortic depressor nerve was identified and placed on a pair of platinum electrodes, which is connected to an amplifier. Abdomen was exposed and the abdominal aorta was identified. An inflation cuff was mounted around the aorta above the branches of renal artery. A pressure pump was connected to the cuff for inflation, which simultaneously clamp the aorta to elevate the arterial blood pressure at upper body. B, photos showing the actual scenario in an experiment.

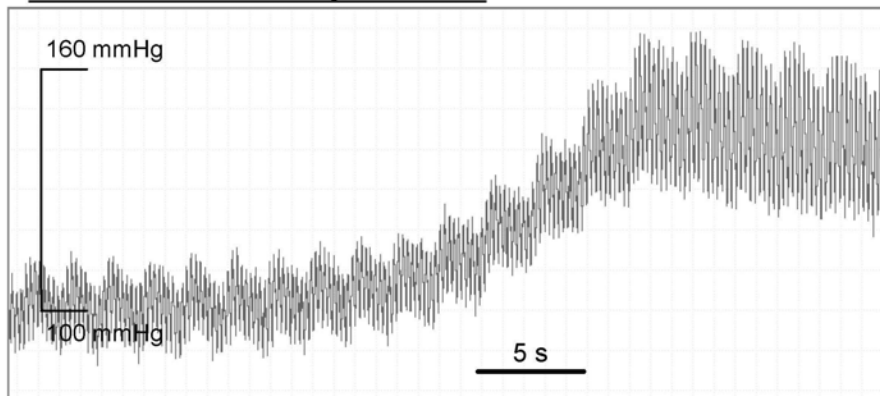
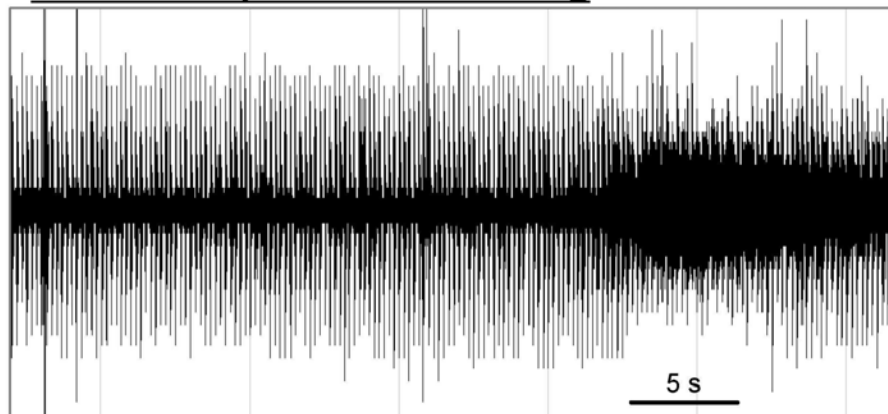
A. Arterial blood pressure**B. Aortic depressor nerve firing**

Figure 5.19 Baroreceptor activity as a function of arterial pressure elevation

A, representative time course of arterial blood pressure change during clamping of abdominal aorta. B, amplified signals from the aortic depressor nerve corresponding to the time course in A. Frequency of the action potential discharge represents the baroreceptor activity.

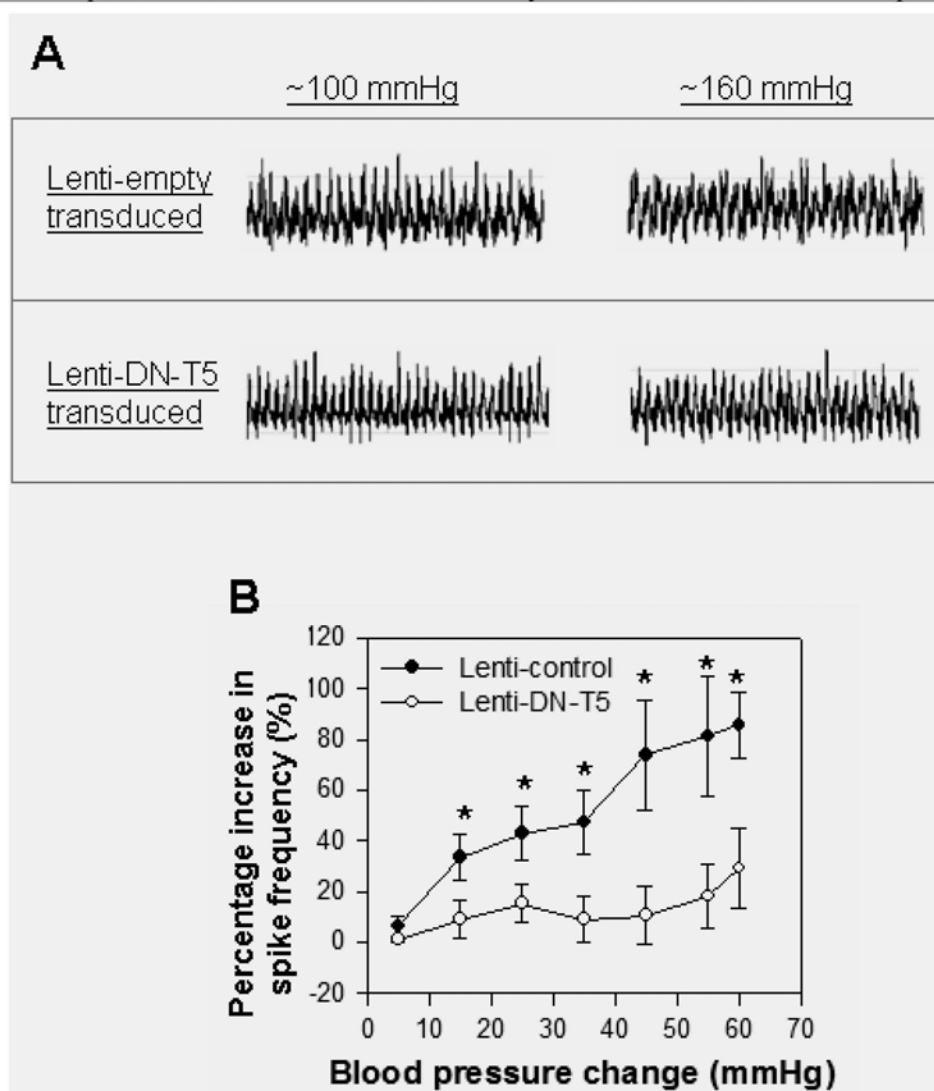


Figure 5.20 Baroreceptor activity is diminished by TRPC5 functional knock-down

A, a typical action potential discharge recorded from aortic depressor nerve at ~100 mmHg and ~160 mmHg of arterial blood pressure in rat transduced with empty lentiviral vector (lenti-empty transduced, upper panel) and in rat transduced with lentiviral vector carrying dominant-negative TRPC5 (lenti-DN-T5 transduced). B, summarized comparison of baroreceptor activity in rats transduced with lenti-control (n=6) and lenti-DN-T5 (n=5). Percentage increase in action potential discharge frequency was analyzed at successive blood pressure steps during the pressure ramp induced by clamping aorta. * $p < 0.05$.

5.3 Discussion

In the present study, I tested the hypothesis that TRPC5 is sensitive to membrane tension. Membrane stretch was exerted by cell swelling induced by external hypotonicity, a method that has been applied previously by others to demonstrate mechanosensitive channels (Cunningham *et al.*, 1995; Hamill *et al.*, 2001; Oliet *et al.*, 1993; Viana *et al.*, 2001). TRPC5-expressing HEK cells showed moderate and robust Ca^{2+} influx when external osmolarity was lowered to 240 mOsm and 210 mOsm respectively. Pharmacological blocker 2-APB and antibody blocker T5E3 abolished the Ca^{2+} influx at hypotonicity. The closely-related TRP isoform TRPC6 failed to mimic such property of TRPC5. The sensitivity of TRPC5 to cell swelling was not dependent on PLC activity, but relied on the intact function of cytoskeletal proteins. The results are in line with another study which shows TRPC5 activation by hypo-osmolarity and cell-swelling (Gomis *et al.*, 2008). That TRPC5 is sensitive to mechanical stress was further confirmed by direct stretching of membrane patch. Single TRPC5 channels expressed in CHO cells were stimulated by applying negative pressure (suction) on the membrane patch. To investigate the function of TRPC5 mechanosensitivity in physiological system, the afferent pathway of arterial baroreceptor was studied. TRPC5 expression was found in rat baroreceptor neurons and the sensory nerve terminals at aortic arch. Isolated baroreceptor neurons showed TRPC5-mediated Ca^{2+} influx in response to hypotonicity-induced cell swelling. TRPC5 function in the baroreceptor neurons was down-regulated by a dominant-negative TRPC5 construct carried by a lentivirus. In vivo recording of the afferent signal on the aortic depressor nerve demonstrated that baroreceptor activity was lowered when TRPC5 function was compromised. The results suggest that TRPC5 contributes to the

transduction of mechanical signal into electric signals in arterial baroreceptors.

Structural proteins, e.g. extracellular matrix and cytoskeleton, participate in the membrane bilayer mechanics (Hamill *et al.*, 2001; Janmey, 1998). These proteins tether to some of the ion channels and have been found to mediate the channel stimulation induced by mechanical force (Janmey, 1998; Kung, 2005; Parker *et al.*, 2007). The cytoskeletal proteins that tether ion channels may transmit mechanical force to regulate the channel activity. Furthermore, in isolated baroreceptor neurons, cytoskeletal actin filaments are crucial for mechanosensitive cation influx (Cunningham *et al.*, 1997). In the present study, when TRPC5-expressing HEK cells were pretreated with cytochalasin D, a microfilament-disrupting agent, the hypotonicity-induced Ca^{2+} influx was impaired. The data suggest that an intact cytoskeleton function is critical to the mechanosensing of TRPC5. Notably, Kim *et al.* show that the receptor activation of TRPC5 could be inhibited by cytochalasin D treatment (Kim *et al.*, 2008). Hence, it is also possible that multiple activation modes of TRPC5, not only mechanical force, rely on cytoskeletal function. Inhibition of TRPC5 vesicle translocation by cytochalasin D is unlikely to explain the absence of mechanosensitivity (Greka *et al.*, 2003), since enhancement of single TRPC5 channel opening could be seen upon stretching membrane patch. TRPC5 has been shown to interact with cytoskeletal proteins via C-terminal PDZ-binding domain (Tang *et al.*, 2000). However, the PDZ-binding domain is unlikely to take part in the observed mechanosensitivity, since the TRPC5 mutant ΔC -TRPC5 lacking the PDZ-binding domain showed sensitivity to hypotonic shock. Further investigation is needed to determine whether cytoskeleton tethered to other TRPC5 domains, e.g. N-terminal coiled-coil domain,

influences the mechanosensitivity of the channel.

In the present study, individual cells showed elevated $[Ca^{2+}]_i$ with different latency period after external osmolarity decreased. The cells did not show synchronized and immediate $[Ca^{2+}]_i$ rise at hypotonicity. It is previously suggested that a mechanically-gated channel should respond to mechanical stress almost instantaneously, with delay in only milliseconds (Christensen *et al.*, 2007). However, the results are not in conflict with a mechanosensitive-TRPC5 scenario. Latency in $[Ca^{2+}]_i$ elevation at hypotonicity may be due to the time for building up the membrane tension as external water flux into the cells. Coupling of primary force sensor, for example cytoskeletal proteins, to TRPC5 for channel activation may contribute to the delay in response. Alternatively, decoupling of inhibitory components from TRPC5 upon mechanical stress may be required for the observed mechanosensitivity.

The functional importance of TRPC5 mechanosensitivity is demonstrated on arterial baroreceptor neurons. Mechanical deformation by external hypo-osmolarity has been previously used by others to study mechanosensitive channel on baroreceptor neurons (Cunningham *et al.*, 1995; Ditting *et al.*, 2003). Experiments on isolated baroreceptor neurons reveal TRPC5 as a component of Ca^{2+} influx pathway upon hypotonic shock. TRPC5 has been previously shown to be a Ca^{2+} influx channel that initiates neurite outgrowth and regulates growth cone morphology (Greka *et al.*, 2003; Hui *et al.*, 2006; Wu *et al.*, 2007). Expression of dominant-negative TRPC5 results in modification of growth cone morphology. In the present study, functional knock-down of TRPC5 on the baroreceptor neurons was achieved by the

dominant-negative construct; however, the observed reduction in osmolarity-sensitive Ca^{2+} influx is not caused by perturbation of neuronal growth. It is because the reduction in Ca^{2+} influx was also observed by acute blockade of TRPC5 with antibody, which is unlikely to influence neuronal growth in vitro.

One of the distinctive characteristics of TRPC5 is the potentiation of channel activity by gadolinium and lanthanum (Jung *et al.*, 2003). Gadolinium (Gd^{3+}) has been commonly used to block mechanosensitive channels (Yang *et al.*, 1989). On isolated baroreceptor neurons, it has been shown that micromolar extracellular Gd^{3+} effectively blocks the cation influx upon stimulation by mechanical deformation (Cunningham *et al.*, 1997; Cunningham *et al.*, 1995; Ditting *et al.*, 2003; Hajduczuk *et al.*, 1994; Sharma *et al.*, 1995; Sullivan *et al.*, 1997). Results from these reports seem not supportive to the mechanosensory role by TRPC5 on baroreceptor. However, it should be noted that, in addition to mechanosensitive channels, Gd^{3+} block a variety of non-selective cation channels. Whole-cell ion homeostasis is inevitably altered by Gd^{3+} application, which could then suppress the contribution of cation influx by TRPC5. On the other hand, Andresen & Yang observed that Gd^{3+} did not affect baroreceptor activity on ex vivo preparation (Andresen *et al.*, 1992). And notably, lanthanum (La^{3+}), also a TRPC5 potentiator, has no effect on this Gd^{3+} -sensitive influx (Cunningham *et al.*, 1995; Sullivan *et al.*, 1997). Hence, TRPC5 participation in baroreceptor mechanosensory is tenable.

Recent studies provide evidence for the role of amiloride sensitive ion channels of the DEG/ENaC family (degenerin/epithelial Na^+ -channel) in regard of

mechanosensation on arterial baroreceptor (Ditting *et al.*, 2003; Drummond *et al.*, 2001). Pharmacological blockade of ENaC channels attenuated the baroreceptor activity in response to arterial pressure in *ex vivo* preparation (Drummond *et al.*, 2001). Nevertheless, the mechanosensitivity of ENaC proteins are poorly characterized and their mandatory role in baroreceptor mechanosensation is questionable (Ditting *et al.*, 2003; Rossier, 1998). The current study suggesting TRPC5 as a mechanosensitive component in regulating baroreceptor activity does not exclude the participation of ENaC proteins. In fact, it is possible that an orchestra of mechanosensitive components is required for the fine sensing of pressure change. By mean of a lentivirus vector, dominant-negative TRPC5 was introduced to the rat baroreceptor neurons. These rats showed less firing of small-amplitude spikes, which are fired by the high-threshold non-myelinated C-fiber (Kirchheim, 1976), when arterial pressure was elevated. This means that TRPC5 may function in C-fiber, and is responsible for sensing high pressure. Since the electrical signal from a whole bundle of fibers was recorded in the present study, it is insufficient to conclude that TRPC5 functions solely on C-fiber but not in others, for example A-fiber. Further experiments are needed to determine which type(s) of fiber TRPC5 is attributed to. It is noteworthy that the results from hypotonic shock experiment on over-expressed TRPC5 suggest a threshold of activation at low external osmolarity. Altogether, the results suggest that TRPC5 contributes to the generation of action potential at high arterial blood pressure, possibly by setting the depolarization signal arisen from its non-selective ion conduction.

Available information about the non-selective cation channels expressed on the

baroreceptor nerve terminals is inadequate. Glazebrook et al. identified the expression of TRPC1, and TRPC3-5 at the aortic baroreceptor sensory terminals (Glazebrook *et al.*, 2005). While the present study identifies TRPC5 as a component in the mechanotransduction at baroreceptor, involvement of other TRP isoforms in the process cannot be excluded, particularly since heteromultimerization between TRP isoforms commonly occurs at physiological context. Expression data of other mechanosensitive TRP isoforms, for example TRPV4 and TRPA1, at baroreceptor sensory terminals is lacking. In addition, whether a mechanosensitive channel plays a role in the decreased baroreceptor activity in pathological states is worthy to investigation. On the other hand, functional contribution by other TRP isoforms may not be confined by mechanotransduction. Regarding that most TRP channels are Ca²⁺-permeable, they may contribute to the raise intracellular calcium and play a role in the release of neurotransmitters, autocrines and paracrines, which would modulate the baroreceptor sensitivity and discharge (Chapleau *et al.*, 2001; Glazebrook *et al.*, 2005).

6 Chapter 6 General Conclusion and Future Work

6.1 Concluding remarks

The present study focuses on the cation channel TRPC5. The study has been divided into three major parts: 1) testing the effect of nitric oxide (NO) on TRPC5; 2) modulation of TRPC5 by isoflavones genistein; and 3) mechanosensitivity of TRPC5 and the relevant physiological function. Comprehensive techniques, covering molecular biology, cell biology, virus-based gene transfer, fluorescent imaging, electrophysiology, and in vivo experiments, have been applied to verify the experimental results. The findings implicate several previously unknown regulatory mechanisms and physiological functions of TRPC5.

A heterologously expression system has been constructed by over-expressing TRPC5 in HEK cells. The expressed TRPC5 displays characteristics that were previously reported by others. Those include stimulation by La^{3+} and carbachol, and inhibition by 2-APB and specific blocking antibody. TRPC5 is also found to be a component mediating the Ca^{2+} influx in bovine aortic endothelial cells (BAECs). In contrast to a previous report, the present study provides evidence against direct stimulatory effect of NO to TRPC5. Two chemically distant NO donors, SNAP and DEA-NONOate, fail to stimulate TRPC5 expressed in both HEK cells and BAECs. In addition, NO donor treatment decreases the Ca^{2+} influx in BAECs, consistent with many other studies showing inhibitory effect of NO to endothelial Ca^{2+} influx.

The present study also identifies the first TRP channel being stimulated by isoflavone genistein. Genistein, and the analogous isoflavone daidzein, stimulate TRPC5 expressed in HEK cells to induce Ca^{2+} influx. Genistein acts synergistically with La^{3+} to stimulate TRPC5. The effect is independent of tyrosine kinases, estrogen receptors and phospholipase C activity. The genistein action on TRPC5 can be recorded in excised membrane patches, suggesting a relatively direct action. Furthermore, genistein acts on native TRPC5 by stimulating cytosolic Ca^{2+} elevation in primary endothelial cells. The sensitivity to the lipophilic genistein implicates that TRPC5 is modulated by the biophysical property of the membrane lipid bilayer.

Lastly, participation of TRPC5 in mechanotransduction has been revealed by both *in vitro* and *in vivo* studies. Cell swelling induced by external hypotonicity was accompanied by TRPC5-mediated Ca^{2+} influx. The hypotonicity-induced stimulation is independent of PLC activity, but relies on intact cytoskeletal functions. Negative pressure applied to the membrane patch stimulates the opening of single TRPC5 channels, supporting that TRPC5 is sensitive to membrane stretch. Primary isolated rat arterial baroreceptor neurons express TRPC5. Hypotonic stress elevates cytosolic Ca^{2+} level in these neurons. Blockade of TRPC5 function by specific blocking antibody or dominant-negative construct drastically reduces the Ca^{2+} rise in response to hypotonicity, indicating that TRPC5 acts as a membrane stretch-sensitive channel in baroreceptor neurons. Finally, functional contribution of TRPC5 to baroreceptor activity has been revealed by *in vivo* experiment. Baroreceptor activity in response to blood pressure elevation was significantly reduced after lentiviral vector transduction of baroreceptor neurons with dominant-negative

TRPC5. The results indicate that TRPC5 functions as a mechanosensitive channel in arterial baroreceptor.

6.2 Future work

To follow up the findings from the present study, several lines of direction are suggested to carry out further study:

1. Inhibitory effect of NO-mediated pathways on TRPC5

Although NO does not stimulate TRPC5, it inhibits the Ca^{2+} influx in endothelial cells, in which TRPC5 functions as a cation influx component. It is therefore logical to test whether NO inhibits the function of a TRPC5-containing channel through, for example cyclic nucleotides or protein kinase G mediated pathway.

2. Effect of other isoflavones on TRPC5 activity

Isoflavones comprise of a family of compounds that share similar chemical structure (Barnes *et al.*, 2000). Given that genistein and daidzein stimulate TRPC5, other chemically analogous compounds may share their capability.

3. Effect of genistein and daidzein on TRPC4

TRPC4 shares that highest degree of similarity with TRPC5. TRPC4 is also expressed in endothelial cells (Kwan *et al.*, 2007). It is therefore possible that genistein and daidzein can also modulate TRPC4 activity.

4. Participation of TRPC5 in other mechanotransduction physiology

TRPC5 is expressed in other cell types that possess mechanotransduction signaling pathways. Hence, it is highly possible that the functional role of TRPC5 mechanosensitivity is not confined to arterial baroreceptor. In particular, cell migration involves opening of stretch-sensitive channel(s) and rearrangement of cytoskeleton (Schwab, 2001). Since TRPC5 mediates cell motility of several cell type (Beech, 2007b), it is of interest whether it may function as a stretch-sensitive channel in the process.

5. Participation of other TRP channels in arterial baroreceptor mechanotransduction

Previous study shows expression of other TRP channels in baroreceptor (Glazebrook *et al.*, 2005). Moreover, some TRP isoforms have been suggested as mechanosensitive (Pedersen *et al.*, 2007). There may be other TRP channels that act as the pressure sensor in baroreceptor.

References

- Akiyama T, Ishida J, Nakagawa S, Ogawara H, Watanabe S, Itoh N, *et al.* (1987). Genistein, a specific inhibitor of tyrosine-specific protein kinases. *J Biol Chem* **262**(12): 5592-5595.
- Alfonso S, Benito O, Alicia S, Angelica Z, Patricia G, Diana K, *et al.* (2008). Regulation of the cellular localization and function of human transient receptor potential channel 1 by other members of the TRPC family. *Cell Calcium* **43**(4): 375-387.
- Altavilla D, Crisafulli A, Marini H, Esposito M, D'Anna R, Corrado F, *et al.* (2004). Cardiovascular effects of the phytoestrogen genistein. *Curr Med Chem Cardiovasc Hematol Agents* **2**(2): 179-186.
- Ambudkar IS, Ong HL (2007a). Organization and function of TRPC channelosomes. *Pflugers Arch* **455**(2): 187-200.
- Ambudkar IS, Ong HL, Liu X, Bandyopadhyay BC, Cheng KT (2007b). TRPC1: the link between functionally distinct store-operated calcium channels. *Cell Calcium* **42**(2): 213-223.
- Andresen MC, Yang M (1992). Gadolinium and mechanotransduction of rat aortic baroreceptors. *Am J Physiol* **262**(5 Pt 2): H1415-1421.
- Arora A, Byrem TM, Nair MG, Strasburg GM (2000). Modulation of liposomal membrane fluidity by flavonoids and isoflavonoids. *Arch Biochem Biophys* **373**(1): 102-109.
- Bahnasi YM, Wright HM, Milligan CJ, Dedman AM, Zeng F, Hopkins PM, *et al.* (2008). Modulation of TRPC5 cation channels by halothane, chloroform and propofol. *Br J Pharmacol* **153**(7): 1505-1512.
- Barnes S, Boersma B, Patel R, Kirk M, Darley-Usmar VM, Kim H, *et al.* (2000). Isoflavonoids and chronic disease: mechanisms of action. *Biofactors* **12**(1-4): 209-215.
- Barry SC, Harder B, Brzezinski M, Flint LY, Seppen J, Osborne WR (2001). Lentivirus vectors encoding both central polypurine tract and posttranscriptional

regulatory element provide enhanced transduction and transgene expression. *Hum Gene Ther* **12**(9): 1103-1108.

Beech DJ (2007a). Bipolar phospholipid sensing by TRPC5 calcium channel. *Biochem Soc Trans* **35**(Pt 1): 101-104.

Beech DJ (2007b). Canonical transient receptor potential 5. *Handb Exp Pharmacol*(179): 109-123.

Beech DJ (2009). Harmony and discord in endothelial calcium entry. *Circ Res* **104**(2): e22-23.

Belevych AE, Warriar S, Harvey RD (2002). Genistein inhibits cardiac L-type Ca(2+) channel activity by a tyrosine kinase-independent mechanism. *Mol Pharmacol* **62**(3): 554-565.

Bezzarides VJ, Ramsey IS, Kotecha S, Greka A, Clapham DE (2004). Rapid vesicular translocation and insertion of TRP channels. *Nat Cell Biol* **6**(8): 709-720.

Bicker G (2005). STOP and GO with NO: nitric oxide as a regulator of cell motility in simple brains. *Bioessays* **27**(5): 495-505.

Bodding M (2007). TRPM6: A Janus-like protein. *Handb Exp Pharmacol*(179): 299-311.

Bush EW, Hood DB, Papst PJ, Chapo JA, Minobe W, Bristow MR, *et al.* (2006). Canonical transient receptor potential channels promote cardiomyocyte hypertrophy through activation of calcineurin signaling. *J Biol Chem* **281**(44): 33487-33496.

Cantor RS (1997). Lateral pressures in cell membranes: a mechanism for modulation of protein function. *J Phys Chem B* **101**(10): 1723-1725.

Chapleau MW, Cunningham JT, Sullivan MJ, Wachtel RE, Abboud FM (1995a). Structural versus functional modulation of the arterial baroreflex. *Hypertension* **26**(2): 341-347.

Chapleau MW, Hajduczuk G, Sharma RV, Wachtel RE, Cunningham JT, Sullivan MJ, *et al.* (1995b). Mechanisms of baroreceptor activation. *Clin Exp Hypertens* **17**(1-2): 1-13.

- Chapleau MW, Li Z, Meyrelles SS, Ma X, Abboud FM (2001). Mechanisms determining sensitivity of baroreceptor afferents in health and disease. *Ann NY Acad Sci* **940**: 1-19.
- Chaudhuri P, Colles SM, Bhat M, Van Wagoner DR, Birnbaumer L, Graham LM (2008). Elucidation of a TRPC6-TRPC5 channel cascade that restricts endothelial cell movement. *Mol Biol Cell* **19**(8): 3203-3211.
- Chen Y, Lin MC, Yao H, Wang H, Zhang AQ, Yu J, *et al.* (2007). Lentivirus-mediated RNA interference targeting enhancer of zeste homolog 2 inhibits hepatocellular carcinoma growth through down-regulation of stathmin. *Hepatology* **46**(1): 200-208.
- Cheng KT, Leung YK, Shen B, Kwok YC, Wong CO, Kwan HY, *et al.* (2008). CNGA2 channels mediate adenosine-induced Ca²⁺ influx in vascular endothelial cells. *Arterioscler Thromb Vasc Biol* **28**(5): 913-918.
- Chiang CE, Chen SA, Chang MS, Lin CI, Luk HN (1996). Genistein directly inhibits L-type calcium currents but potentiates cAMP-dependent chloride currents in cardiomyocytes. *Biochem Biophys Res Commun* **223**(3): 598-603.
- Chiang CE, Luk HN, Chen LL, Wang TM, Ding PY (2002). Genistein inhibits the inward rectifying potassium current in guinea pig ventricular myocytes. *J Biomed Sci* **9**(4): 321-326.
- Christensen AP, Corey DP (2007). TRP channels in mechanosensation: direct or indirect activation? *Nat Rev Neurosci* **8**(7): 510-521.
- Chung HT, Choi BM, Kwon YG, Kim YM (2008). Interactive relations between nitric oxide (NO) and carbon monoxide (CO): heme oxygenase-1/CO pathway is a key modulator in NO-mediated antiapoptosis and anti-inflammation. *Methods Enzymol* **441**: 329-338.
- Clapham DE, Julius D, Montell C, Schultz G (2005). International Union of Pharmacology. XLIX. Nomenclature and structure-function relationships of transient receptor potential channels. *Pharmacol Rev* **57**(4): 427-450.
- Cruz MN, Agewall S, Schenck-Gustafsson K, Kublickiene K (2008). Acute dilatation

to phytoestrogens and estrogen receptor subtypes expression in small arteries from women with coronary heart disease. *Atherosclerosis* **196**(1): 49-58.

Cruz MN, Luksha L, Logman H, Poston L, Agewall S, Kublickiene K (2006). Acute responses to phytoestrogens in small arteries from men with coronary heart disease. *Am J Physiol Heart Circ Physiol* **290**(5): H1969-1975.

Cunningham JT, Wachtel RE, Abboud FM (1997). Mechanical stimulation of neurites generates an inward current in putative aortic baroreceptor neurons in vitro. *Brain Res* **757**(1): 149-154.

Cunningham JT, Wachtel RE, Abboud FM (1995). Mechanosensitive currents in putative aortic baroreceptor neurons in vitro. *J Neurophysiol* **73**(5): 2094-2098.

Dalmazzo S, Antoniotti S, Ariano P, Gilardino A, Lovisolo D (2008). Expression and localisation of TRPC channels in immortalised GnRH neurons. *Brain Res* **1230**: 27-36.

De Koninck P, Carbonetto S, Cooper E (1993). NGF induces neonatal rat sensory neurons to extend dendrites in culture after removal of satellite cells. *J Neurosci* **13**(2): 577-585.

Dedkova EN, Blatter LA (2002). Nitric oxide inhibits capacitative Ca²⁺ entry and enhances endoplasmic reticulum Ca²⁺ uptake in bovine vascular endothelial cells. *J Physiol* **539**(Pt 1): 77-91.

Dietrich A, Kalwa H, Fuchs B, Grimminger F, Weissmann N, Gudermann T (2007). In vivo TRPC functions in the cardiopulmonary vasculature. *Cell Calcium* **42**(2): 233-244.

Ditting T, Linz P, Hilgers KF, Jung O, Geiger H, Veelken R (2003). Putative role of epithelial sodium channels (ENaC) in the afferent limb of cardio renal reflexes in rats. *Basic Res Cardiol* **98**(6): 388-400.

Drummond HA, Welsh MJ, Abboud FM (2001). ENaC subunits are molecular components of the arterial baroreceptor complex. *Ann N Y Acad Sci* **940**: 42-47.

Du J, Ding M, Sours-Brothers S, Graham S, Ma R (2008). Mediation of angiotensin II-induced Ca²⁺ signaling by polycystin 2 in glomerular mesangial cells. *Am J*

Physiol Renal Physiol **294**(4): F909-918.

Escande A, Pillon A, Servant N, Cravedi JP, Larrea F, Muhn P, *et al.* (2006). Evaluation of ligand selectivity using reporter cell lines stably expressing estrogen receptor alpha or beta. *Biochem Pharmacol* **71**(10): 1459-1469.

Espey MG, Miranda KM, Thomas DD, Xavier S, Citrin D, Vitek MP, *et al.* (2002). A chemical perspective on the interplay between NO, reactive oxygen species, and reactive nitrogen oxide species. *Ann N Y Acad Sci* **962**: 195-206.

Feelisch M (1998). The use of nitric oxide donors in pharmacological studies. *Naunyn Schmiedebergs Arch Pharmacol* **358**(1): 113-122.

Flemming PK, Dedman AM, Xu SZ, Li J, Zeng F, Naylor J, *et al.* (2006). Sensing of lysophospholipids by TRPC5 calcium channel. *J Biol Chem* **281**(8): 4977-4982.

Garcia-Martinez C, Morenilla-Palao C, Planells-Cases R, Merino JM, Ferrer-Montiel A (2000). Identification of an aspartic residue in the P-loop of the vanilloid receptor that modulates pore properties. *J Biol Chem* **275**(42): 32552-32558.

Glazebrook PA, Schilling WP, Kunze DL (2005). TRPC channels as signal transducers. *Pflugers Arch* **451**(1): 125-130.

Goel M, Sinkins WG, Schilling WP (2002). Selective association of TRPC channel subunits in rat brain synaptosomes. *J Biol Chem* **277**(50): 48303-48310.

Gomez TM, Zheng JQ (2006). The molecular basis for calcium-dependent axon pathfinding. *Nat Rev Neurosci* **7**(2): 115-125.

Gomis A, Soriano S, Belmonte C, Viana F (2008). Hypoosmotic- and pressure-induced membrane stretch activate TRPC5 channels. *J Physiol* **586**(Pt 23): 5633-5649.

Gottlieb P, Folgering J, Maroto R, Raso A, Wood TG, Kurosky A, *et al.* (2008). Revisiting TRPC1 and TRPC6 mechanosensitivity. *Pflugers Arch* **455**(6): 1097-1103.

Gouni-Berthold I, Sachinidis A (2004). Possible non-classic intracellular and molecular mechanisms of LDL cholesterol action contributing to the development and progression of atherosclerosis. *Curr Vasc Pharmacol* **2**(4): 363-370.

- Greka A, Navarro B, Oancea E, Duggan A, Clapham DE (2003). TRPC5 is a regulator of hippocampal neurite length and growth cone morphology. *Nat Neurosci* **6**(8): 837-845.
- Hajduczuk G, Chapleau MW, Ferlic RJ, Mao HZ, Abboud FM (1994). Gadolinium inhibits mechanoelectrical transduction in rabbit carotid baroreceptors. Implication of stretch-activated channels. *J Clin Invest* **94**(6): 2392-2396.
- Hamill OP, Martinac B (2001). Molecular basis of mechanotransduction in living cells. *Physiol Rev* **81**(2): 685-740.
- Hardie RC (2003). Regulation of TRP channels via lipid second messengers. *Annu Rev Physiol* **65**: 735-759.
- Hardie RC, Minke B (1993). Novel Ca²⁺ channels underlying transduction in Drosophila photoreceptors: implications for phosphoinositide-mediated Ca²⁺ mobilization. *Trends Neurosci* **16**(9): 371-376.
- Hess DT, Matsumoto A, Kim SO, Marshall HE, Stamler JS (2005). Protein S-nitrosylation: purview and parameters. *Nat Rev Mol Cell Biol* **6**(2): 150-166.
- Hoenderop JG, Voets T, Hoefs S, Weidema F, Prenen J, Nilius B, *et al.* (2003). Homo- and heterotetrameric architecture of the epithelial Ca²⁺ channels TRPV5 and TRPV6. *EMBO J* **22**(4): 776-785.
- Hofmann T, Schaefer M, Schultz G, Gudermann T (2002). Subunit composition of mammalian transient receptor potential channels in living cells. *Proc Natl Acad Sci U S A* **99**(11): 7461-7466.
- Hu G, Oboukhova EA, Kumar S, Sturek M, Obukhov AG (2009). Canonical transient receptor potential channels expression is elevated in a porcine model of metabolic syndrome. *Mol Endocrinol* **23**(5): 689-699.
- Hughes AR, Putney JW, Jr. (1988). Metabolism and functions of inositol phosphates. *Biofactors* **1**(2): 117-121.
- Hui H, McHugh D, Hannan M, Zeng F, Xu SZ, Khan SU, *et al.* (2006). Calcium-sensing mechanism in TRPC5 channels contributing to retardation of

neurite outgrowth. *J Physiol* **572**(Pt 1): 165-172.

Hwang TC, Koeppe RE, 2nd, Andersen OS (2003). Genistein can modulate channel function by a phosphorylation-independent mechanism: importance of hydrophobic mismatch and bilayer mechanics. *Biochemistry* **42**(46): 13646-13658.

Ignarro LJ (2002). Nitric oxide as a unique signaling molecule in the vascular system: a historical overview. *J Physiol Pharmacol* **53**(4 Pt 1): 503-514.

Jaffrey SR, Erdjument-Bromage H, Ferris CD, Tempst P, Snyder SH (2001). Protein S-nitrosylation: a physiological signal for neuronal nitric oxide. *Nat Cell Biol* **3**(2): 193-197.

Janmey PA (1998). The cytoskeleton and cell signaling: component localization and mechanical coupling. *Physiol Rev* **78**(3): 763-781.

Jung S, Muhle A, Schaefer M, Strotmann R, Schultz G, Plant TD (2003). Lanthanides potentiate TRPC5 currents by an action at extracellular sites close to the pore mouth. *J Biol Chem* **278**(6): 3562-3571.

Kanki H, Kinoshita M, Akaike A, Satoh M, Mori Y, Kaneko S (2001). Activation of inositol 1,4,5-trisphosphate receptor is essential for the opening of mouse TRP5 channels. *Mol Pharmacol* **60**(5): 989-998.

Kawasaki BT, Liao Y, Birnbaumer L (2006). Role of Src in C3 transient receptor potential channel function and evidence for a heterogeneous makeup of receptor- and store-operated Ca²⁺ entry channels. *Proc Natl Acad Sci U S A* **103**(2): 335-340.

Kaziro Y, Itoh H, Kozasa T, Nakafuku M, Satoh T (1991). Structure and function of signal-transducing GTP-binding proteins. *Annu Rev Biochem* **60**: 349-400.

Kedei N, Szabo T, Lile JD, Treanor JJ, Olah Z, Iadarola MJ, *et al.* (2001). Analysis of the native quaternary structure of vanilloid receptor 1. *J Biol Chem* **276**(30): 28613-28619.

Kelly MJ, Levin ER (2001). Rapid actions of plasma membrane estrogen receptors. *Trends Endocrinol Metab* **12**(4): 152-156.

Kim BJ, Kim MT, Jeon JH, Kim SJ, So I (2008). Involvement of

phosphatidylinositol 4,5-bisphosphate in the desensitization of canonical transient receptor potential 5. *Biol Pharm Bull* **31**(9): 1733-1738.

Kim MT, Kim BJ, Lee JH, Kwon SC, Yeon DS, Yang DK, *et al.* (2006). Involvement of calmodulin and myosin light chain kinase in activation of mTRPC5 expressed in HEK cells. *Am J Physiol Cell Physiol* **290**(4): C1031-1040.

Kinoshita-Kawada M, Tang J, Xiao R, Kaneko S, Foskett JK, Zhu MX (2005). Inhibition of TRPC5 channels by Ca²⁺-binding protein 1 in *Xenopus* oocytes. *Pflugers Arch* **450**(5): 345-354.

Kirchheim HR (1976). Systemic arterial baroreceptor reflexes. *Physiol Rev* **56**(1): 100-177.

Klionsky L, Tamir R, Holzinger B, Bi X, Talvenheimo J, Kim H, *et al.* (2006). A polyclonal antibody to the prepore loop of transient receptor potential vanilloid type 1 blocks channel activation. *J Pharmacol Exp Ther* **319**(1): 192-198.

Kunert-Keil C, Bisping F, Kruger J, Brinkmeier H (2006). Tissue-specific expression of TRP channel genes in the mouse and its variation in three different mouse strains. *BMC Genomics* **7**: 159.

Kung C (2005). A possible unifying principle for mechanosensation. *Nature* **436**(7051): 647-654.

Kwan HY, Huang Y, Yao X (2004). Regulation of canonical transient receptor potential isoform 3 (TRPC3) channel by protein kinase G. *Proc Natl Acad Sci U S A* **101**(8): 2625-2630.

Kwan HY, Huang Y, Yao X (2000). Store-operated calcium entry in vascular endothelial cells is inhibited by cGMP via a protein kinase G-dependent mechanism. *J Biol Chem* **275**(10): 6758-6763.

Kwan HY, Huang Y, Yao X (2007). TRP channels in endothelial function and dysfunction. *Biochim Biophys Acta* **1772**(8): 907-914.

Lee J, Cha SK, Sun TJ, Huang CL (2005). PIP₂ activates TRPV5 and releases its inhibition by intracellular Mg²⁺. *J Gen Physiol* **126**(5): 439-451.

- Lee YM, Kim BJ, Kim HJ, Yang DK, Zhu MH, Lee KP, *et al.* (2003). TRPC5 as a candidate for the nonselective cation channel activated by muscarinic stimulation in murine stomach. *Am J Physiol Gastrointest Liver Physiol* **284**(4): G604-616.
- Li Z, Chapleau MW, Bates JN, Bielefeldt K, Lee HC, Abboud FM (1998). Nitric oxide as an autocrine regulator of sodium currents in baroreceptor neurons. *Neuron* **20**(5): 1039-1049.
- Liao Y, Erxleben C, Abramowitz J, Flockerzi V, Zhu MX, Armstrong DL, *et al.* (2008). Functional interactions among Orai1, TRPCs, and STIM1 suggest a STIM-regulated heteromeric Orai/TRPC model for SOCE/Icrac channels. *Proc Natl Acad Sci U S A* **105**(8): 2895-2900.
- Lin SY, Corey DP (2005). TRP channels in mechanosensation. *Curr Opin Neurobiol* **15**(3): 350-357.
- Liu D, Liman ER (2003a). Intracellular Ca²⁺ and the phospholipid PIP₂ regulate the taste transduction ion channel TRPM5. *Proc Natl Acad Sci U S A* **100**(25): 15160-15165.
- Liu DY, Thilo F, Scholze A, Wittstock A, Zhao ZG, Harteneck C, *et al.* (2007). Increased store-operated and 1-oleoyl-2-acetyl-sn-glycerol-induced calcium influx in monocytes is mediated by transient receptor potential canonical channels in human essential hypertension. *J Hypertens* **25**(4): 799-808.
- Liu X, Singh BB, Ambudkar IS (2003b). TRPC1 is required for functional store-operated Ca²⁺ channels. Role of acidic amino acid residues in the S5-S6 region. *J Biol Chem* **278**(13): 11337-11343.
- Maroto R, Raso A, Wood TG, Kurosky A, Martinac B, Hamill OP (2005). TRPC1 forms the stretch-activated cation channel in vertebrate cells. *Nat Cell Biol* **7**(2): 179-185.
- Mery L, Strauss B, Dufour JF, Krause KH, Hoth M (2002). The PDZ-interacting domain of TRPC4 controls its localization and surface expression in HEK293 cells. *J Cell Sci* **115**(Pt 17): 3497-3508.
- Messina M (1999). Soy, soy phytoestrogens (isoflavones), and breast cancer. *Am J Clin Nutr* **70**(4): 574-575.

- Minke B, Cook B (2002). TRP channel proteins and signal transduction. *Physiol Rev* **82**(2): 429-472.
- Mio K, Ogura T, Hara Y, Mori Y, Sato C (2005). The non-selective cation-permeable channel TRPC3 is a tetrahedron with a cap on the large cytoplasmic end. *Biochem Biophys Res Commun* **333**(3): 768-777.
- Mishra SK, Abbot SE, Choudhury Z, Cheng M, Khatab N, Maycock NJ, *et al.* (2000). Endothelium-dependent relaxation of rat aorta and main pulmonary artery by the phytoestrogens genistein and daidzein. *Cardiovasc Res* **46**(3): 539-546.
- Moiseenkova-Bell VY, Stanciu LA, Serysheva, II, Tobe BJ, Wensel TG (2008). Structure of TRPV1 channel revealed by electron cryomicroscopy. *Proc Natl Acad Sci U S A* **105**(21): 7451-7455.
- Montell C, Rubin GM (1989). Molecular characterization of the *Drosophila* *trp* locus: a putative integral membrane protein required for phototransduction. *Neuron* **2**(4): 1313-1323.
- Morikawa H, Fukuda K, Mima H, Shoda T, Kato S, Mori K (1998). Tyrosine kinase inhibitors suppress N-type and T-type Ca²⁺ channel currents in NG108-15 cells. *Pflugers Arch* **436**(1): 127-132.
- Nadal A, Ropero AB, Fuentes E, Soria B, Ripoll C (2004). Estrogen and xenoestrogen actions on endocrine pancreas: from ion channel modulation to activation of nuclear function. *Steroids* **69**(8-9): 531-536.
- Naylor J, Milligan CJ, Zeng F, Jones C, Beech DJ (2008). Production of a specific extracellular inhibitor of TRPM3 channels. *Br J Pharmacol* **155**(4): 567-573.
- Nevala R, Paukku K, Korpela R, Vapaatalo H (2001). Calcium-sensitive potassium channel inhibitors antagonize genistein- and daidzein-induced arterial relaxation in vitro. *Life Sci* **69**(12): 1407-1417.
- Nilius B, Mahieu F, Prenen J, Janssens A, Owsianik G, Vennekens R, *et al.* (2006). The Ca²⁺-activated cation channel TRPM4 is regulated by phosphatidylinositol 4,5-bisphosphate. *EMBO J* **25**(3): 467-478.

- Nilius B, Owsianik G, Voets T (2008). Transient receptor potential channels meet phosphoinositides. *EMBO J* **27**(21): 2809-2816.
- Nilius B, Prenen J, Janssens A, Owsianik G, Wang C, Zhu MX, *et al.* (2005). The selectivity filter of the cation channel TRPM4. *J Biol Chem* **280**(24): 22899-22906.
- Obukhov AG, Nowycky MC (2005). A cytosolic residue mediates Mg²⁺ block and regulates inward current amplitude of a transient receptor potential channel. *J Neurosci* **25**(5): 1234-1239.
- Obukhov AG, Nowycky MC (2004). TRPC5 activation kinetics are modulated by the scaffolding protein ezrin/radixin/moesin-binding phosphoprotein-50 (EBP50). *J Cell Physiol* **201**(2): 227-235.
- Obukhov AG, Nowycky MC (2008). TRPC5 channels undergo changes in gating properties during the activation-deactivation cycle. *J Cell Physiol* **216**(1): 162-171.
- Ogata R, Kitamura K, Ito Y, Nakano H (1997). Inhibitory effects of genistein on ATP-sensitive K⁺ channels in rabbit portal vein smooth muscle. *Br J Pharmacol* **122**(7): 1395-1404.
- Okada T, Shimizu S, Wakamori M, Maeda A, Kurosaki T, Takada N, *et al.* (1998). Molecular cloning and functional characterization of a novel receptor-activated TRP Ca²⁺ channel from mouse brain. *J Biol Chem* **273**(17): 10279-10287.
- Oliet SH, Bourque CW (1993). Mechanosensitive channels transduce osmosensitivity in supraoptic neurons. *Nature* **364**(6435): 341-343.
- Ordaz B, Tang J, Xiao R, Salgado A, Sampieri A, Zhu MX, *et al.* (2005). Calmodulin and calcium interplay in the modulation of TRPC5 channel activity. Identification of a novel C-terminal domain for calcium/calmodulin-mediated facilitation. *J Biol Chem* **280**(35): 30788-30796.
- Otsuguro K, Tang J, Tang Y, Xiao R, Freichel M, Tsvilovskyy V, *et al.* (2008). Isoform-specific inhibition of TRPC4 channel by phosphatidylinositol 4,5-bisphosphate. *J Biol Chem* **283**(15): 10026-10036.
- Paillart C, Carlier E, Guedin D, Dargent B, Couraud F (1997). Direct block of voltage-sensitive sodium channels by genistein, a tyrosine kinase inhibitor. *J*

Pharmacol Exp Ther **280**(2): 521-526.

Parker KK, Ingber DE (2007). Extracellular matrix, mechanotransduction and structural hierarchies in heart tissue engineering. *Philos Trans R Soc Lond B Biol Sci* **362**(1484): 1267-1279.

Pedersen SF, Nilius B (2007). Transient receptor potential channels in mechanosensing and cell volume regulation. *Methods Enzymol* **428**: 183-207.

Pena F, Ordaz B (2008). Non-selective cation channel blockers: potential use in nervous system basic research and therapeutics. *Mini Rev Med Chem* **8**(8): 812-819.

Philipp S, Hambrecht J, Braslavski L, Schroth G, Freichel M, Murakami M, *et al.* (1998). A novel capacitative calcium entry channel expressed in excitable cells. *EMBO J* **17**(15): 4274-4282.

Potier M, Trebak M (2008). New developments in the signaling mechanisms of the store-operated calcium entry pathway. *Pflugers Arch* **457**(2): 405-415.

Prescott ED, Julius D (2003). A modular PIP2 binding site as a determinant of capsaicin receptor sensitivity. *Science* **300**(5623): 1284-1288.

Raz L, Khan MM, Mahesh VB, Vadlamudi RK, Brann DW (2008). Rapid estrogen signaling in the brain. *Neurosignals* **16**(2-3): 140-153.

Rindone JP, Sloane EP (1992). Cyanide toxicity from sodium nitroprusside: risks and management. *Ann Pharmacother* **26**(4): 515-519.

Rossier BC (1998). Mechanosensitivity of the epithelial sodium channel (ENaC): controversy or pseudocontroversy? *J Gen Physiol* **112**(2): 95-96.

Schaefer M, Plant TD, Obukhov AG, Hofmann T, Gudermann T, Schultz G (2000). Receptor-mediated regulation of the nonselective cation channels TRPC4 and TRPC5. *J Biol Chem* **275**(23): 17517-17526.

Schofield JN, Day IN, Thompson RJ, Edwards YH (1995). PGP9.5, a ubiquitin C-terminal hydrolase; pattern of mRNA and protein expression during neural development in the mouse. *Brain Res Dev Brain Res* **85**(2): 229-238.

Schwab A (2001). Function and spatial distribution of ion channels and transporters in cell migration. *Am J Physiol Renal Physiol* **280**(5): F739-747.

Semtner M, Schaefer M, Pinkenburg O, Plant TD (2007). Potentiation of TRPC5 by protons. *J Biol Chem* **282**(46): 33868-33878.

Sharma RV, Chapleau MW, Hajduczuk G, Wachtel RE, Waite LJ, Bhalla RC, *et al.* (1995). Mechanical stimulation increases intracellular calcium concentration in nodose sensory neurons. *Neuroscience* **66**(2): 433-441.

Shen B, Cheng KT, Leung YK, Kwok YC, Kwan HY, Wong CO, *et al.* (2008). Epinephrine-induced Ca²⁺ influx in vascular endothelial cells is mediated by CNGA2 channels. *J Mol Cell Cardiol* **45**(3): 437-445.

Si H, Liu D (2007). Phytochemical genistein in the regulation of vascular function: new insights. *Curr Med Chem* **14**(24): 2581-2589.

Smirnov SV, Aaronson PI (1995). Inhibition of vascular smooth muscle cell K⁺ currents by tyrosine kinase inhibitors genistein and ST 638. *Circ Res* **76**(2): 310-316.

Snyder SH (1994). Nitric oxide. More jobs for that molecule. *Nature* **372**(6506): 504-505.

Sossey-Alaoui K, Lyon JA, Jones L, Abidi FE, Hartung AJ, Hane B, *et al.* (1999). Molecular cloning and characterization of TRPC5 (HTRP5), the human homologue of a mouse brain receptor-activated capacitative Ca²⁺ entry channel. *Genomics* **60**(3): 330-340.

Spassova MA, Hewavitharana T, Xu W, Soboloff J, Gill DL (2006). A common mechanism underlies stretch activation and receptor activation of TRPC6 channels. *Proc Natl Acad Sci U S A* **103**(44): 16586-16591.

Stamler JS, Toone EJ, Lipton SA, Sucher NJ (1997). (S)NO signals: translocation, regulation, and a consensus motif. *Neuron* **18**(5): 691-696.

Strubing C, Krapivinsky G, Krapivinsky L, Clapham DE (2003). Formation of novel TRPC channels by complex subunit interactions in embryonic brain. *J Biol Chem* **278**(40): 39014-39019.

- Strubing C, Krapivinsky G, Krapivinsky L, Clapham DE (2001). TRPC1 and TRPC5 form a novel cation channel in mammalian brain. *Neuron* **29**(3): 645-655.
- Sullivan MJ, Sharma RV, Wachtel RE, Chapleau MW, Waite LJ, Bhalla RC, *et al.* (1997). Non-voltage-gated Ca²⁺ influx through mechanosensitive ion channels in aortic baroreceptor neurons. *Circ Res* **80**(6): 861-867.
- Sutton KA, Jungnickel MK, Wang Y, Cullen K, Lambert S, Florman HM (2004). Enkurin is a novel calmodulin and TRPC channel binding protein in sperm. *Dev Biol* **274**(2): 426-435.
- Tabata H, Tanaka S, Sugimoto Y, Kanki H, Kaneko S, Ichikawa A (2002). Possible coupling of prostaglandin E receptor EP(1) to TRP5 expressed in *Xenopus laevis* oocytes. *Biochem Biophys Res Commun* **298**(3): 398-402.
- Takeuchi K, Watanabe H, Tran QK, Ozeki M, Sumi D, Hayashi T, *et al.* (2004). Nitric oxide: inhibitory effects on endothelial cell calcium signaling, prostaglandin I₂ production and nitric oxide synthase expression. *Cardiovasc Res* **62**(1): 194-201.
- Tang J, Lin Y, Zhang Z, Tikunova S, Birnbaumer L, Zhu MX (2001). Identification of common binding sites for calmodulin and inositol 1,4,5-trisphosphate receptors on the carboxyl termini of trp channels. *J Biol Chem* **276**(24): 21303-21310.
- Tang Y, Tang J, Chen Z, Trost C, Flockerzi V, Li M, *et al.* (2000). Association of mammalian trp4 and phospholipase C isozymes with a PDZ domain-containing protein, NHERF. *J Biol Chem* **275**(48): 37559-37564.
- Trebak M, Hempel N, Wedel BJ, Smyth JT, Bird GS, Putney JW, Jr. (2005). Negative regulation of TRPC3 channels by protein kinase C-mediated phosphorylation of serine 712. *Mol Pharmacol* **67**(2): 558-563.
- Trebak M, Lemonnier L, Dehaven WI, Wedel BJ, Bird GS, Putney JW, Jr. (2008). Complex functions of phosphatidylinositol 4,5-bisphosphate in regulation of TRPC5 cation channels. *Pflugers Arch*.
- Valero MS, Garay RP, Gros P, Alda JO (2006). Cystic fibrosis transmembrane conductance regulator (CFTR) chloride channel and Na-K-Cl cotransporter NKCC1 isoform mediate the vasorelaxant action of genistein in isolated rat aorta. *Eur J Pharmacol* **544**(1-3): 126-131.

- Vanhoutte PM (1992). Role of calcium and endothelium in hypertension, cardiovascular disease, and subsequent vascular events. *J Cardiovasc Pharmacol* **19** Suppl 3: S6-10.
- Vannier B, Zhu X, Brown D, Birnbaumer L (1998). The membrane topology of human transient receptor potential 3 as inferred from glycosylation-scanning mutagenesis and epitope immunocytochemistry. *J Biol Chem* **273**(15): 8675-8679.
- Venkatachalam K, Zheng F, Gill DL (2003). Regulation of canonical transient receptor potential (TRPC) channel function by diacylglycerol and protein kinase C. *J Biol Chem* **278**(31): 29031-29040.
- Viana F, de la Pena E, Pecson B, Schmidt RF, Belmonte C (2001). Swelling-activated calcium signalling in cultured mouse primary sensory neurons. *Eur J Neurosci* **13**(4): 722-734.
- Voets T, Janssens A, Prenen J, Droogmans G, Nilius B (2003). Mg²⁺-dependent gating and strong inward rectification of the cation channel TRPV6. *J Gen Physiol* **121**(3): 245-260.
- Voets T, Nilius B (2007). Modulation of TRPs by PIPs. *J Physiol* **582**(Pt 3): 939-944.
- Voets T, Prenen J, Vriens J, Watanabe H, Janssens A, Wissenbach U, *et al.* (2002). Molecular determinants of permeation through the cation channel TRPV4. *J Biol Chem* **277**(37): 33704-33710.
- Voets T, Talavera K, Owsianik G, Nilius B (2005). Sensing with TRP channels. *Nat Chem Biol* **1**(2): 85-92.
- Vriens J, Watanabe H, Janssens A, Droogmans G, Voets T, Nilius B (2004). Cell swelling, heat, and chemical agonists use distinct pathways for the activation of the cation channel TRPV4. *Proc Natl Acad Sci U S A* **101**(1): 396-401.
- Whaley WL, Rummel JD, Kastropeli N (2006). Interactions of genistein and related isoflavones with lipid micelles. *Langmuir* **22**(17): 7175-7184.
- Worley PF, Zeng W, Huang GN, Yuan JP, Kim JY, Lee MG, *et al.* (2007). TRPC channels as STIM1-regulated store-operated channels. *Cell Calcium* **42**(2): 205-211.

- Wu G, Lu ZH, Obukhov AG, Nowycky MC, Ledeen RW (2007). Induction of calcium influx through TRPC5 channels by cross-linking of GM1 ganglioside associated with alpha5beta1 integrin initiates neurite outgrowth. *J Neurosci* **27**(28): 7447-7458.
- Xu SZ, Boulay G, Flemming R, Beech DJ (2006a). E3-targeted anti-TRPC5 antibody inhibits store-operated calcium entry in freshly isolated pial arterioles. *Am J Physiol Heart Circ Physiol* **291**(6): H2653-2659.
- Xu SZ, Muraki K, Zeng F, Li J, Sukumar P, Shah S, *et al.* (2006b). A sphingosine-1-phosphate-activated calcium channel controlling vascular smooth muscle cell motility. *Circ Res* **98**(11): 1381-1389.
- Xu SZ, Sukumar P, Zeng F, Li J, Jairaman A, English A, *et al.* (2008). TRPC channel activation by extracellular thioredoxin. *Nature* **451**(7174): 69-72.
- Xu SZ, Zeng F, Boulay G, Grimm C, Harteneck C, Beech DJ (2005a). Block of TRPC5 channels by 2-aminoethoxydiphenyl borate: a differential, extracellular and voltage-dependent effect. *Br J Pharmacol* **145**(4): 405-414.
- Xu SZ, Zeng F, Lei M, Li J, Gao B, Xiong C, *et al.* (2005b). Generation of functional ion-channel tools by E3 targeting. *Nat Biotechnol* **23**(10): 1289-1293.
- Yamada H, Wakamori M, Hara Y, Takahashi Y, Konishi K, Imoto K, *et al.* (2000). Spontaneous single-channel activity of neuronal TRP5 channel recombinantly expressed in HEK293 cells. *Neurosci Lett* **285**(2): 111-114.
- Yamamoto M, Chen MZ, Wang YJ, Sun HQ, Wei Y, Martinez M, *et al.* (2006). Hypertonic stress increases phosphatidylinositol 4,5-bisphosphate levels by activating PIP5K1beta. *J Biol Chem* **281**(43): 32630-32638.
- Yang XC, Sachs F (1989). Block of stretch-activated ion channels in *Xenopus* oocytes by gadolinium and calcium ions. *Science* **243**(4894 Pt 1): 1068-1071.
- Yao X, Garland CJ (2005a). Recent developments in vascular endothelial cell transient receptor potential channels. *Circ Res* **97**(9): 853-863.
- Yao X, Kwan HY, Huang Y (2005b). Regulation of TRP channels by phosphorylation.

Neurosignals **14**(6): 273-280.

Yip H, Chan WY, Leung PC, Kwan HY, Liu C, Huang Y, *et al.* (2004). Expression of TRPC homologs in endothelial cells and smooth muscle layers of human arteries. *Histochem Cell Biol* **122**(6): 553-561.

Yoshida T, Inoue R, Morii T, Takahashi N, Yamamoto S, Hara Y, *et al.* (2006). Nitric oxide activates TRP channels by cysteine S-nitrosylation. *Nat Chem Biol* **2**(11): 596-607.

Yuan JP, Zeng W, Huang GN, Worley PF, Muallem S (2007). STIM1 heteromultimerizes TRPC channels to determine their function as store-operated channels. *Nat Cell Biol* **9**(6): 636-645.

Zeng F, Xu SZ, Jackson PK, McHugh D, Kumar B, Fountain SJ, *et al.* (2004). Human TRPC5 channel activated by a multiplicity of signals in a single cell. *J Physiol* **559**(Pt 3): 739-750.

Zhang W, Tong Q, Conrad K, Wozney J, Cheung JY, Miller BA (2007). Regulation of TRP channel TRPM2 by the tyrosine phosphatase PTPL1. *Am J Physiol Cell Physiol* **292**(5): C1746-1758.

Zhang Y, Davies LR, Martin SM, Coddington WJ, Miller FJ, Jr., Buettner GR, *et al.* (2003). The nitric oxide donor S-nitroso-N-acetylpenicillamine (SNAP) increases free radical generation and degrades left ventricular function after myocardial ischemia-reperfusion. *Resuscitation* **59**(3): 345-352.

Zhang Z, Tang J, Tikunova S, Johnson JD, Chen Z, Qin N, *et al.* (2001). Activation of Trp3 by inositol 1,4,5-trisphosphate receptors through displacement of inhibitory calmodulin from a common binding domain. *Proc Natl Acad Sci U S A* **98**(6): 3168-3173.

Zhu MH, Chae M, Kim HJ, Lee YM, Kim MJ, Jin NG, *et al.* (2005). Desensitization of canonical transient receptor potential channel 5 by protein kinase C. *Am J Physiol Cell Physiol* **289**(3): C591-600.

Zhu X, Chu PB, Peyton M, Birnbaumer L (1995). Molecular cloning of a widely expressed human homologue for the *Drosophila* trp gene. *FEBS Lett* **373**(3): 193-198.

Zhu X, Jiang M, Peyton M, Boulay G, Hurst R, Stefani E, *et al.* (1996). trp, a novel mammalian gene family essential for agonist-activated capacitative Ca²⁺ entry. *Cell* **85**(5): 661-671.